Luigi Margarucci

UNIVERSITÀ DEGLI STUDI DI SALERNO
DIPARTIMENTO DI SCIENZE FARMACEUTICHE

Dottorato di Ricerca in Scienze Farmaceutiche
IX-Ciclo NS
2007-2010

CHEMICAL PROTEOMICS ON LIGAND-PROTEIN INTERACTION

Luigi Margarucci

Dipartimento di Scienze Farmaceutiche
Via Ponte Don Melillo 84084
Fisciano, Salerno

Chemicla Proteomics on Ligand Protein Interaction

UNIVERSITÀ DEGLI STUDI DI SALERNO

DIPARTIMENTO DI SCIENZE FARMACEUTICHE

Dottorato di ricerca in Scienze Farmaceutiche

IX ciclo NS (XXIII)

2007-2010

Chemical Proteomics on Ligand Protein Interaction

Tutor
Prof. Raffaele Riccio

PhD Student
Luigi Margarucci

Coordinator
Prof.ssa Nunziatina De Tommasi

To my Parents

Preface

In November 2007, I enrolled in PhD three years course in Pharmaceutical Sciences at the Department of Pharmaceutical Sciences of Salerno University under the supervision of Prof. Raffaele Riccio.

My research activity was mainly focused onto the development of mass spectrometry-based chemical proteomics. These approaches were successfully applied to the interactome characterization of three bioactive marine metabolites, Petrosaspongiolide M, Bolinaquinone and Perthamide C. The entire work was carried out under the direct supervision of Prof. A. Casapullo and Dr. Maria Chiara Monti.

Since our methodology required some biochemical efforts, I also joined forces of Dr. Alessandra Tosco and Dr. Bianca Fontanella from the biochemistry section of our Department.

Furthermore, to improve my knowledge on the quantitative features of chemical proteomics, I moved to the Department of Biomolecular Mass Spectrometry and Proteomic Group of the Utrecht University in 2009. There, my research was carried out under the supervision of Prof. Albert J.R. Heck and Dr. Arjen Scholten and was mainly focused on the application of targeted quantitative chemical proteomics to uncover spatial reorganization of cAMP and cGMP signaling scaffolds in collagen stimulated platelets.

In addition to PhD course activities, I was involved in different side projects, mainly regarding the molecular recognition processes of small marine metabolites with phospholipase A_2 and tau protein.

List of publications related to the scientific activity performed during the three years PhD course in Pharmaceutical Sciences:

Papers:

- ✓ M. C. Monti, A. Casapullo, C. N. Cavasotto, A.Tosco, F. Dal Piaz, A. Ziemys, **L.Margarucci**, R. Riccio "The Binding Mode of Petrosaspongiolide M to the Human Group IIA PhospholipaseA2: Exploring the Role of Covalent and Non-Covalent Interactions in the Inhibition Process", *Chem. Eur. J.*, **2009**, *15*, 1155-1163.
- ✓ M. C. Monti, M. G. Chini, **L. Margarucci**, A. Tosco, R. Riccio, G. Bifulco, A. Casapullo "The Molecular Mechanism of Human Group IIA Phospholipase A2 Inactivation by Bolinaquinone", *J Mol. Recognit.*, **2009**, *22*, 530-537.
- ✓ **L. Margarucci,** M. C. Monti, A. Tosco, R. Riccio, A. Casapullo "Chemical Proteomics Discloses Petrosapongiolide M, an Anti-inflammatory Marine Sesterterpene, as a New Proteasome Inhibitor", *Angew. Chem. Int. Ed.* **2010,** *49,* 3960 –3963.
- ✓ **L. Margarucci,** M. C. Monti, B. Fontanella, R. Riccio, A. Casapullo "Chemical Proteomics Reveals Bolinaquinone as a Clathrin-Mediated Endocytosis Inhibitor", *Mol. BioSyst.,* **2011**, 7, 480–485
- ✓ **C. Petronzi, R**. Filosa, A. Peduto, M. C. Monti, **L. Margarucci**, A. Massa, S. F. Ercolino, V. Bizzarro, L. Parente, R. Riccio, P. de Caprariis "Structure-Based *Design, Synt*he**sis** and Preliminary Anti-inflammatory Activity of Boli**naquinone Ana**logues" *Eur J Med Chem*, **2011**, *In press* **DOI**: 10.1016/j.ejmech.2010.11.028.
- ✓ **L.Margarucci**, T. C. van Holten, C. Preisinger, O. B. Bleijerveld, M. Roest, A. J.R. Heck, A. Scholten,"Collage*n stimulation of* **pla**tel*ets induc***es** rapid spatial reorganizations in cAMP and cGMP signaling scaffolds" *Mol. BioSyst.*, **2011** *Manuscript submitted-under review.*

- ✓ **L. Margarucci,** M. C. Monti, A. Vilasi, A. Tosco, R. Riccio, Agostino Casapullo "Towards the Identification of Perthamide C Biological Partners" *Manuscript in preparation* (Full Paper).
- ✓ M.C. Monti, **L.Margarucci**, A. Tosco, R. Riccio, A. Casapullo "New insights on the interaction mechanism between tau protein and Oleochantal, an extra-virgin olive-oil bioactive component" *Manuscript in preparation*.

Conference proceedings:

- ✓ **L.Margarucci**, M. C. Monti, B. Fontanella, R. Riccio, A. Casapullo "Bolinaquinone, a New Clathrin-Mediated Endocytosis Inhibitor by Chemical Proteomics", *Journal of Biotechnology*, **2010**, 150, Supplement 1, 458-459.
- ✓ **L. Margarucci,** M.Chiara Monti, R. Riccio, A. Casapullo, "Chemical Proteomics as a Tool in Target Discovery of Bioactive Small Molecules", 2010, *Journal of Biotechnology*, *150*, Supplement 1, 576

Table of Contents

Abstract.....**I**

Page

Introduction.....**1-26**

Chapter 1 Mass spectrometry-based chemical proteomics: an overview **3**

Results and Discussion.....**27-96**

Chapter 2 Chemical Proteomics Discloses Petrosapongiolide M, an Anti-inflammatory Marine Sesterterpene, as a Proteasome Inhibitor **29**

Chapter 3 Chemical Proteomics Reveals Bolinaquinone as a Clathrin-Mediated Endocytosis Inhibitor **47**

Chapter 4 Towards the Identification of Perthamide C Biological Partners **63**

Chapter 5 Collagen Stimulation of Platelets Induces Rapid Spatial Reorganizations in cAMP and cGMP Signaling Scaffolds **77**

Conclusions.....**97-104**

Chapter 6 Conclusions **97**

Experimental Section.....**105-136**

Chapter 7 Chemical proteomics applied to Petrosaspongiolide M, Bolinaquinone, Perthamide C target discovery: Experimental procedures **107**

Chapter 8 Collagen stimulation of platelets induces rapid spatial reorganizations in cAMP and cGMP signaling scaffolds: Experimental procedures. **127**

Bibliography.....**137-148**

List of Abbreviations.....**149-152**

Abstract

The emerging field of mass spectrometry-based chemical proteomics provides a powerful instrument in the target discovery of bioactive small-molecules, such as drugs or natural products[1]. The identification of their macromolecular targets is required for a comprehensive understanding of their bio-pharmacological role and for unraveling their mechanism of action[1, 2]. Indeed, the target discovery of bioactive molecules endowed with intriguing pharmacological profiles is one of the main issues in the field of pharmaceutical sciences, since this is necessary for a rational development of potential drugs. Nevertheless, several bioactive compounds have been mainly evaluated for their pharmacological effects, whereas the exact mechanism of action at molecular level still remains unknown[3, 4].

Moreover, a complementary point of view about the effect of a small bioactive molecule on a cellular system can be given by label-based quantitative proteomic analysis[5]. Indeed, the identification of biologically relevant changes in the expression of proteins in a cell, after a treatment with a bioactive compound, could help to understand the exact mechanism of action of such active compound.

Here, we report the application of chemical proteomics to the analysis of the cellular interactome of three marine bioactive metabolites, all showing an intriguing anti-inflammatory pharmacological profile, and the application of quantitative chemical proteomics to the platelets activation mechanism by collagen. In more detail, the chemical proteomic approach was applied to Petrosaspongiolide M (PM)[6-8], Bolinaquinone (BLQ)[9-11] and Perthamide C (PRT)[12] target discovery. Thus, these molecules were immobilized onto agarose beads through an α,ω-diamino polyethylene glycol spacer. The

modified beads were then used as baits for fishing the potential partners of the bioactive compounds in macrophages cell lysate. The application of such technique allowed us to identify 20S proteasome, clathrin and endoplasmin (GRP94) as main partners of PM, BLQ and PRT, respectively.

Then, *in vitro* and *in cell* fluorescence assays were developed to assess the effect of PM onto the 20S proteasome enzymatic system, allowing us to measure the inhibition potency of this sesterterpene on the different proteolytic sites of the proteasome machinery.

The BLQ ability to modulate clathrin mediated endocytosis has been assessed through cytofluorimetric and microscopy analysis, suggesting a new application of BLQ as biotechnological tool in the modulation of trafficking pathways.

SPR technology has been employed to prove the ability of PRT to interact with GRP94 and Hsp90, opening the way to further investigations on the role of PRT in the modulation of heat shock protein functions.

Finally, we report the application of quantitative chemical proteomics to discover the effect of collagen on platelet activation. Since cAMP and cGMP plays a key role in platelet activation[13], we combined quantitative chemical proteomics approach with the specific enrichment of cAMP/cGMP signaling nodes[14], to investigate how PKA but also cGMP-dependent protein kinases (PKG) spatially reorganizes in activated human platelets.

Bibliography

[1] U. Rix, G. Superti-Furga. *Nat. Chem. Biol.* **2009**, *5*(9), 616-624.

[2] M. Bantscheff, A. Scholten, A. J. Heck. *Drug Discov. Today* **2009**, *14*(21-22), 1021-1029.

[3] U. Rix, O. Hantschel, G. Durnberger, L. L. Remsing Rix, M. Planyavsky, N. V. Fernbach, I. Kaupe, K. L. Bennett, P. Valent, J. Colinge, T. Kocher, G. Superti-Furga. *Blood* **2007**, *110*(12), 4055-4063.

[4] D. A. Jeffery, M. Bogyo. *Curr. Opin. Biotechnol.* **2003**, *14*(1), 87-95.

[5] J. L. Hsu, S. Y. Huang, N. H. Chow, S. H. Chen. *Anal. Chem.* **2003**, *75*(24), 6843-6852.

[6] J. Busserolles, M. Paya, M. V. D'Auria, L. Gomez-Paloma, M. J. Alcaraz. *Biochem. Pharmacol.* **2005**, *69*(10), 1433-1440.

[7] I. Posadas, M. C. Terencio, A. Randazzo, L. Gomez-Paloma, M. Paya, M. J. Alcaraz. *Biochem. Pharmacol.* **2003**, *65*(5), 887-895.

[8] M. C. Monti, A. Casapullo, C. N. Cavasotto, A. Tosco, P. F. Dal, A. Ziemys, L. Margarucci, R. Riccio. *Chemistry* **2009**, *15*(5), 1155-1163.

[9] R. Lucas, C. Giannini, M. V. D'Auria, M. Paya. *J. Pharmacol. Exp. Ther.* **2003**, *304*(3), 1172-1180.

[10] J. Busserolles, M. Paya, M. V. D'Auria, L. Gomez-Paloma, M. J. Alcaraz. *Biochem. Pharmacol.* **2005**, *69*(10), 1433-1440.

[11] M. C. Monti, M. G. Chini, L. Margarucci, A. Tosco, R. Riccio, G. Bifulco, A. Casapullo. *J. Mol. Recognit.* **2009**, *22*(6), 530-537.

[12] C. Festa, S. De Marino, V. Sepe, M. C. Monti, P. Luciano, M. V. D'Auria, C. Dèbitus, M. Bucci, V. Vellecco, A. Zampella. *Tetrahedron* **2009**, *65*(50), 10424-10429.

[13] U. R. Schwarz, U. Walter, M. Eigenthaler. *Biochem. Pharmacol.* **2001**, *62*(9), 1153-1161.

[14] T. T. Aye, S. Mohammed, H. W. van den Toorn, T. A. van Veen, M. A. van der Heyden, A. Scholten, A. J. Heck. *Mol. Cell Proteomics.* **2009**, *8*(5), 1016-1028.

INTRODUCTION

-CHAPTER 1-

Mass spectrometry-based chemical proteomics: an overview

1.1 Target discovery and "omics" sciences

One of the main purpose of pharmaceutical companies is the finding of new druggable targets, whereas the exact targets of some drugs, actually in clinical or under development, remain unknown. Besides, a lot of compounds show a jumbled pharmacological profile with a modulation of several targets, providing advanced therapeutic effects, particularly for complex diseases . The simplified "one molecule, one target" concept seems to be by now out-of-date[1]. The main advantage for a drug hitting more than one target is the possible application in a plethora of diseases, even if the multi-target interaction could also lead to harmful side effects, reducing the potency and efficiency of the drugs. Thus, the only way to better understand the poly-pharmacological activities and toxicity of a drug is the comprehensive characterization of its target interaction profile inside a complex mixture, such as the cellular environment[2].

The identification of a drug interactome followed by biological assays for the measure of its activity against the identified target proteins, is actually one of the key processes in the drug development process. Several approaches mainly based on protein array and reverse docking have been developed to reach this goal even if gaining only a partial coverage of the full interactome, due to the absence of a biological context.

Recent developments in analytical methods, mainly in mass spectrometry and liquid chromatography, have had an important impact in the field of target discovery. In particular, mass spectrometry-based chemical proteomics has been emerging as a powerful tool to a comprehensive characterization of a drug interactome under physiological relevant conditions. Moreover, such method enables the analysis of the drug mechanism of action, in the context of a complex proteome accelerating the difficult process of target validation and drug discovery[3].

1.2 Chemical proteomics

Chemical proteomics is considered a combination of affinity purification and mass spectrometric identification of a set of proteins targeted (or captured) by a small molecule. It is a multidisciplinary technique, involving different research areas such as biochemistry, cell biology, organic synthesis and mass spectrometry. This technique allows the analysis of all potential targets of a molecule in a single experiment, leading to a complete and selective target mapping of a drug candidate. This means that the drug is able to fish out its own targets directly from the biological sample of interest.

Chemical proteomics approaches include several different experimental procedures, however three of them have emerged as most popular: (i) fishing for partners (or pull down), which employs a ligand immobilized onto a solid support, (ii) global proteomics (quantitative proteomics), in which isobaric tags are used to asses changing in protein concentration upon drug treatment, and (iii) ABPP, activity-based protein profiling, which uses active site-directed probes to record variations in the activity of enzymes in a whole proteome (**figure 1**).

Since the first approach (i) is the main method used in the development of the research projects concerning this thesis, I will focus on it giving some examples which clearly show the success of the technique in target discovery applications.

Rix and co-workers, for instance, applied chemical proteomics to the analysis of imatinib, nilotinib and dasatinib, three BCR-ABL inhibitors[4]. The approach successfully led to the identification of the 30 Tyr and Ser/Thr kinases which bound to dasatinib, and the receptor tyrosine kinase DDR1 as partner of nilotinib. Finally, the oxidoreductase NQO2, the first non- kinase target of these drugs, has been found to bind and inhibit imatinib and nilotinib at physiologically relevant concentrations.

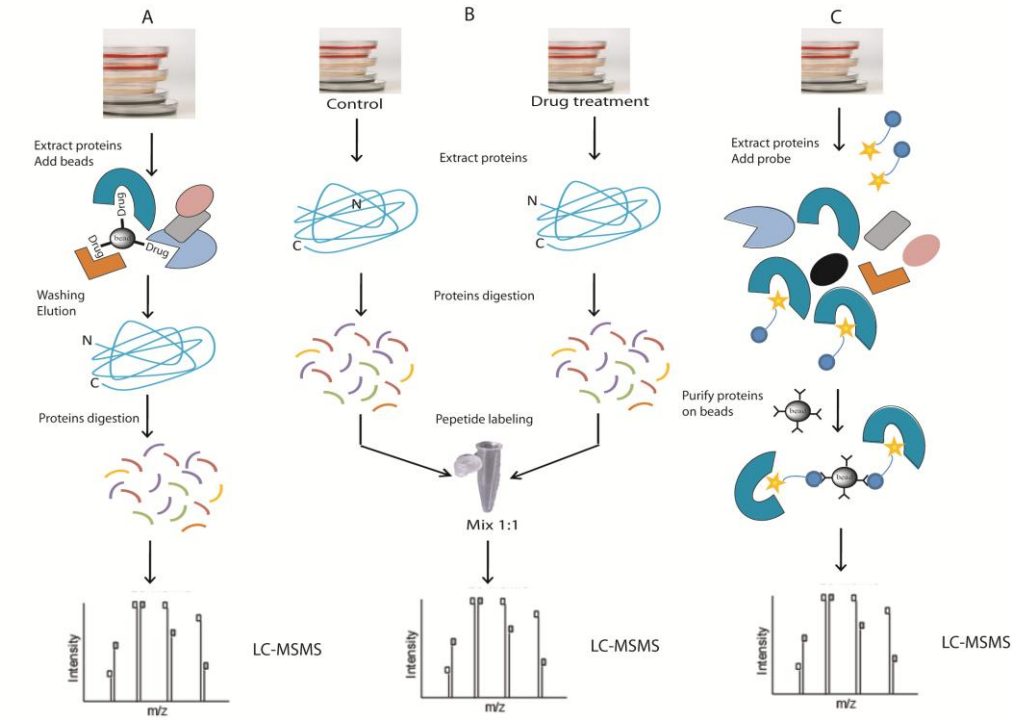

Fig. 1 Experimental workflows of three different approach in chemical proteomics. (**A**) "fishing for partners", the compound under investigation is anchored on a solid support. The immobilized compound is then incubated with a protein sample to fish its specific partners sequentially identify by LC-MSMS. (**B**) Global proteomic approach. Cell cultures (control and drug treatment) are lysed, the obtained proteins digested and peptides analyzed by liquid chromatography coupled to tandem mass spectrometry. The quantification is achieved through stable isotope labeling. (**C**) Affinity-based protein profiling (ABPP) involves the incubation of the cell extract with a probe able to bind only a subset of all proteins. The tagged protein are then recover using affinity chromatography before digestion and LC-MSMS analysis.

Later, pyrido [2,3-*d*] pyrimidine kinase inhibitors have been used as bait to fish out their specific targets from a cell lysate. With this approach, Wissing and co-workers identified more than 30 human protein kinases affected by this class of compounds[5]. The profile of these inhibitors has been clarified, revealing their selectivity for protein kinases possessing a conserved small amino acid residue, such as threonine, in a critical site of the ATP binding

pocket[5]. Again, a chemical proteomic based approach applied to flavopiridol, a CDK inhibitors revealed its ability to bind two additional targets, such as aldehyde dehydrogenase and glycogen phosphorylase[6, 7].
Based on these example, it is clear that chemical proteomics could have a deep impact on the characterization of small molecule biological targets.

1.3.1 Fishing for partners: Outline

The first step in chemical proteomics based experiments consists in enriching the small molecule interactome through a pull down affinity assay. The pull down assay is based on the development of non covalent and specific interactions occurring between the small molecule and its potential binders, and the following purification and mass spectrometric identification of these interacting proteins[3].
In more details, the compound of interest (with known or unknown biological activity) has to be anchored to a solid support through a spacer arm. This matrix is then treated with an opportune lysate, from cells or tissue, to promote the interaction between the bait (the anchored compound) and its specific protein binders. After several washing steps, useful to reduce the amount of non-specific binding proteins, the captured proteins are eluted and subjected to either 1D or 2D SDS PAGE, or gel free chromatography.
The peptide mixtures obtained after trypsin digestion are then submitted to MS analysis (usually nano-LC-MSMS) and database search for the final protein identification.
More in general, the procedure should be divided into three main steps: (i) drug on-beads immobilization, (ii) affinity purification of the interacting proteins and (iii) mass spectrometry identification of the specifically bound proteins, as reported in **figure 2**.

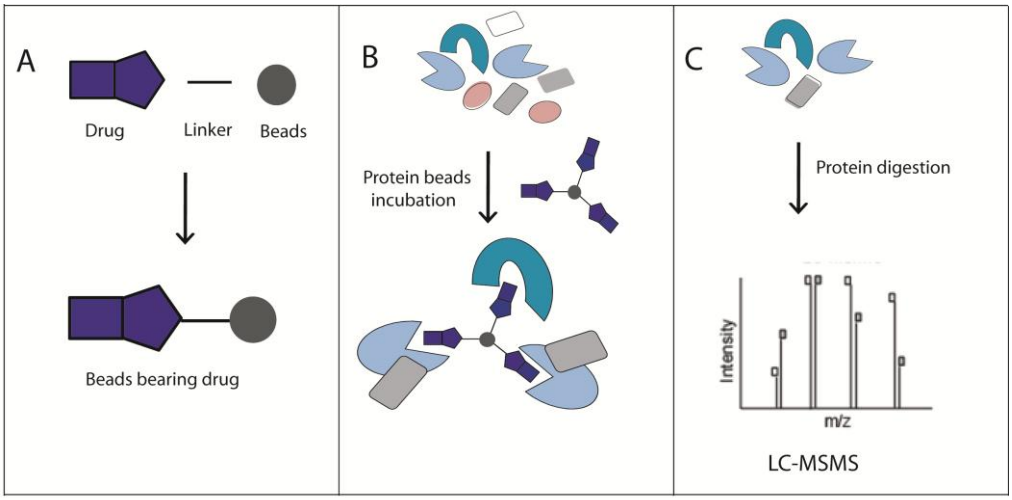

Fig. 2. The three main steps of fishing for partner approach are depicted. (**A**) drug on beads immobilization, (**B**) affinity purification of the interacting protein by the beads bearing drug, (**C**) Mass spectrometry identification of the peptides originating from specifically bound proteins.

1.3.2 "Drug on-beads" immobilization

The drug on-beads immobilization is usually achieved through a set of pre-activated support such as sepharose or agarose. Several activated, able to promote the linkage of specific reactive groups, such as sulfhydryl, amino, hydroxyl, carboxyl or aldehyde resins, are commercially available. One of the main drawbacks of this technique is that only molecules containing one or more reactive sites can be attached to a such solid support.

Otherwise, if synthetic modifications are needed before immobilization, *in vitro* or cell-based assays are required to confirm the activity to be maintained. To avoid or reduce steric interferences between the targets and the ligand-bearing matrix, the solid support is usually modified with an opportune spacer arm. The spacer arm provides an suitable distance between the beads and the small molecule that can enhance the binding efficiency between the

bait and the interacting proteins. Different possible linkers have been described in literature, based on polyethylene glycol (PEG)[8, 9], epoxide [10] (ethyleneglycol diglycidylether) or an aminocaproylaminopentyloxy, skeletons, but more in general the choice is based on the drug chemical structure.

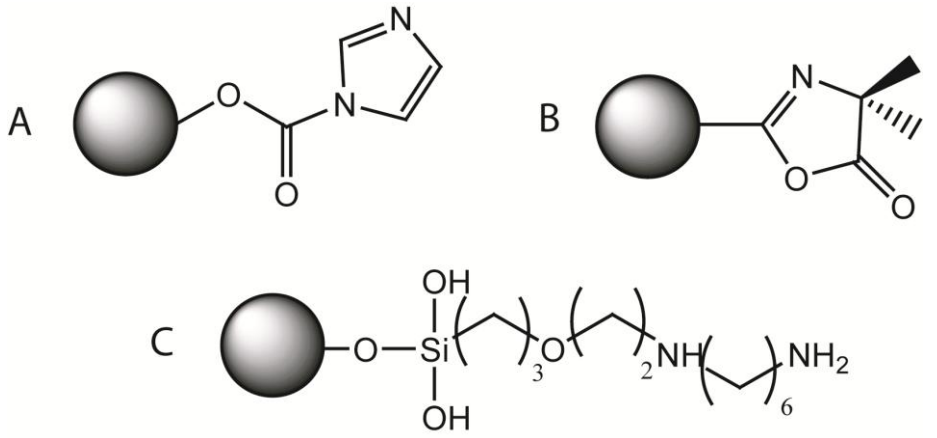

Fig. 3. Matrix bearing three different reactive group. (**A**) 1,1´-carbonyl diimidazole, (**B**) azalactone and (**C**) amino spacer group.

One of the most used is the PEG spacer since it increases the hydrophilicity of the resin reducing the percentage of non-specific binding proteins, while leaving the amount of the specific binders unaffected[11]. On the contrary, a hydrophobic spacer increases dramatically non-specific binding, making much more difficult the following target identification. As a matter of fact, the amount of non specific binding proteins could affect the purification efficiency because they co-elute with the main targets.

Another important factor to take into account is the amount of the immobilized drug used to fish out the interacting proteins. Indeed, an overloading of the drug onto the beads can disturb the interaction between the bait and the putative targets (**figure 4**).

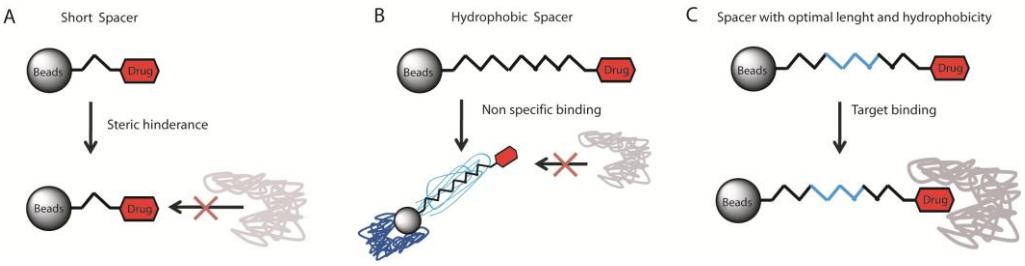

Fig. 4. Effect of choice and positioning of the chemical linker. (**A**) Short spacer linking the matrix and the drug increase the steric hindrance and prevents the drug/target interaction. (**B**) A spacer too hydrophobic generates unspecific interaction increasing the amount of non specific binding and also preventing targets binding. (**C**) An optimal chemical spacer with mild hydrophobicity grade and with the right length avoids steric hindrance and increases targets binding.

On the other hand, a very low immobilization level leaves a high percentage of matrix surface for non specific binding. In general, as reported by Guiffant and co workers[12], 3 μ mol of drug/mL resin is an optimal concentration to minimize the non-specific binding and to increase the specific interactions.
Therefore, the optimization of "on-beads" drug immobilization is the key step of a successful experiment.

1.3.3 Affinity purification of the interacting proteins

Actually, affinity chromatography is one of most powerful technique for the enrichment of specific binders in a chemical proteomics experiment.
The small molecule anchored to the solid support is added to an opportune protein extract, coming from a cell culture, tissue or serum, to promote ligand-protein interaction. After the treatment, the bait-bearing matrix is repeatedly washed to reduce the amount of the non-specific binding proteins and finally the elution of the retained ones is carried on.

The eluted proteins are sequentially separated by gel electrophoresis, *in situ* or *in solution* digested with trypsin, and finally analyzed and identified by HPLC-MSMS and data base search.

The identified proteins could be usually divided into several classes: (i) proteins exclusively interacted with the linker or the beads, (ii) proteins highly abundant with low affinity for the bait, and (iii) proteins with high affinity for the bait. Several approaches to distinguish specific from non-specific binding partners could be employed. One of the main strategy is to perform a parallel experiment using the matrix with only the spacer or an inactive structural analog of the drug, as control. Comparison between the protein lists of the ligand and the negative control experiments provides the identification of non-biologically relevant interactions[13].

In another approach an aqueous solution of the free ligand is added at the end of the experiment to the beads suspension, enabling the release of the specific partners from the beads. This method, often, suffers of the slow dissociation kinetics of the specific binding protein from the ligand anchored on the affinity resin[14].

Furthermore, if the free ligand is added to the protein mixture before the affinity step, it will interact with its partners in solution reducing their binding to the beads (bearing the ligand itself)[14, 15]. Nevertheless, the use of both methods could be limited by the low solubility of the ligand in aqueous solution, which does not contain any organic solvent but high concentration of several salts and reagents to stabilize protein and to mime physiological condition. Dadvar and co-workers successfully applied this approach to the discovery of the interactome of the PDE5 inhibitor, PF-3717842[15]. By applying this method, they were able to enrich for PDE5 and a few other PDEs. Moreover, phosphatidylethanolamine-binding protein 2, a protein involved in various important signal transduction pathways, has been identified and validated as PF-3717842 interactor demonstrating that chemical

proteomic is a valid technique to discover the interactome of small molecule inhibitors.

In 2006 Yamamoto and co-workers[14] described an alternative method to distinguish non-specific and specific bound protein based on a serial affinity chromagraphy approach (**figure 5**).

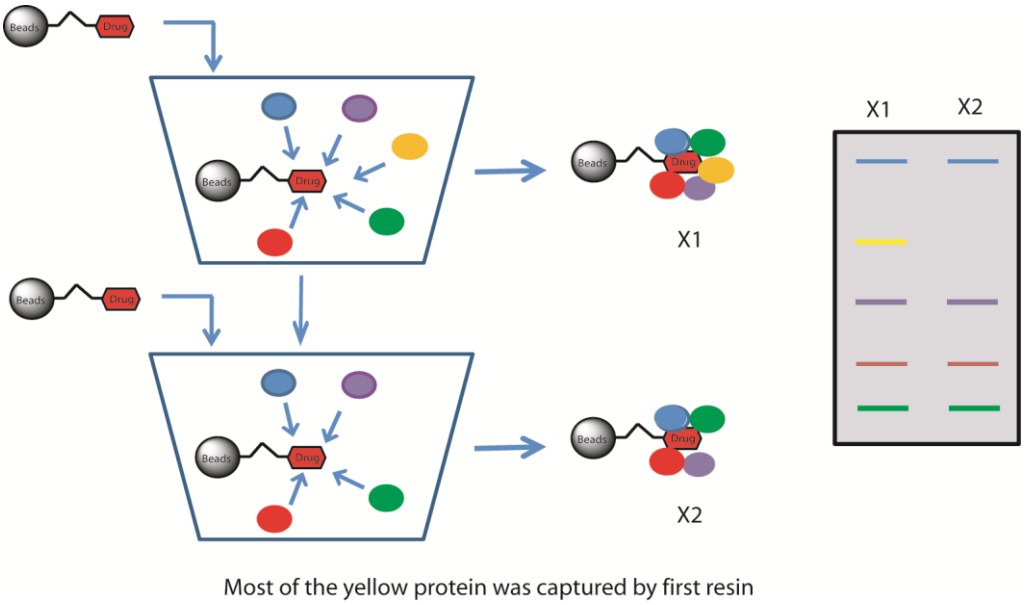

Fig. 5. A schematic comparison of serial affinity chromatography is depicted. In serial affinity chromatography, specific binding protein is usually captured by the first resin (X1) due to its high affinity for the ligand. This causes a large decrease in the amount of protein in the remaining lysate. Therefore, the amount of protein on the second affinity resin (X2) should decrease[14].

The matrix bearing an active compound was incubated with a protein mixture. After the removal of the first beads fraction, the same amount of freshly prepared beads is added to the same lysate.

In this case, both resins should capture almost the same amount of background proteins, while the specific targets preferentially bind the resin in the first chromatographic step instead that in the second one.

Thus, a negative control is not needed even if the method condition can be employed only if the bait-compound shown an high affinity for a specific target. As reported in literature, this approach was successfully applied to three drugs namely FK506, benzenesulfonamide, and metotrexate. All three compounds, immobilized onto a solid support, were subjected to serial affinity chromatography revealing their ability to bind selectively FKBP12, carbonic anhydrase II and dihydrofolate reductase, respectively[14].

1.3.4 Mass spectrometry identification

The key step in proteomics is the identification of the proteins. Actually, two complementary approaches, the "top down"[16, 17] and "bottom up" [17, 18] , have been developed. The top-down proteomics has been introduced several years ago and is based on the fragmentation of the intact protein by tandem mass spectrometry. The fragments are then analyzed giving a direct information on the protein identity. This method is not well established because requires ultra-high resolution instruments and bioinformatics supports, not yet well implemented. The bottom up approach is actually the most popular method in terms of protein identification. It is based on a previous enzymatic digestion of the proteins and the tandem mass spectrometric analysis of the complex peptide mixtures. The most important aspect and probably the main drawback of the bottom up proteomics is the handling and processing of a large amount of data[18].

The usual proteolytic enzyme in bottom up proteomics is trypsin, a protease that cleaves peptides at C-terminus of arginine and lysine residues (**figure 6**).

The peptides originated by proteolytic cleavage have a size less than 3 kDa and a free amino group at C-terminus, and give rise to doubly and triply charged peptides, when exposed to a mass spectrometer.

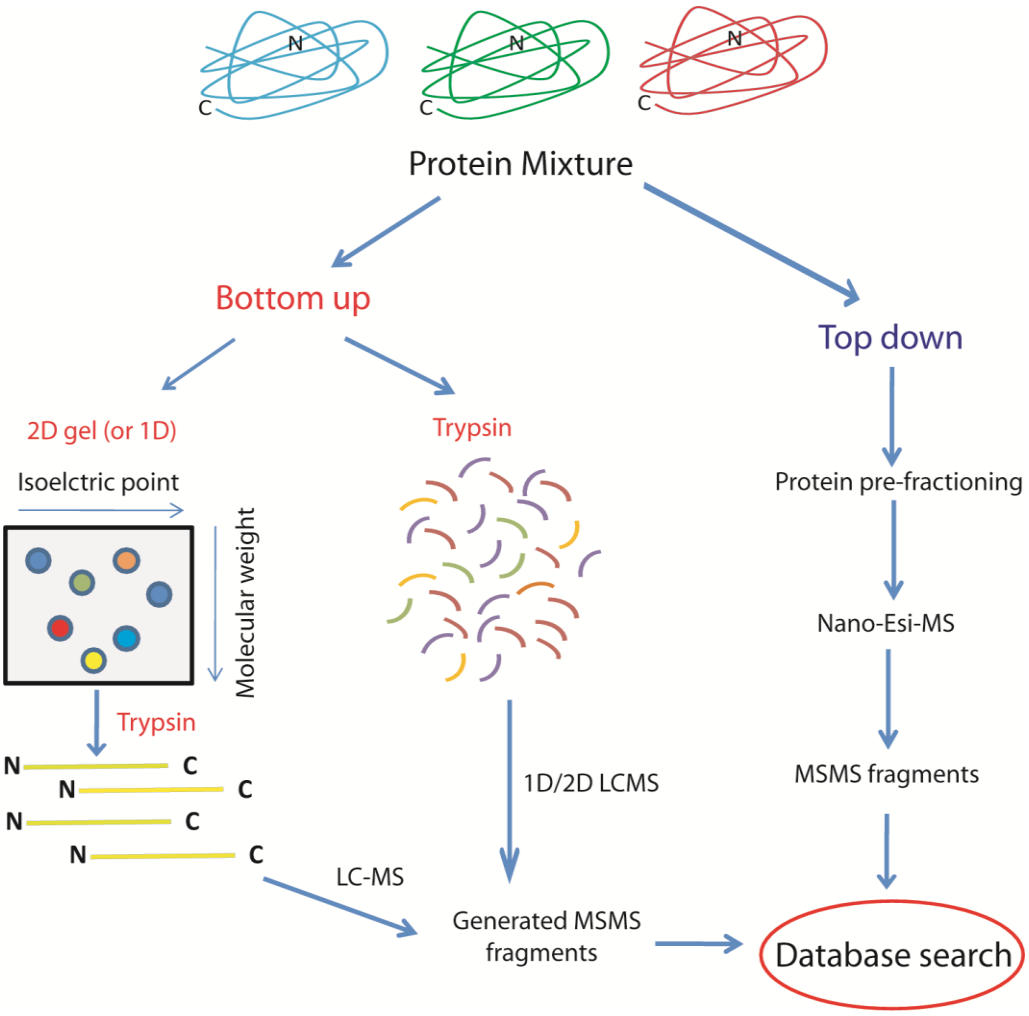

Fig. 6. Schematic representation of bottom-up and top-down proteomics. In bottom-up approach protein identification is achieved through the comparison of the fragmented peptides with predicted tryptic fragments deposited in a public database. In contrast, top-down methods measure fragments originating by intact proteins. In bottom up, one of the method is based on the gel electrophoresis whereas the second method uses two-dimensional liquid chromatography (gel free approach) coupled to mass spectrometry.

The mass spectra of these peptides, especially after CID fragmentation, can be easily interpreted due to their *y* and *b* fragment types. A combination of different proteolytic enzymes, such as Lyc-C and Lys-N, and also the application of different fragmentation techniques, like ETD, can improve

protein identification level. The accurate measurement of the peptides masses could be compared with "in silico" proteolytic fragments reported in public databases. This method, called peptide mass fingerprint (PMF)[19] is mostly used with simple peptide mixtures, for example after digestion of a single protein spot from 2D electrophoresis. The peptides are extracted from the gel and then submitted to MALDI-ToF analysis. Their mass values are then used to reveal the identity of the protein by searching in a database.

With more complex protein mixtures PMF is ineffective, and more information about the amino acid sequence and the exact mass of the precursor peptides are needed before database search[20]. Thus, the peptide mixture is subjected to liquid chromatography coupled tandem MS analysis, and the raw data are processed to give a peak list submitted to a protein search engine.

A number of MS/MS web database exist today[21, 22] but, probably, the most popular one is Mascot[23], which identifies peptides using a probability based algorithm. This web program compares the experimental MS^2 spectra versus theoretical fragment spectra generated "in silico". The search is user dependent, indeed all the parameters like peptide tolerance, proteolytic enzyme, miss cleavage and variable modifications have to be defined.

The search engine collects the identified peptides giving a list of proteins, clustered by score, as output.

1.3.5 Biological assays to test the identified target

Chemical proteomics experiments are indicative of specific interactions, driven by affinity, established between a small bioactive compound and a cellular component. The biological relevance of such interactions in terms of enzyme inhibition or activation ability is an issue to be determined later on and could be considered as a sort of validation of the chemical proteomics

results. If the identified protein is an enzyme, an *in vitro* assay is useful to assess the ability of the ligand to modulate its activity. However, the main purpose is to provide evidence that the physical association between the ligand and the target could affect some biological processes in a living system. This goal can be achieved by measuring enzymatic activity, cell proliferation and apoptosis at a cellular level. In the case of a protein without enzymatic activity, one of the more convincing way to validate proteomics data is to generate quantitative interaction parameters, by measuring protein-ligand affinity with technique like surface plasmon resonance (SPR) or isothermic titration calorimetry (ITC). Nevertheless, the success of both approaches depends on availability of the recombinant and purified protein of interest.
Eventually, it could be very interesting to carried out STD-NMR or co-crystallization[24] experiments to gain information about the protein-ligand interaction mode.

1.4.1 Global proteomics

The aim of global proteomics approaches is the evaluation of the whole cellular response to drug treatment. Cell cultures or primary cell lines are treated with a putative bioactive molecule and the changing in the protein expression level are then evaluated in a global and unbiased fashion[25, 26].
This kind of analysis is usually performed without target enrichment, thus the changes observed are often limited to the most abundant proteins. Sometimes the analysis is more complicated by the fact that the proteins differentially expressed could be unrelated to the pathway modulated by the drug, but often represent only highly abundant proteins.
Moreover, due to the multi-target interaction profile of the drug, several cellular pathways can be modulated upon the treatment, complicating the

proteomic analysis. Global proteomics coupled with target enrichment (targeted quantitative chemical proteomics), allows in the analysis of a specific intracellular pathway and the measurement of low abundant protein amounts, often missed in large-scale studies.

1.4.2 An overview of global proteomics approaches

The analysis of the biological processes or protein expression levels occurring upon a drug treatment can be done using qualitative or quantitative based approaches. The qualitative approach is only able to assess the presence or absence of a specific protein failing in profiling dynamics of protein expression. In this cases a quantitative approach is required.
In the last years, plethora of techniques have been proposed with the aim of "absolutely" quantifying differences between two (or more) physiological states of a cell system[27-29].Essentially, the global chemical proteomics approaches can be divided into two main classes: (i) label-based chemical proteomics, in which proteins or peptides are labeled with differential isotopic tag (SILAC, ICAT[31], iTRAQ[32] or dimethyl labeling[33]), and (ii) label-free based approaches, in which protein abundance is extimated by peptide counts. In the next paragraph the label-based approach will be deeply discussed as part of this thesis, while only a small section will be dedicated to the label-free techniques.

1.4.3 Label-based global proteomics

The most used method to quantify different protein levels in different samples is the application of the differential isotopic labeling[27] (f**igure 7**).

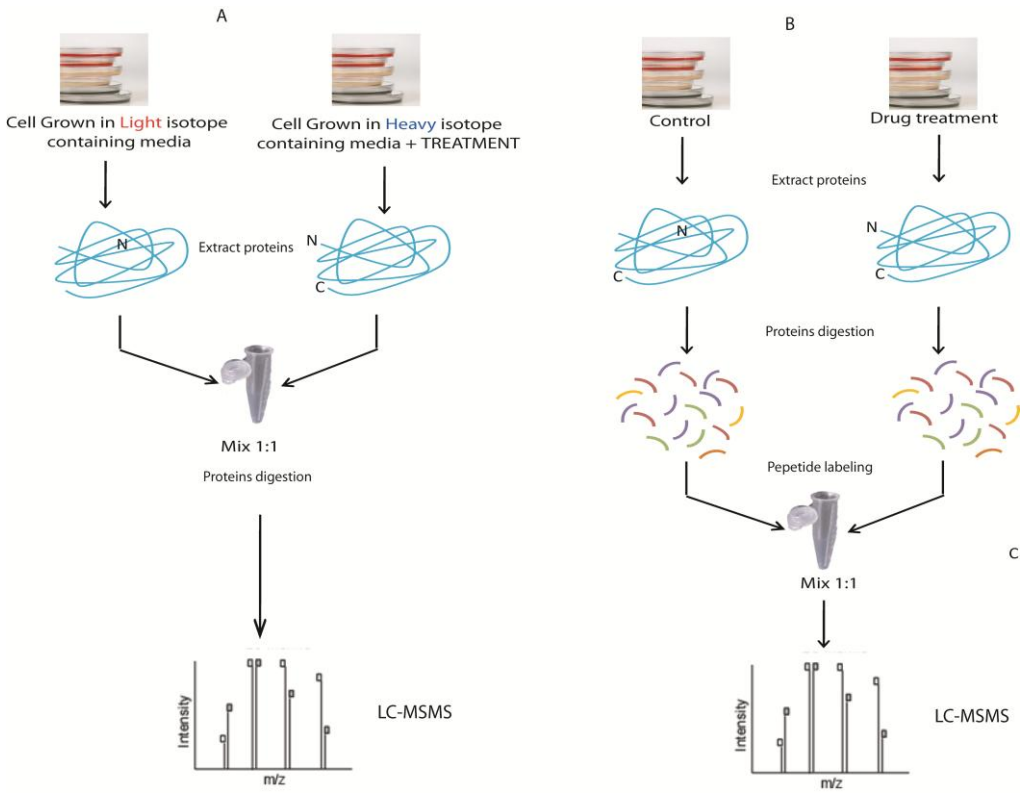

Fig. 7. Schematic representation of metabolic and chemical labeling. (**A**)Metabolic labeling (SILAC). Cells are grown using a media containing respectively SILAC light and SILAC heavy aminoacids; after 100% label incorporation, heavy-labeled cells are treated with the compound under investigation for 24 hours. Cells from each sample are lysed, the obtained protein mixed and analyzed by LC-MSMS after protelytic digestion. (**B**) Chemical labeling. Cells subjected tosolvent and drug treatment are separately lysed to give a protein sample, then digeste using a proteolytic anzyme. The obtained peptides are labelled by iTRAQ or dimethyl labelling, mixed and analyzed by LC-MSMS.

Nowadays, stable isotope labeling can be performed at protein and peptide levels. In both cases, two cell samples (one of them treated with a drug) are differentially exposed to different isotopes. This method allows the analysis of two (or more) biological samples in a single analytical experiment, and the quantification of the proteins simply by comparing their relative peptide ions abundance[28]. The strategies for introducing heavy isotopes into protein

samples make use of metabolic or chemical labeling (f**igure 7**). The stable isotope labeling by amino acids in cell culture (SILAC) is a metabolic labeling which employs *in vivo* incorporation of stable isotopes (auxotrophic amino acids)[30].The amino acids are supplied in either their natural or in a stable isotope form to two cell medium to facilitate their incorporation in the protein sequence. One of the cell culture is then subjected to drug treatment and both are finally lysed to give two proteins mixture. The differentially labeled samples are mixed before protease digestion (usually with trypsin) and then subjected to MS analysis and quantitation.

In another experiment, an isotope tag can be chemically attached onto a specific aminoacid at either protein (ICAT)[31] or peptide (iTRAQ)[32] level.

The quantitation through iTRAQ labeling is based onto the reaction of the free amino group of a peptide with N-hydroxysuccinimide esters containing either light or heavy isotopes. Nevertheless, the cost of the iTRAQ reagent and the request for a mass spectrometer able of measuring MS/MS fragments at very low *m*/*z* have limited the use of this technique.

An useful technique for labeling at peptide level is the so-called stable isotope dimethyl labeling[33, 34]. It is virtually applicable to any kind of samples and it is less expensive if compared to the other labeling methodologies, and will be discuss more in detail in the next paragraph.

1.4.4 Stable isotope dimethyl labeling

This method is based onto the condensation of a primary amine (e.g. the free amino terminal group of a peptide) with an aldehyde (or ketone) in presence of reducing agent[33]. Therefore, the peptides are converted in a mixture of N,N-dimethylamino peptides by treating the sample with formaldehyde and cyanoborohydride. Formaldehyde can react with the primary amino group or

epsilon amino group of a peptide side chain giving a Schiff base, then reduced to a secondary amine by cyanoborohydride. An extra reductive alkylation occurs immediately after the formation of the secondary amine, giving a tertiary amine. By combining different isotope of formaldehyde, a minimum of 4 Da difference between two samples could be gained[35]. In more details, each peptide could be labeled at the N-termini or at ε-amino group of lysine residues with light (d0) or heavy (d2) formaldehyde originating an increase in mass of 28 Da and 32 Da respectively.

A third label employs the treatment of peptides mixture with ^{13}C-labeled (d2)-formaldehyde and cyanoborodeuteride leading to a mass increase of 36 Da[34, 35] (**figure 8**).

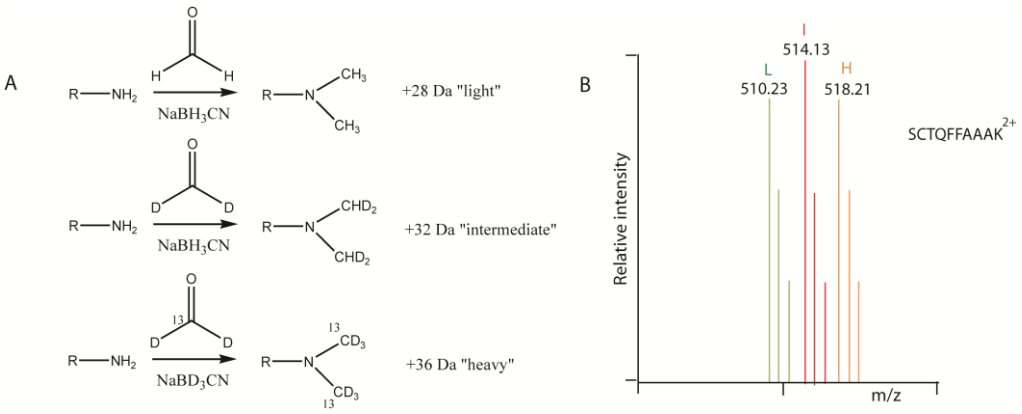

Fig. 8. (A)Triplex stable isotope dimethyl labeling, (B) Mass spectrum of the triplet of the labeled isotopomers of the same peptide (the light, intermediate and heavy labeled peptides are indicated in green, red orange, respectively).

In a mass spectrometer, the chemical peptide labeled with heavy reagents will lead to a mass shift when compared with the light labeled peptide. Therefore, the intensity of the peaks in the mass spectrometer is directly connected with the relative abundance of the peptides (and of the proteins for inference) in the original samples (**figure 8**). The stable isotope dimethyl labeling opens the

way to analyze three different samples, allowing the quantification of their protein expression levels in a single LC-MS run[36]. Compared with other labeling technique, stable isotope dimethyl labeling can be used with any kind of biological samples. Moreover, the labeling reaction is quick, the reagents are relatively stable and cheep and it is a high throughput method[37].
Finally, this tagging approach could be performed also on intact proteins, even if the main drawback is the choice of the protease, since trypsin and Lys-C are not able to cleave modified lysine residues.

1.4.5 Protein identification and quantitation

An important point in performing a correct global proteomics experiment is strictly connected with the mass spectrometer performances. As already discussed, the heavy and light labeled peptides are mixed and analyzed by mass spectrometry in a single analysis.
The correct assessment of the mass differences between the light and heavy peptides requires a high-resolution mass spectrometer, with Time-of-flight, Fourier Transform Orbitrap or Fourier Transform Ion Cyclotron Resonance, analyzers, capable of determining peptide precursor charge states and fully resolving all ions. These instruments can measure peptide masses and induce fragmentation (tandem MS) for determination of their amino acid sequence at high resolution. The protein identification is given by matching the MS/MS spectra against theoretical spectra generated in protein databases, such as MASCOT[23] and SEQUEST[38]. These databases are accessible on the Web and use different algorithm to score identified proteins through the identification of peptide bearing different kind of labeling. After protein identification, quantification could be achieved by comparing the peak areas of the differentially labeled peptide ions. This operation can be done manually,

even if software packages, like Mascot Distiller or open source software such as MSQuant[39] (http://msquant.sourceforge.net/), are preferred.

1.4.6 Label free based approaches

Recently, it has been observed that the number of MS/MS counted during a LC-MSMS run is connected to the protein abundance. Thus, the proteins with high concentration produce more MS/MS spectra when compared with proteins less abundant[40].

Based on this evidence, label-free based approaches have been developed to estimate the protein abundance between two different biological samples[41]. In this approach, usually named "spectral counting", samples are analyzed and processed separately and the identified proteins are compared in term of number of assigned spectra per protein.

Despite in literature this method is considered as accurate, it fails when only small changes occur between two proteins[42].

1.5 ABPP: activity based protein profiling

ABPP is a functional proteomics technology which employs chemical probes specifically designed to react with one class of enzyme[43]. An ABPP probe consists of two elements: a reactive group containing an electrophilic site, designed to react with a nucleophilic residue in the active site of an enzyme, and a tag which is the reporter, like a fluorophore or biotin group[44, 45].

These radioactive groups (fluorophores) or even affinity tags (biotin), can be used as reporters to detect their targets by activity-based probes[13]. The approach is essentially based on the fact that the ligand under consideration

will interact with its targets reducing the ability of the probe to reveal (fluorofore) or enrich (biotin) the enzyme itself [46] (**figure 9**).

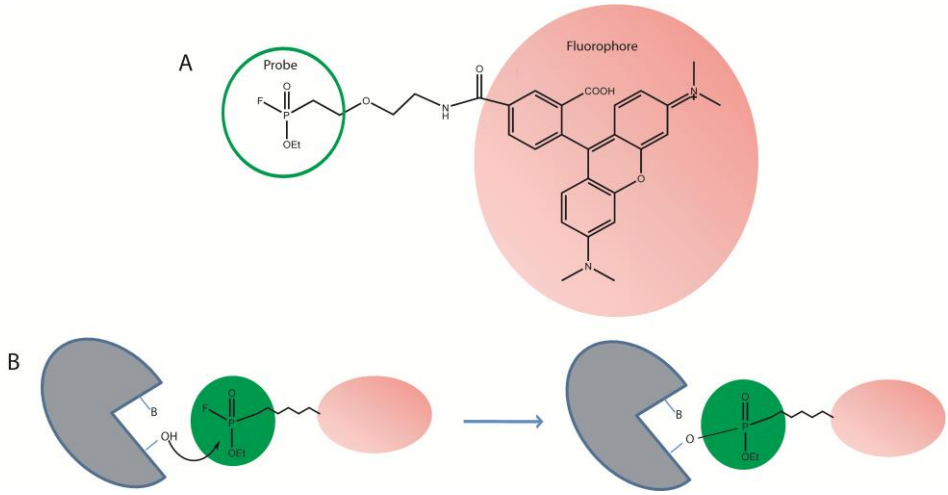

Fig. 9. ABPP based approach (A) Structure of a probe, and (B) Reaction between probe and target enzyme. The fluorescence tag allow the enzyme detection.

The major advantage of ABPP is the ability to directly monitor the availability of the enzyme active site. The combination of tandem mass spectrometry with ABPP enables the identification of hundreds of active enzymes from a single sample and it is mainly useful for profiling inhibitor selectivity against hundreds of targets simultaneously.

1.6 Scope and outline of this thesis

Several of the drugs commercially available today are natural products obtained from plants, from marine sponges and microorganisms[47]. Indeed, nowadays natural products isolated from marine sources are emerging as potential drug for a plethora of diseases[48, 49]. The sponges are one of the main

source of marine natural products, since they have developed an ability to produce secondary metabolites as a defense mechanism against their predators[48], and these compounds may have relvant bioactivites and applications in human diseases.

Petrosaspongiolide M (PM)[50], Bolinaquinone (BLQ)[51] and Perthamides (PRT)[52] are examples of bioactive marine metabolites with a relevant effect in experimental models of acute or chronic inflammation.

PM and BLQ exert their pharmacological activities through the phospholipase A_2[51, 53, 54] inhibition, as well as through the control of nuclear factor-kB activation and NO syntase[50, 55-57], while the exact mechanism of action of PRT, in acute inflammation, is currently under investigation.

The pharmacological properties showed by these metabolites seem not be related to a single enzyme inhibition, for instance $sPLA_2$ or NF-kB.

Thus, a fully investigation of their interactome has been considered of a broad interest to better understand their mechanism of action and potential multiple effects.

As reported previously, the only way to better understand the drug's poly-pharmacological activities and toxicity is a comprehensive characterization of the drug interaction with cellular components.

Therefore, the primary purpose of the projects involved in my PhD thesis has been a comprehensive characterization of the interactome profile of the above mentioned marine metabolites. I have applied a chemical proteomics-based approach to discovery the main cellular partners of each compound validating all the results through biological assays.

In **chapter 2** the determination of the interactome of Petrosaspongiolide M is described. This metabolite has been anchored to a solid support to fish out its proteins partners from a complex cell lysate. The 20S proteasome has been identified as main partner. *In vitro* and *in cell* fluorescence assays have assessed the effect of the free metabolite onto the proteasome enzymatic

system. The results have clarified Petrosaspongiolide M effects at NF-KB level.

In **chapter 3** the same approach has been applied to the analysis of the interactome of the marine metabolite Bolinaquinone. In this case clathrin, an "unexpected" target not directly connected with the BLQ anti-inflammatory properties, was identified. The BLQ ability to modulate clathrin mediated endocytosis has been assessed trough cytofluorimetric and microscopy analysis, suggesting a new application of BLQ as biothecnological tool in the modulation of trafficking pathways.

In **chapter 4** Perthamide C, a novel cyclopeptide showing anti-inflammatory properties, has been analyzed by chemical proteomics and Endoplasmin, an endoplasmic reticulum heat shock protein, has been identified as its main partner.

Finally, to expand my knowledge in chemical proteomics-based approaches, I have applied quantitative chemical proteomics to discover the effect of collagen on platelet activation. Since cAMP and cGMP play a key role in platelet activation, I have described, in **chapter 5**, the combination of quantitative chemical proteomics approach with the specific enrichment of cAMP/cGMP signaling nodes, with the aim to understand how PKA but also cGMP-dependent protein kinases (PKG) spatially reorganizes in activated human platelets.

RESULTS AND DISCUSSION

-CHAPTER 2-

Chemical Proteomics Discloses Petrosapongiolide M, an Antiinflammatory Marine Sesterterpene, as a Proteasome Inhibitor

Based on: *Angew. Chem. Int. Ed*. **2010**, 49, 1 – 5

2.1 Gone Fishing: Petrosaspongiolide M

Marine sesterterpenes containing γ-hydroxybutenolide moiety have been studied for their potent anti-inflammatory activity since the discovery in 1980 of manoalide, which is considered the reference compound in this research field [58]. Since then, a number of γ-hydroxybutenolide-containing metabolites have been isolated, for instance luffariellolides, luffariellins, luffolide, cacospongionolides and petrosaspongiolides, each capable of irreversible inhibition of PLA_2[59, 60].

Among the γ-hydroxybutenolide-containing compounds, Petrosaspongiolide M (**PM**, **figure 10**) has been subjected to a comprehensive *in vitro*[61] and *in vivo* [62] pharmacological investigation. In more detail, PM shows an IC_{50} of 0.8 μM toward human synovial PLA_2[63, 64] and is able to reduce the levels of prostaglandin E2, tumor necrosis factor α, and leucotriene B4 in a dose-dependent fashion[62, 65].

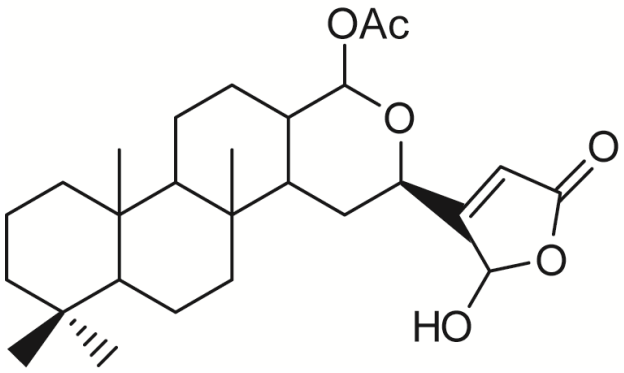

Fig. 10. Chemical Structure of Petrosaspongiolide M.

In addition, an in-depth pharmacological investigation has revealed that PM also interferes with NF-κB pathway, strongly decreasing NF-kB–DNA binding[62]. Nonetheless, whether PM exerts its pharmacological effects through binding and/or modifying specific proteins remained unknown[62].

Since the NF-kB pathway plays a crucial role in the development of the inflammation response, it would be desirable to identify the primary PM partners, suitable as potential therapeutic targets. To reach this goal, a chemical proteomic strategy, using affinity chromatography coupled with mass spectrometry, has been applied to macrophage cell proteomes[66-68].

From an experimental point of view, our work can be divided into the following steps: (i) chemical immobilization of PM on a solid support; (ii) incubation of PM-modified beads with cell lysates; (iii) MS identification of PM interactors; (iv) determination of physical interaction between PM and the identified partners; (v) evaluation of PM bioactivity *in vitro* and in living cells.

2.2 Chemical immobilization of PM on a solid support

The chemical immobilization of a small molecule ligand is usually achieved through suitable functional group. PM was anchored onto a solid support, taking advantage of its electrophilic functional group, the masked aldehyde on the γ-hydroxybutenolide ring.

We selected a Reacti-Gel (6X) matrix beads consisting of agarose activated by 1-1'-carbonyl-di-imidazole functions. In addition, to the introduction of a spacer between PM and the Reacti-Gel (6X) beads was necessary to avoid possible steric hindrance between the macromolecular target(s) and the immobilized ligand. A set of possible linkers, such as 1,5-di-amino-pentane (DAP), 1,12-di-amino-dodecane (DAD), 4,7,10-Trioxa-1,13-tridecanediamine (PEG), different in terms of length and hydrophilic properties, have been tested to minimize non-specific protein binding and maximize purification efficiency. The linkers were bound to the matrix via nucleophilic attack of their terminal amino group onto the carbonyl function of Reacti-Gel (**figure**

11). The linker-bearings matrix were then subjected to Kaiser test, prior PM immobilization, to verify the presence of free NH_2 function on the beads.

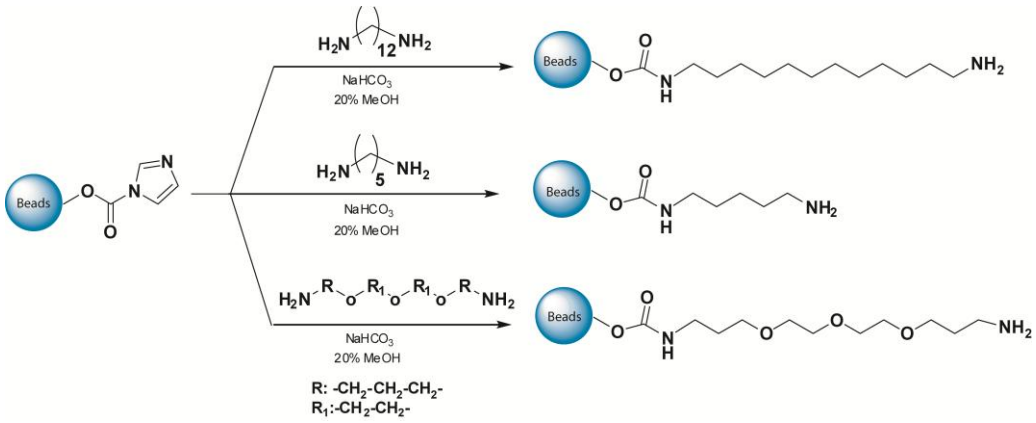

Fig. 11. Reaction scheme of the beads with 1,12-di-amino-dodecane, 5-di-amino-pentane, and 4,7,10-Trioxa-1,13-tridecanediamine.

Then, PM was treated with the amine-modified beads to obtain PM-DAP-beads, PM-DAD-beads and PM-PEG-beads, respectively. As reported in **figure 12**, the imine bond occurring between the masked aldehyde at C-25 of PM γ-hydroxybutenolide ring and the free amino group of the linker was selectively reduced by $NaBH_4$.

The experimental conditions (buffer, pH, reaction time and temperature) were optimized in order to reach a final concentration of 1.8 μmol drug/mL resin, as reported in literature[69].

The yield was calculated by the integration of RP-HPLC peaks relative to the PM concentration before and after the treatment with the different beads. The coupling process was completed by blocking the remaining active groups with acetic anhydride.

As a control, a portion of the activated Reacti-Gel (6X) support was mixed with the three different diamines and the free amino groups were capped with acetic anhydride.

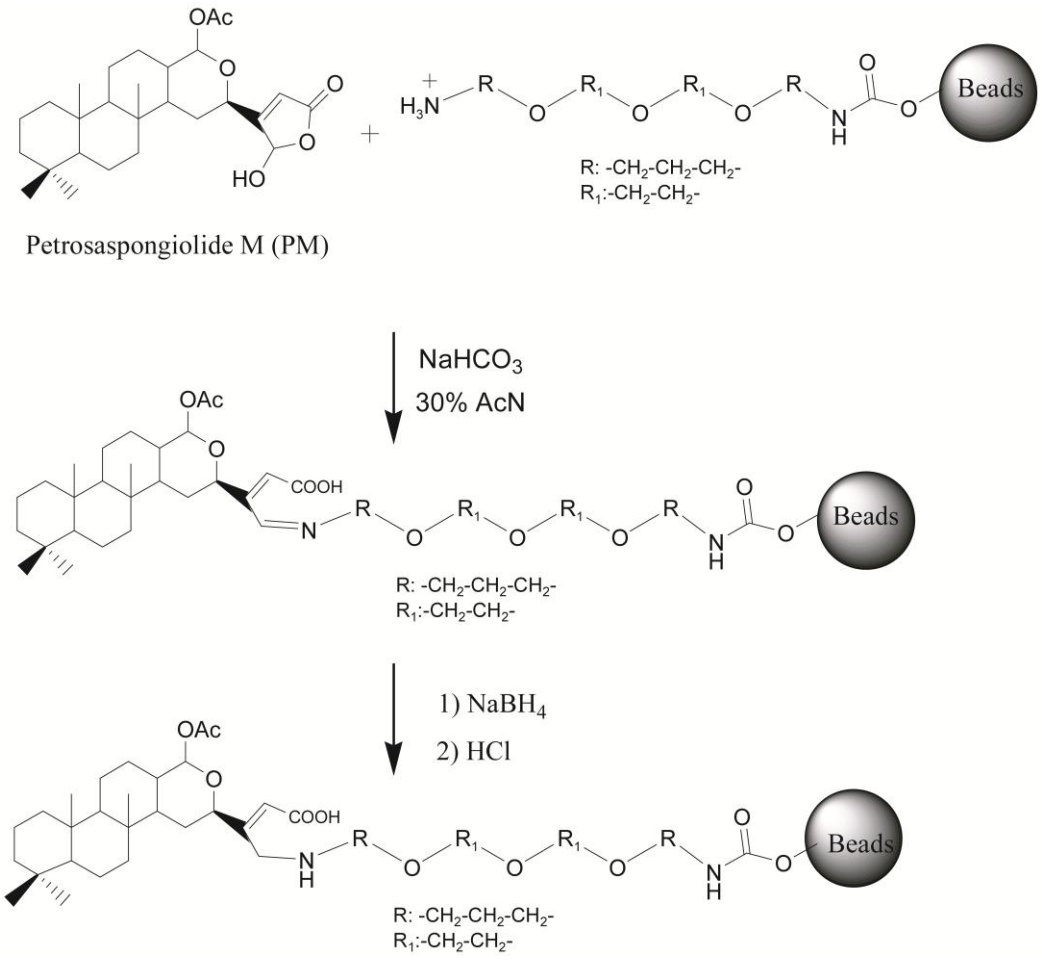

Fig. 12. Preparation of PM-modified beads.

2.3 Affinity purification of PM interacting proteins

2.3.1 Cell lysate

Since PM has been investigated for its anti-inflammatory properties, we selected the same model system for our analysis[62].

Thus, THP1 monocytic cells were differentiated in macrophages by treating them with phorbol ester (PMA) upon LPS treatment to induce an

inflammatory response. Finally, the cells were scraped out and lysed to obtaine the whole cell lysate used for the following affinity purification experiments.

2.3.2 Affinity purification and mass spectrometry analysis of PM partners

Before starting PM target purification, we evaluated the effects of the above mentioned spacers on the non-specific protein binding level. Indeed, non-specific binding of cellular proteins to affinity matrices is a significant limitation to this approach, and the reduction of such binding is an important outcome. Thus, we compared the gel electrophoretic profile of PM-DAP-beads, PM-DAD-beads and PM-PEG-beads after the incubation with the THP-1 cell lysate (**figure 13**).

The resin bearing hydrophilic PEG spacers showed a moderate degree of nonspecific binding proteins, when compared with the other samples, and was then used in the affinity purification step (**figure 13**).

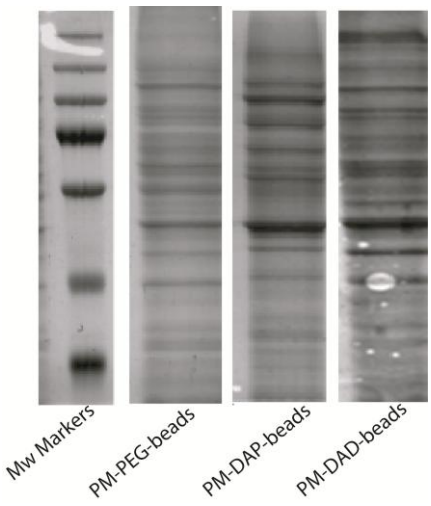

Fig. 13. Electrophoretic profile of PM beads bearing three different spacer arm. The amount of total proteins eluted is reduced by beads modification with hydrophilic PEG spacers.

The crude cell extracts of LPS induced THP-1 were treated with the PM-PEG-beads to promote the interaction between PM and its potential partners in the cell lysate. Cell extracts were also incubated with a PM free matrix, as a control experiment, to distinguish between specifically bound components and background contaminants.

After extensive washings, the PM interacting proteins were released from the resin by elution with SDS-gel loading buffer. The protein mixtures were then resolved by SDS-PAGE[70, 71], and the gel lanes, of the PM beads and control experiments were cut in 13 pieces, digested with trypsin, and analyzed by mass spectrometry through nanoflow reversed-phase HPLC MS/MS (**figure 14**).

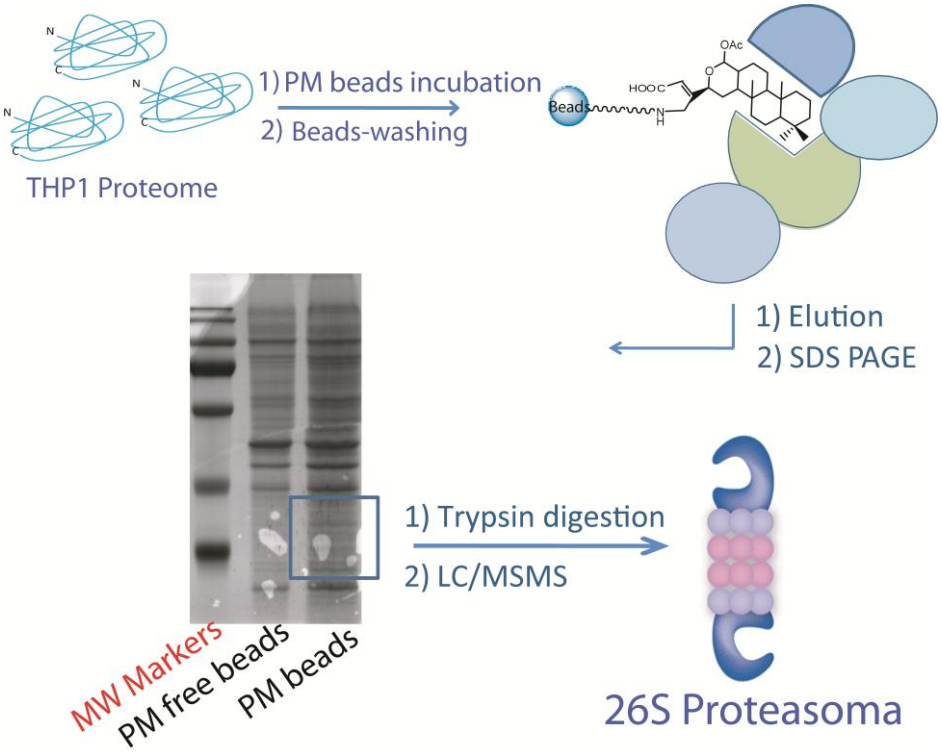

Fig. 14. Representation of the chemical proteomic experiments applied to the discovery of PM targets. The proteins retained in the PM-affinity step were eluted from the support, subjected to SDS PAGE separation, digested *in situ*, and identified by mass spectrometry.

Doubly and triply charged peptide species obtained in the conventional MS spectrum were fragmented, and all the MS/MS spectra converted into a peak list. All peak lists were then submitted to a Mascot database search for the protein identification.

2.3.3 PM interactors

The outcome of the Mascot database search revealed the whole interactome of PM. A list of identified proteins, from both gel lanes (control and matrix bearing PM), was obtained and compared to establish which proteins were specifically captured by PM. As reported in the Venn diagram (**figure 15**), 325 proteins were observed in both experiments while 29 only were exclusively identified in the binding experiment (**figure 15**).

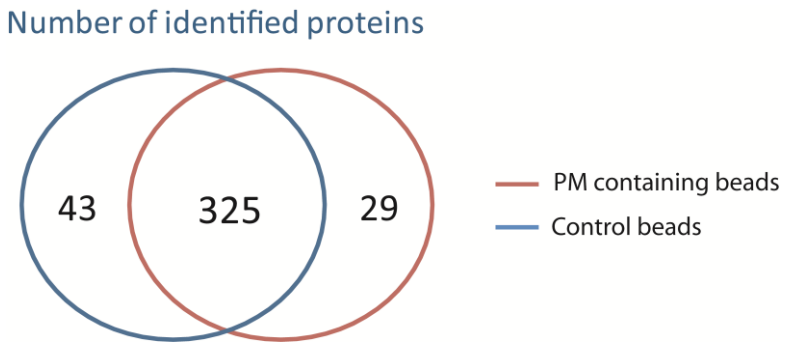

Fig. 15. Venn diagram showing the number of proteins identified in either or both binding experiments.

These proteins were considered as potential PM interactors (**table 1**). Several of the proteins reported in Table 1 are highly expressed in THP-1 cells[72], and their presence, typical in this kind of analysis, is due mostly to their abundance rather than to a real affinity to the ligands[67, 72].

SwissProt Code	Identified proteins	Mw (KDa)	Sequence Coverage	No of Queries	Unique Spectra	SCR
Proteasome Machinery						
PSME2_HUMAN	Proteasome activator complex subunit 2	28	55%	20	10	471
PSME1_HUMAN	Proteasome activator complex subunit 1	26	10%	3	2	161
PSA2_HUMAN	Proteasome subunit alpha type-2	25	8%	5	2	149
PSA4_HUMAN	Proteasome subunit alpha type-4	29	28%	6	5	101
PSA5_HUMAN	Proteasome subunit alpha type-5	26	31%	7	5	119
PSB1_HUMAN	Proteasome subunit beta type-1	26	5%	2	1	47
PSB4_HUMAN	Proteasome subunit beta type-4	29	28%	6	4	79
PSA7_HUMAN	Proteasome susunit alpha type-7	27	23%	5	4	89
PRS6B HUMAN	26S protease regulatory sub 6B	47	12%	6	2	48
Cytoskeletal						
ARP3_HUMAN	Actin-related protein 3	47	11%	9	4	178
ACTN1_HUMAN	alpha-actinin-1	103	9%	5	4	237
Ras-related protein						
RAC2-HUMAN	Ras-related C3 botulinum toxin substrate	21	22%	9	5	120
RAB14_HUMAN	Ras-related protein Rab-14	23	23%	5	3	119
RAB1B_HUMAN	Ras-related protein Rab-8B	22	17%	6	3	177
RAB5C_HUMAN	Ras-related protein Rab-5C	23	40%	8	6	100
Kinases						
NDKA_HUMAN	Nucleoside diphosphate kinase A	17	11%	3	2	42
NDKB_HUMAN	Nucleoside diphosphate kinase B	17	10%	4	3	38
Oxidative stress proteins						
PRDX6_HUMAN	Peroxiredoxin-2	25	14%	10	2	219
PRDX3_HUMAN	Thioredoxin-dep peroxide reductase	27	14%	5	3	73
Ribosomal proteins						
R13AX_HUMAN	60S ribosomal protein L13a-like	12	10%	2	2	129
EF1A_HUMAN	Elongation factor 1-alpha	50	21%	8	4	111
Others						
ENPL_HUMAN	Endoplasmin	92	8%	10	7	237
SYG_HUMAN	Glycyl-tRNA synthetase	83	14%	6	4	81
IFIT1_HUMAN	Interferon-induced protein	55	22%	12	7	286
PDIA6_HUMAN	Protein disulfide-isomerase A6	48	13%	7	4	266
1433E_HUMAN	14-3-3 protein epsilon	29	25%	10	5	251
DECR_HUMAN	2,4-dienoyl-CoA reductase	36	46%	21	11	380
VIME HUMAN	Vimentin	53	15%	5	5	74

Tab. 1. Proteins identified as PM interactors (clustered by function).

We were particularly intrigued by the presence of several components of the proteasome enzymatic machinery, since the ubiquitin–proteasome system (UPS) is responsible for the degradation of most intracellular proteins, including those that control cell cycle progression, apoptosis, signal transduction, and the NF-kB transcriptional pathway[73-75]. As these findings were strictly connected with the previously reported pharmacological evidence[62], we performed an in-depth investigation on the biological role of PM in the interaction with the proteasome machinery, through *in vitro* and in living cells assays.

2.4 Characterization of physical interactions between PM and 20S proteasome

Surface plasmon resonance (SPR) Biacore technology was employed to quantify the interactions of PM with the human recombinant 20S proteasome[76]. SPR is an optical technique, based on the evanescent wave phenomenon, able to measure changes in refractive index onto a sensor surface, and it is suitable for characterizing macromolecular interactions[77-79]. The binding between a compound in solution and its ligand immobilized on the sensor surface results in a change of the refractive index, that could be monitored in real time allowing the measurement of association and dissociation rates.

We attempted to measure the kinetic dissociation constants between PM and the 20S proteasome by anchoring PM onto the chip surface through a di-amine PEG spacer (PEG). More in details, the PEG spacer, containing an NH_2 group coupled with a trityl group (trt), was bound onto the chip surface pre-activated by EDC/NHS. The trt group was removed by injection of 1% TFA solution, to give a free amine group able to react with the PM aldehyde function.

Indeed, PM was injected on the chip surface, and the Schiff base formed between the masked aldehyde on PM and the free amino groups on the chip, was then reduced by $NaBH_4$ (**figure 16**). The PM immobilization was assessed by measuring an increase of response units (RU) of 800 on the SPR trace.

As additional test to prove the PM immobilization, a sample of bee venom PLA_2, a well known PM interactor[80], was injected onto the chip surface and a strong binding (K_D in the low nano molar range) was calculated that gave us the confidence of a successful ligand immobilization.

Then, different concentrations of 20S Proteasome (1 to 100 nM), in presence or absence of its activator PA28[81], were injected over the PM-modified sensor chip.

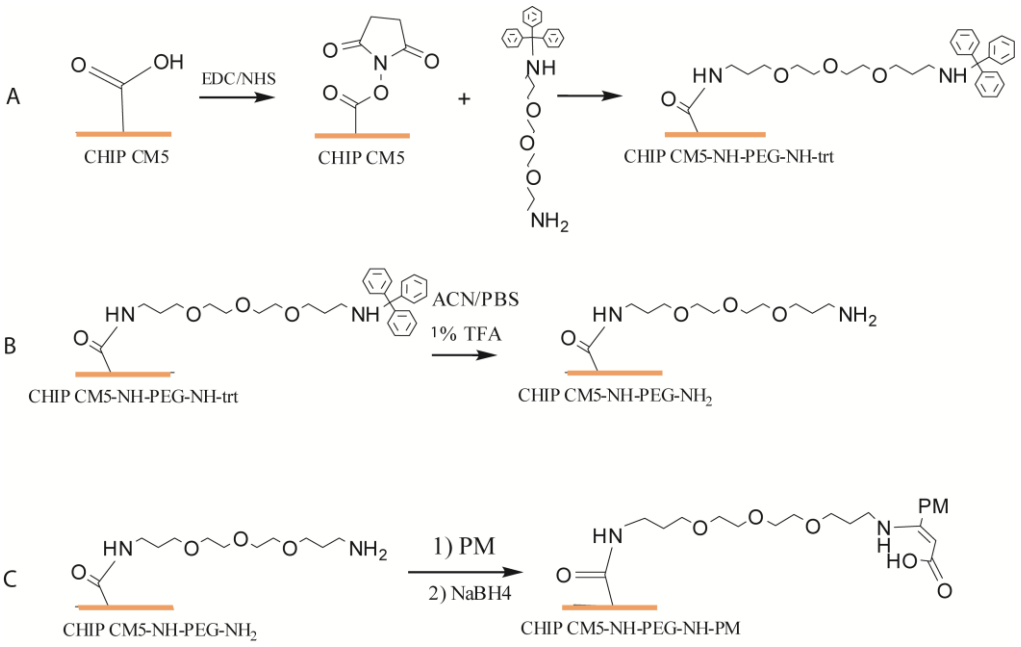

Fig. 16. PM on chip immobilization**.** (**A**) Sensor surface activated with EDC/NHS mixture has been modified with trt-NH-PEG-NH_2; (**B**) To give a free amine a solution containing 1% TFA has been injected onto the chip surface; (**C**) The free amine on chip surface reacts with PM aldehyde and was reduced by $NaBH_4$.

In **figure 17** are shown the sensograms detected after the binding of 20S-PA28 complex to PM, at two different concentrations. The increase of response units (RU) in the association phase and the slope of the dissociation phase of the complex are clearly dependent on the analyte concentration.

Association and dissociation rate constants were determined, and equilibrium binding constants (K_D) of 8 (±3.1), and 0.7 (±1.1) nM were calculated for 20S and 20S-PA28 complex respectively, demonstrating the strong interaction occurring between the marine metabolite PM and proteasome subunits.

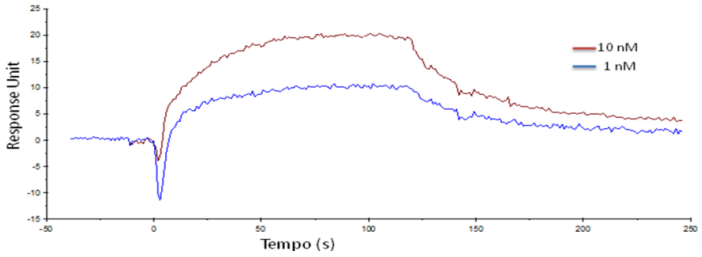

Fig. 17. Sensograms obtained from the binding of PM to 20S-PA28 in presence of $CaCl_2$ at two different concentrations.

2.5 20S proteasome inhibition by PM: *in vitro* assay

Proteasome is a large protein complex inside all eukaryotes and archaea, as well as in some bacteria[82]. The main proteasome function is to induce the degradation of unneeded or damaged proteins by proteolysis. All proteins tagged with poly-ubiquitin chains are recognized and hydrolized by the proteasome[83, 84], yielding short peptides (seven to eight amino acids long), following converted into amino acids. Proteasome is a large barrel-like complex consisting of a "core" of four rings around a central hole. Each ring is composed of seven different proteins; two rings are made of seven β subunits

and the other two contain seven α subunit each.[85] Moreover, β subunits ring contains six protease active sites located in the β1, β3 and β5 subunits. The roles of the α rings are to maintain a "gate" through which proteins can enter the barrel and bind a "cap" structures or regulatory particles that recognize poly-ubiquitin tags.

After an initial recognition step, proteins are degraded by three catalytic β subunits (β1, β3 and β5). Although they have a common mechanism, they have slightly different substrate specificities, which are considered chymotrypsin-like (β5), trypsin-like (β1), and peptidyl-glutamyl peptide-hydrolyzing (PHGH)-like (or caspase-like, β3)[85].

The activity of PM on the 20S human proteasome (the catalytic subunit of the entire 26S proteasome) was tested *in vitro* by detecting its ability to modulate the 20S-mediated proteolysis of fluorogenic peptide substrates, each specific for a particular catalytic subunit of the enzyme (see experimental section for details)[86, 87]. All these peptides are enzymatic substrates containing 7-amino-4-methylcoumarin (AMC) as fluorophore. In such substrates, the AMC is typically linked to the peptide through formation of an amide bond between the coumarin amino group and the carboxylic group of the C-terminal amino-acid residue.

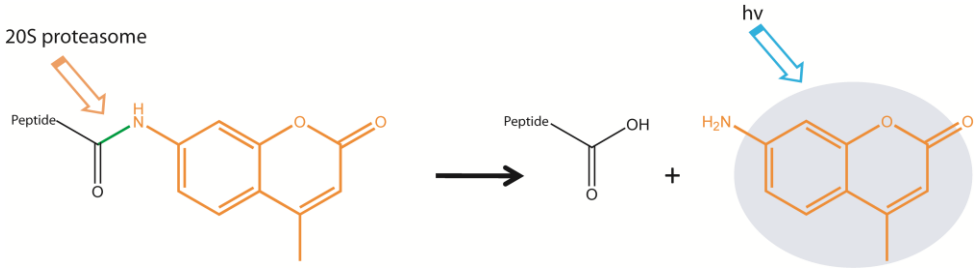

Fig. 18. Principle of AMC-labeled fluorogenic substrates.

Proteolysis of this amide bond gives free AMC, resulting in a large increase in fluorescence that can be detected at 460 nm upon excitation at 350 nm. As

reported in literature, to prime 20S proteasome activity we incubated it with Proteasome activator complex (PA28)[81, 88]. Then, we treated the activated proteasome with different concentrations of PM (0.5–5 μM) before the addition of a site specific fluorogenic substrate. The proteasome degradation occurs and the fluorescence moiety is released in solution, leading to a large increase in fluorescence, upon excitation. The comparison of the fluorescence emission of the PM-treated enzyme mixture with that of control (DMSO) allowed us to demonstrate the PM effect on each proteolytic site. In more details, we found that PM directly inhibits the proteasomal activity, in particular its caspase- and chymotrypsin-like activities with IC_{50} of 1.8 (±0.23) e 3.1 (± 0.15) μM respectively (**figure 19**).

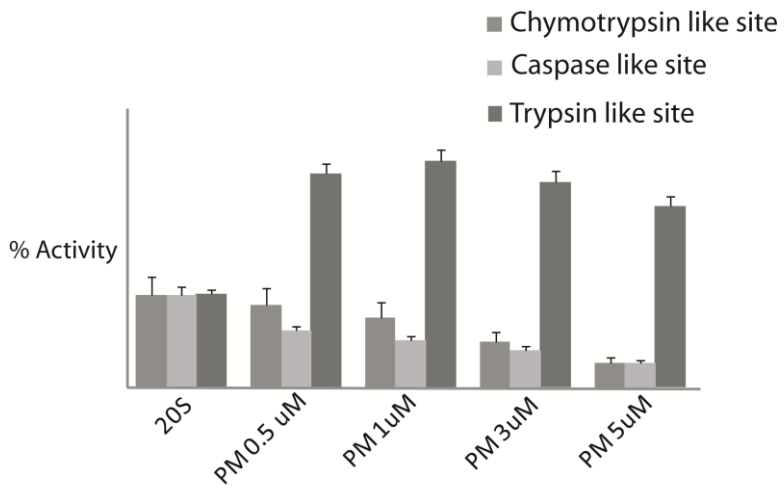

Fig. 19. *In vitro* Petrosaspongiolide M inhibition of 20S proteasome. Bars shows PM effect (0.5-5 μM) on recombinant 20S-PA28 proteasome complex activities. The caspase and chymotrypsin-like activity are inhibited by PM, whereas the trypsin like activity is fully activated. The data confirm a direct interaction between PM and proteasome**.**

As shown in **figure 19**, PM stimulates the trypsin-like activity of the proteasome at the tested concentrations. This is not surprising, since this effect

has been already reported for several inhibitors of caspase-like site which allosterically stimulates the trypsin-like activity[87]. Furthermore, it is well known that the inactivation of the chymotrypsin-like site is the main event determining the inhibition degree of protein degradation[86].

2.6 Cellular Inhibition of 26S Proteasome Activity by Petrosaspongiolide M

In a following experiment, we have assessed the ability of PM to inhibit proteasome functions inside the cell. Since proteasome inhibitors are known to be extremely cytotoxic, a MTT cell viability assay was performed to evaluate PM cytotoxic effects at the appropriate concentration for proteasome inhibition. Indeed, as reported in **figure 20**, PM did not produce significant cytotoxic effects, even at 1 μM, after 24 h of incubation.

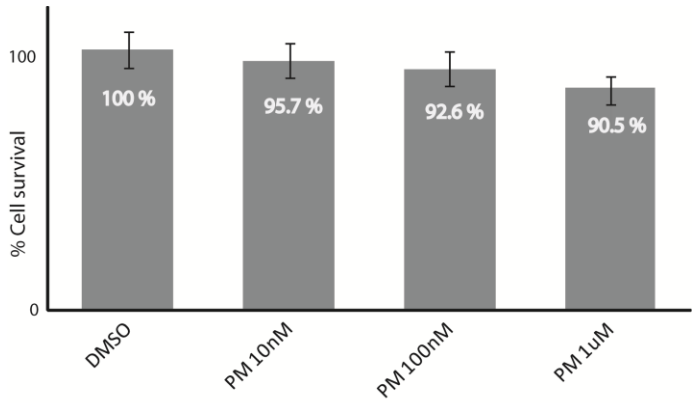

Fig. 20. PM effect on cell viability. % Cell survival of THP1-LPS induced macrophages at different concentration of PM All the experiment were triplicate and normalized to control (DMSO).

Then, THP-1 macrophages were incubated with PM in a concentration range between 0.1–1 μM. After 24 h, PM treated and control (DMSO) cells were

scraped out and lysed. Proteasome activity inside the cell lysates was measured by addition of site specific fluorogenic peptides.

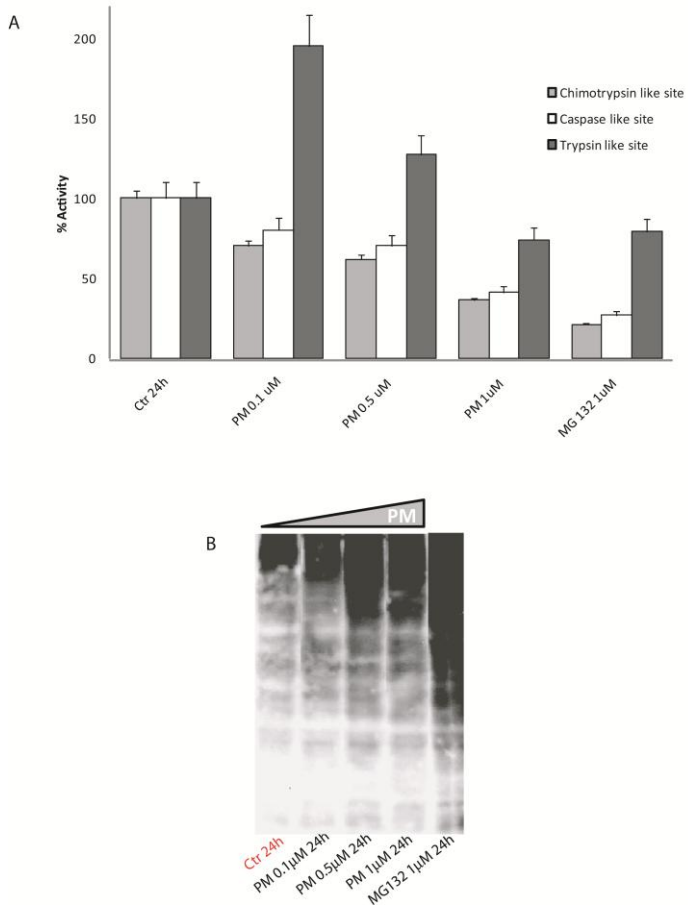

Fig. 21. Effect of PM inhibition on 26S proteasome in cells. (**A**) Effect of PM (0.1–1 μM) and MG132 (1 μM) on 26S proteasome activities in cells. (**B**) Western blot analysis of polyUP accumulation after treatment with PM (0.1–1 μM) and MG132 (1 μM).

The fluorescence emission of PM treated cell lysate was compared with that of control (DMSO), as for *in vitro* experiments, showing a significant inhibition by PM of the caspase- and the chymotrypsinlike activity, with IC_{50} values of 0.85 (±0.15) μM and 0.64 (±0.11) μM, respectively. The trypsin-like activity resulted to be activated, as already reported for *in vitro* based assays (**figure**

21A). In the same test, the reference compound MG132, a well-known proteasome inhibitor[89], was found to be slightly more effective than PM on the inhibition of chymotrypsin and caspase activity, and a similar behavior was observed for the modulation of the trypsin-like activity (**figure 21A**).

Since the specific inhibition of proteasome produces the accumulation of polyubiquitinated proteins, we wanted to improve the biological profile of PM testing its effect on the accumulation of polyubiquitinated proteins (polyUP) by immunoblot analysis. After treatment of THP-1 macrophage cells with PM, lysates were analyzed by western blotting using polyubiquitin antibodies[90].

The immunoblot profile in **figure 21B** demonstrated a relevant degree of polyUP accumulation in the cells treated with PM, increasing in a concentration-dependent manner. A major effect was evident in the case of MG132 due to its higher potency of action.

Since the UPS abnormal activation or failure underlies the pathogenesis of many human diseases[75, 84] (i.e. cancer, inflammation, cardiovascular diseases, neurodegenerative disorders), its modulating agents are considered attractive molecules for pharmacological intervention. In particular, two proteasome inhibitors have entered clinical trials for the treatment of cancer (Bortezomib) and stroke patients (MLN-519)[91], of which the first is already commercially available. On this basis, the relevant blocking of the proteasome activity in the living cells demonstrated by PM suggests this molecule as a potential new lead compound. Detailed investigations on the molecular mechanism of this inhibition are needed with the aim of the rational design of a new class of proteasome inhibitors.

-CHAPTER 3-

Chemical Proteomics Reveals Bolinaquinone as a Clathrin-Mediated Endocytosis Inhibitor

Based on: *Mol. BioSyst.*, **2011**, 7, 480–485

3.1 Fishing out BLQ target

Bolinaquinone (BLQ, **figure 22**) is a sesquiterpene metabolite isolated from the marine sponge *Dysidea sp*. in 1998 by Ireland and co-workers[92].
Chemically, BLQ is a terpenoid derivative characterized by a rearranged drimane skeleton linked at the unusual C-15 position with an hydroxyquinone ring (**Figure 22**)[92].

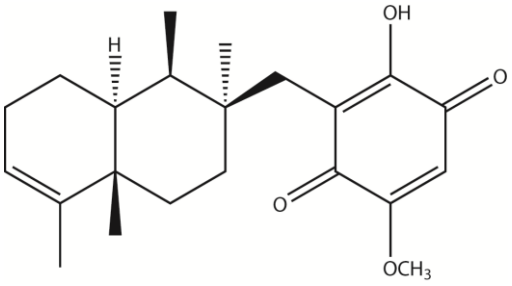

Fig. 22. Bolinaquinone (BLQ) chemical structure.

The field of quinone–protein chemical interactions is quite intriguing, as a result of multiple reaction pathways, including nucleophilic additions and redox processes. Indeed, quinone/hydroquinone redox species are often involved in single-electron transfer (SET) processes, which ultimately elicit chemical inactivation of several proteins and enzymes[93-95].
BLQ was extensively studied as anti-inflammatory compound and its PLA_2-inhibition properties[96, 97] and anti-inflammatory pharmacological profile were thoroughly examined, both *in vitro* and *in vivo*[98].
In particular, BLQ is able to reduce the production of mediators in acute and chronic inflammation and is a modulator of the oxidative stress parameters in 2,4,6-trinitrobenzenesulphonicacid (TNBS)-induced colitis in mice[99].
Moreover, as reported by Busserolles and co-workers, BLQ dramatically reduces nitrotyrosine immunodetection and colonic superoxide anion production, and furthermore decreases the extension of apoptosis, suggesting

potential protective actions in intestinal inflammatory diseases[99]. Due to its interesting anti-inflammatory profile[98, 99], BLQ is a good candidate for a target discovery study aimed to the identification of its primary partners, and to a better understanding of its mechanism of action. To reach this goal, a chemical proteomics-based approach has been employed. From an experimental point of view, our approach to determine the BLQ interactome can be divided into three steps: (i) Generation of functional BLQ-modified beads, (ii) affinity purification and MS identification of BLQ specific interacting partner(s), and (iii) *in cell* assays to test its biological effect(s).

3.2 Generation of functional BLQ-modified beads

The immobilization of a compound on the matrix beads usually requires the interposition of a spacer arm to minimize steric hindrance between the ligand and its macromolecular partners in the following step of affinity purification, as already reported for PM in chapter 1. The spacer arm can be inserted on the particle surface before the immobilization of the compound, even if an increase in the non-specific protein adsorption has to be expected, due to several unmodified reacting groups of the spacer after the following step of immobilization.

An improvement in term of target binding ability and reduction of non-specific binding can be obtained by a prevoious reaction between the spacer and the sample compound and the following immobilization on the resin.

On this basis, BLQ was treated with 4,7,10-trioxa-1,13-tridecanediamine (NH_2-$(PEG)_2$-NH2) to give a covalent adduct (BLQ-NH-$(PEG)_2$-NH_2), through a Michael-like addition of the spacer amino group onto the conjugated quinone moiety followed by methanol loss (**figure 23**), as already reported[96, 97]. The reaction was monitored by HPLC-MS, allowing the identification of

the major product of the reaction as BLQ-NH-$(PEG)_2$-NH_2 adduct (MW 546.7 Da).

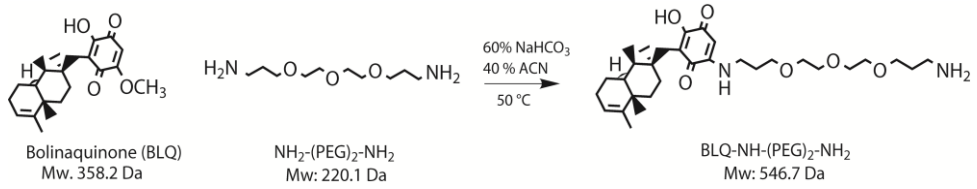

Fig. 23. Reaction scheme of BLQ chemical modification with 7,10-Trioxa-1,13-tridecanediamine.

Finally, several HPLC runs were carried out to isolate enough amount of BLQ modified species. The purified BLQ adduct was then immobilized onto the agarose Reacti-Gel beads by a nucleophilic attack of the terminal NH_2 group onto the activated carbonyl function of the resin, followed by imidazole loss (**figure 24**).

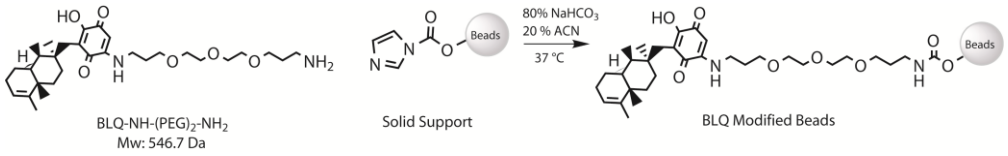

Fig. 24. BLQ immobilization onto the Reacti-Gel (6X) support.

The yield of the immobilization process was evaluated by integration of RP-HPLC peaks of free BLQ-NH-$(PEG)_2$-NH_2 before and after the incubation with the beads. **Figure 25** shows the peaks of free BLQ-NH-$(PEG)_2$-NH_2 in 50 µl of reaction buffer with Reacti-Gel agarose matrix after 0, 2 and 16 h incubation. The high decrease of the peak area revealed the anchorage of the BLQ-NH-$(PEG)_2$-NH_2 adduct onto the beads with a 60% immobilization yield. The experimental conditions such as buffer, pH and temperature (see

Material and Methods section) were optimized to reach final concentration of 2 µmol drug/mL resin, representing an ideal ratio as reported in literature[100].

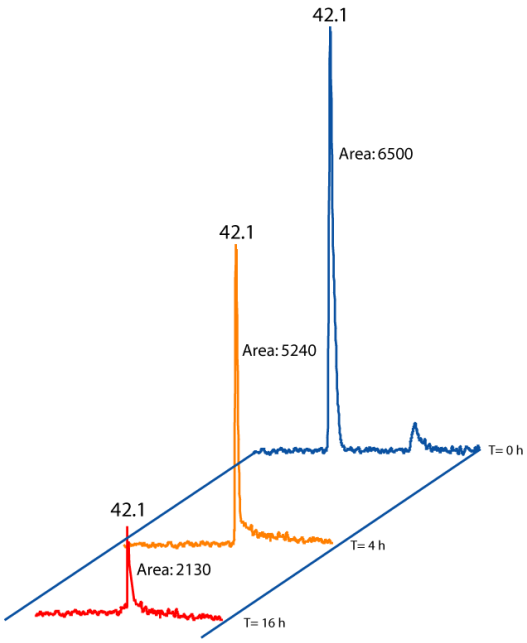

Fig. 25. Chromatographic profile of free BLQ-NH-$(PEG)_2$-NH_2 after 0, 2 and 16 h incubation with Reacti-Gel agarose matrix.

Finally, a control sample was prepared treating a trityl-modified spacer adduct with the Reacti-Gel (6X) resin. Both modified matrix species were then stored in acetone at 4°C.

3.3 Affinity purification and MS identification of BLQ specific interacting partners

3.3.1 Fishing for Partners

The analysis of BLQ-interacting protein(s) started with the treatment of the BLQ modified beads with a lysate of THP1 induced macrophages, the same

model system used in the previous anti-inflammatory pharmacological investigations.[98]

The same amount of protein sample, obtained from LPS induced THP-1, was incubated with the BLQ modified beads and with a BLQ free matrix sample, as control experiment. After incubation, non-specific bound proteins were mostly released by an extensive washing of the beads, while the tightly bound proteins were eluted with SDS loading buffer and then chromatographed by 1D-SDS PAGE. As expected, a clearer electrophoresis profile was obtained if compared with that of the PM experiment (see chapter 2), because of the different approach adopted in the preparation of the beads (**figure 26**).

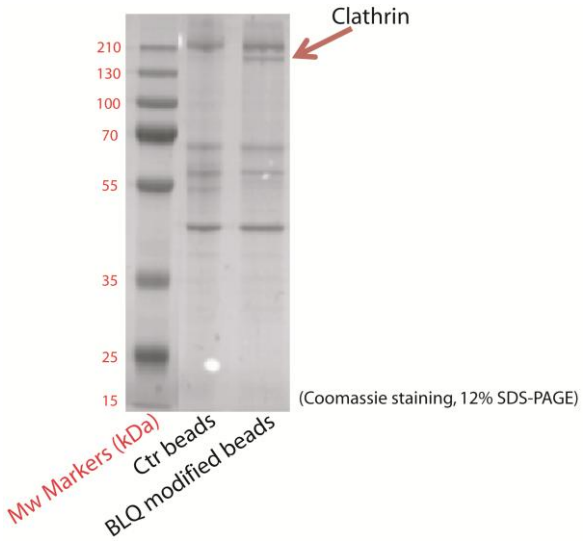

Fig. 26. SDS PAGE analysis of the affinity purified proteins.

In an affinity purification analysis, an unbiased way to perform the identification of the specific interactors of a given compound requires the analysis of the entire gel lanes [101], as performed in the case of the PM interactome analysis (see chapter 1). However, in this case the comparison of the electrophoretic runs (beads-BLQ *vs* control) displayed a major protein

enrichment at an apparent molecular weight of 190 kDa (**figure 26**). On this basis, we focused our attention on this gel region that we cutted out and treated as reported by Schevchenko et al. [102] obtaining tryptic peptide mixtures. Even though the BLQ enrichment on the gel looked convincing, we wanted to take into account the worst case in which a protein smearing from the upper strong band inside the gel giving false positive enrichment. For this reason, we enlarged the cutted region to the upper bands both in control and BLQ-based experiment (**Figure 27A**). The peptide mixtures generated after trypsin digestion were submitted to LC MS/MS analysis. Fragmentation of doubly and triply charged peptide species was performed and all MS/MS spectra were converted into peak lists that were submitted to a Mascot database search for proteins identification.

3.3.2 BLQ interactors identification

The Mascot database search allowed us to identifiy the main BLQ targets. All the proteins identified in the gel region showing the most prominent BLQ enrichment, were compared in term of spectral counts with that of the control ones. As reported in the spectral count table (**Figure 27B**), the upper strong band (in blue) contains different isoforms of myosin with the same extent both in the control and BLQ experiments, whereas clathrin is almost exclusively contained in the strong band enriched in the BLQ experiment (in red). Therefore, the sequence coverage, the Mascot and the peptide scores obtained for clathrin were enough to convince us about the confidence of our identification (**figure 27C**). On this basis, clathrin, a key protein involved in the receptor mediated endocytosis processes, has been recognized as BLQ interactor indicating that this marine metabolite is able to fish out from a cell a main intracellular partner with high specificity. Since BLQ is characterized by

an interesting anti-inflammatory profile[98], this result is somewhat unattended; thus we were intrigued by a new potential application of BLQ and decided to perform additional experiments to confirm clathrin as main BLQ partners.

A)

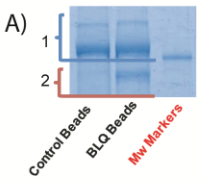

B)

Identified Proteins	Accession Number	Mw	Control*	BLQ beads*
Myosin-9	MYH9_HUMAN	227 kDa	99	52
Myosin-11	MYH11_HUMAN	220 kDa	10	0
Keratin, type II cytoskeletal 1	K2C1_HUMAN	66 kDa	12	22
Myosin-14	MYH14_HUMAN	220 kDa	6	4
Keratin, type II cytoskeletal 2	K22E_HUMAN	66 kDa	5	7
Keratin, type II cytoskeletal 79	K2C79_HUMAN	60kDa	2	3
Keratin, type I cytoskeletal 10	K1C10_HUMAN	60 kDa	3	9
Keratin, type I cytoskeletal 9	K1C9_HUMAN	60 kDa	3	0
Myosin-3	MYH3_HUMAN	220 kDa	2	0
Clathrin heavy chain 1	CLH1_HUMAN	192 kDa	6	68
Clathrin heavy chain 2	CLH2_HUMAN	189kDa	0	12
Myosin-9	MYH9_HUMAN	227 kDa	7	11
Keratin, type II cytoskeletal 1	K2C1_HUMAN	66 kDa	7	2
Keratin, type II cytoskeletal 2	K22E_HUMAN	66 kDa	3	2
Keratin, type I cytoskeletal 10	K1C10_HUMAN	60 kDa	0	1
D-2-hydroxyglutarate dehydrogenase	D2HDH_HUMAN	57 kDa	0	1
		Total Spectr	165	194

*Number of assigned spectra

C)

Swiss Prot Code	Protein name	Mw (Da)	Seq. Coverage	Number oh hit	Unique	Protein Score
CLH1_HUMAN	Clathrin heavy chain 1	193260	50%	67	44	1574

Observed (mz)	Expected (mr)	z	Calculated (mr)	Pep_score	Pep_sequence
472.2634	942.5122	2	942.4923	30.68	K.HELIEFR.R
528.3018	1054.589	2	1054.5699	5.34	K.YIEIYVQK.V
536.321	1070.6274	2	1070.6124	35.03	K.HDVVFLITK.Y
563.8038	1125.593	2	1125.5818	35.53	K.VANVELYYR.A
616.8329	1231.6512	2	1231.6408	32.67	K.VDKLDASESLR.K
626.8367	1251.6588	2	1251.6533	38.39	K.TLQIFNIEMK.S
648.8458	1295.677	2	1295.6622	41.31	K.LLYNNVSNFGR.L
652.8394	1303.6642	2	1303.652	44.57	R.NNLAGAEELFAR.K
667.8295	1333.6444	2	1333.6262	62.66	K.IYIDSNNNPER.F
677.3546	1352.6946	2	1352.6758	48.1	R.VVGAMQLYSVDR.K
677.4312	1352.8478	2	1352.8391	56.73	R.NLQNLLILTAIK.A
694.3778	1386.741	2	1386.7289	26.08	R.QNLQICVQVASK.Y
701.8491	1401.6836	2	1401.6711	53.38	R.CNEPAVWSQLAK.A
717.4111	1432.8076	2	1432.7926	55.77	K.SVDPTLALSVYLR.A
732.8824	1463.7502	2	1463.7296	30.5	R.ALEHFTDLYDIK.R
734.3408	1466.667	2	1466.65	40.19	K.AHTMTDDVTFWK.W
740.4077	1478.8008	2	1478.7922	64.68	K.VGYTPDWIFLLR.R
750.4244	1498.8342	2	1498.8256	37.64	K.WLLLTGISAQQNR.V
750.4249	1498.8352	2	1498.8256	68.58	K.WLLLTGISAQQNR.V
754.3906	1506.7666	2	1506.7501	83.72	K.VIQCFAETGQVQK.I
776.3873	1550.76	2	1550.7464	61.74	R.GQFSTDELVAEVEK.R
776.3881	1550.7616	2	1550.7464	81.57	R.GQFSTDELVAEVEK.R
778.434	1554.8534	2	1554.844	36.67	K.LTDQLPLIIVCDR.F
787.4117	1572.8088	2	1572.793	16.54	R.RPISADSAIMNPASK.V
806.9324	1611.8502	2	1611.8396	54.76	R.ESYVETELIFALAK.T
854.4385	1706.8624	2	1706.8475	8.51	R.GQFSTDELVAEVEKR.N
858.9445	1715.8744	2	1715.8631	7.51	K.VSQPIEGHAASFAQFK.M
879.9474	1757.8802	2	1757.8736	9.46	R.KFNALFAQGNYSEAAK.V
938.9183	1875.822	2	1875.8131	76.1	K.MEGNAEESTLFCFAVR.G
938.9239	1875.8332	2	1875.8131	70.19	K.MEGNAEESTLFCFAVR.G
971.9663	1941.918	2	1941.9068	86.72	R.TSIDAYDNFDNISLAQR.L
971.9672	1941.9198	2	1941.9068	90	R.TSIDAYDNFDNISLAQR.L
974.0134	1946.0122	2	1946.007	22.18	K.AFMTADLPNELIELLEK.I
982.012	1962.0094	2	1962.0019	74.26	K.AFMTADLPNELIELLEK.I
657.6826	1970.026	3	1970.0221	49.98	R.LASTLVHLGEYQAAVDGAR.K
986.0242	1970.0338	2	1970.0221	2.16	R.LASTLVHLGEYQAAVDGAR.K
1021.0594	2040.1042	2	2040.0813	81.63	R.LPVVIGGLLDVDCSEDVIK.N
1036.0273	2070.04	2	2070.0343	51.84	R.GYFEELITMLEAALGLER.A
1036.0303	2070.046	2	2070.0343	58.52	R.GYFEELITMLEAALGLER.A
1061.0251	2120.0356	2	2120.0313	83.81	K.DTELAEELLQWFLQEEK.R
1061.0267	2120.0388	2	2120.0313	79.46	K.DTELAEELLQWFLQEEK.R
1077.0118	2152.009	2	2151.9929	68.39	R.GQCDLELINVCNENSLFK.S
1106.064	2210.1134	2	2210.1001	31.92	K.VGEQAQVVIIDMNDPSNPIR.R
747.3946	2239.162	3	2239.1597	34.52	K.FDVNTSAVQVLIEHIGNLDR.A
785.087	2352.2392	3	2352.2438	43.97	R.ISGETIFVTAPHEATAGIIGVNR.K
785.087	2352.2392	3	2352.2438	68.63	R.ISGETIFVTAPHEATAGIIGVNR.K
1178.0859	2354.1572	2	2354.139	28.85	K.SVNESLNNLFITEEDYQALR.T
1178.0867	2354.1588	2	2354.139	62.85	K.SVNESLNNLFITEEDYQALR.T
790.0921	2367.2545	3	2367.2547	18.26	R.KFDVNTSAVQVLIEHIGNLDR.A

Fig. 27. MS identification of BLQ main target. (**A**) Zoom in the 8% of polyacrylamide gel region around 210 kDa. The upper bands (# 1 in blue) from control and BLQ beads were separately cut and analyzed as well as the lower bands (# 2 in purple). (**B)** Identification of proteins eluted in the upper (in blue) and lower (in purple) bands from control and BLQ beads. Number of assigned spectra for identified protein are reported. The table represents one of three independent experiments. (**C**) Mascot report of all matched peptides of clathrin heavy chain I.

3.3.3 Serial affinity chromatography as a tool for identifying specific BLQ binding protein

In 2006, Yamamoto and co-workers developed a method to distinguish specific bound proteins from the unspecific ones. This method employs the sequentially treatment of the protein mixture with two affinity resin samples bearing the same bioactive ligand. The proteins eluted from each affinity step are chromatographed by 1D-SDS PAGE and comparatively analyzed. The recovery of the specific binding proteins is significantly higher in the first affinity step than in the second one, because of their high affinity for the ligand. On the contrary, nonspecific binding proteins are almost equally captured during the affinity steps, due to their low affinity for the resins[103]. On this basis, we applied the serial chromatography approach to our case.

A THP1 cell lysate was sequentially treated with three batches of affinity beads bearing BLQ, and the proteins bound on each resin (corresponding to A1, A2 and A3 lanes on the gel in **figure 28**) were comparatively analyzed by 1D-SDS PAGE.As expected, the binding of clathrin (the band at around 190 kDa) is significantly reduced on the second and third affinity step (A2 and A3) when compared with the first one (A1), as a sign of a selective capture by BLQ. These findings are extremely convincing about the confidence of clathrin identification as BLQ main partners. The evidence that clathrin binds

BLQ selectively can open the way to further investigation on the role of BLQ in the modulation of clathrin-mediated processes, in a cell system.

Thus, we were intrigued by a new potential application of this molecule in modulating biological processes, such as clathrin-mediated internalization, and we performed additional experiments to confirm this finding.

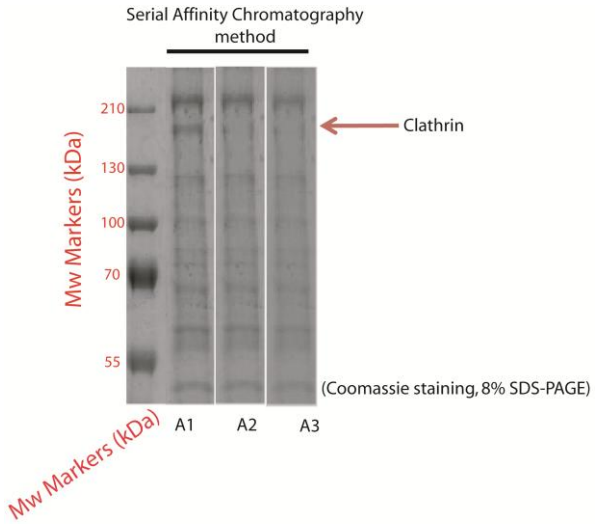

Fig. 28. Serial affinity chromatography experiment. THP1 cell lysate was sequentially treated with three batch of BLQ-modified resins and proteins eluted from each resin (A1, A2 and A3) were resolved using 8% SDS-PAGE.

3.4 *In vivo* BLQ biological effect on Clathrin mediated endocytosis

Endocytosis plays an important role in the selective uptake of proteins, viruses and other biologically important macromolecules at the plasma membrane of eukaryotic cells. Receptor-mediated endocytosis allows the specific removal of cell surface receptors from the plasma membrane and targets them to endosomes[104]. Clathrin is the main component of the coated vesicles that

mediate the selective transfer of molecules from the extracellular environment within cells. In all cell types, clathrin-coated vesicles are responsible for receptor-mediated endocytosis at the plasma membrane and for the receptor-mediated sorting of lysosomal enzyme. In cells with a regulated secretory pathway, clathrin-coated membranes are involved in the formation of secretory granules and in the rapid uptake of plasma membrane following degranulation. A number of protein-protein and protein-lipid interactions underlies the assembly of the clathrin-based endocytic machinery. In addition to clathrin, AP-2, and some other accessory cytosolic proteins, including synaptojanin I and Eps15, are involved in vescicle formation[105, 106].

At each site, clathrin associates indirectly with the membrane by binding to an adaptor protein (AP), which interacts with the cytoplasmic domains of transmembrane receptors. Polymerization of clathrin then catalyze the assembly of adaptors associated receptors and their bound ligands into a coated vesicles.Since the clathrin mediated endocytosis pathway plays an important role in the selective uptake of proteins, viruses and other biologically important macromolecules, the modulating agents of clathrin-mediated endocytosis are considered significant targets for bio-pharmacological studies.

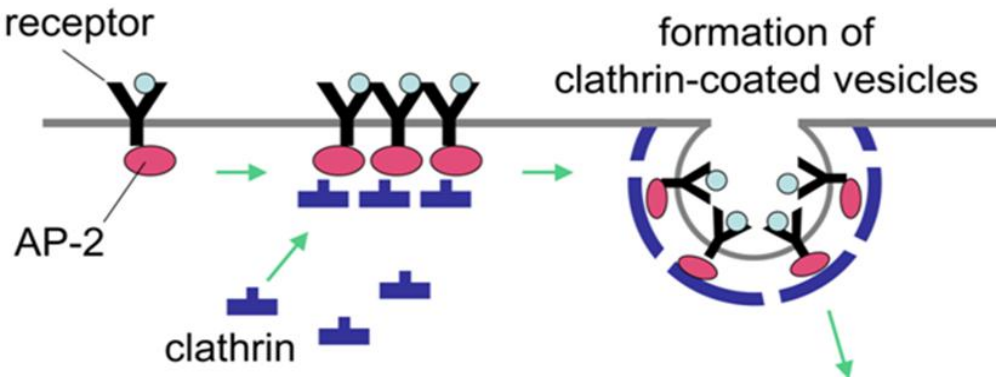

Fig. 29. Schematic rapresentation of clathrin-coated vesicles formation.

On this basis, we decided to verify the biological relevance of BLQ towards clathrin-mediated endocytosis.

More in details, we studied the clathrin dependent internalization of albumin by means of a fluorescence assay. Indeed, since albumin is fully internalized by a pure clathrin-dependent mechanism[107], we chose this protein to test the ability of BLQ to interfere with clathrin dependent internalization. Chlorpromazine (CPZ), a well known inhibitor of clathrin-mediated endocytosis, was selected as refernce compound. Before starting the internalization experiments, an MTT assay was performed to evaluate the cytotoxic effect of BLQ at the concentration used in the clathrin experiment. The cells, seeded into 96 well plate, were exposed to different concentrations of BLQ (0.01 to 100 μM) and incubated for 48 h. The mitochondrial-dependent reduction of 3-(4,5-dimethylthiazol-2-yl)-2,5-diphenyltetrazolium bromide (MTT) to formazan was used to evaluate the possible BLQ cytotoxic effect. As reported in **figure 30**, BLQ did not produce significant cytotoxic effect, even at 100 μM, after 48 h of incubation.

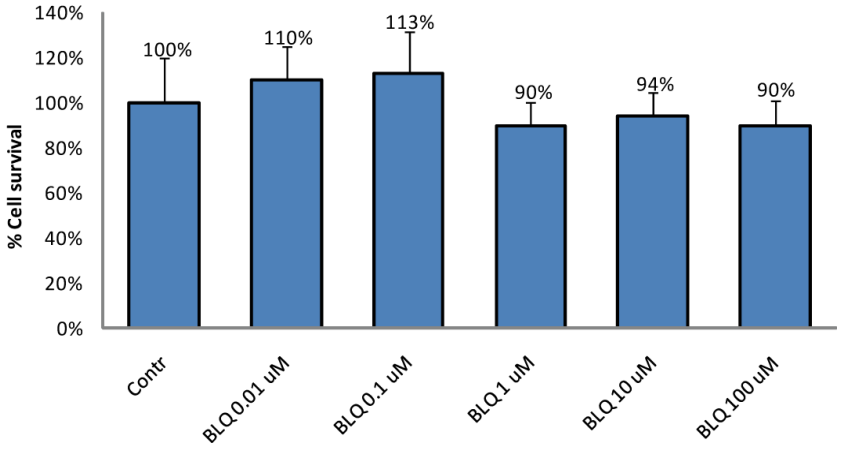

Fig. 30. % cell survival of THP1-LPS induced macrophages at different concentration of BLQ after 48 h of incubation. Each value is the mean ± standard deviation of three different experiment performed in triplicate.

Then, we analyzed the ability of THP1 induced macrophages to internalize a fluorescent-labeled albumin (488-BSA) in presence and absence of BLQ and CPZ[107, 108]. In a first step the internalization assay was optimized by incubating macrophages cells with two different concentration of 488-BSA (10 μg/ml, 20 μg/ml) and with the solvent (control), and then analyzing the cells by flow cytometry.

As depicted in **figure 31**, the shift in the maximum fluorescence intensity in the two experiments *vs* control is clearly due to the BSA internalization. Since the incubation with 10 and 20 μg/ml BSA gave similar results, we decided to use highest BSA concentration.

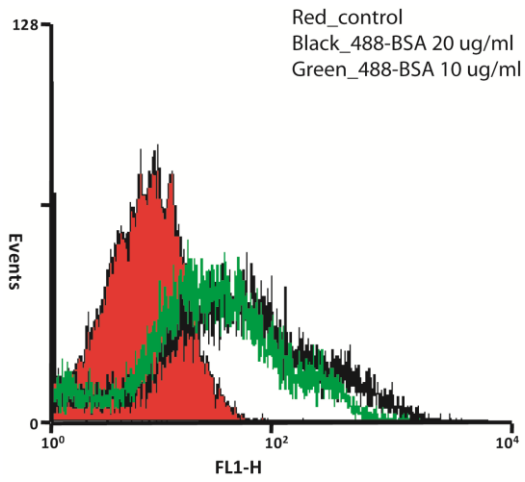

Fig. 31. FACS analysis of 488-BSA uptake, at two different concentrations, in THP1 macrophages.

Once the protocol was optimized, THP1 macrophages were pre-incubated with BLQ or CPZ (50 μM and 100 μM), before the addition of the green fluorescent 488-BSA. **Figure 32** clearly shows the similar effect of BLQ and CPZ on 488-BSA internalization, providing the evidence of BLQ interference on the clathrin-mediated endocytosis.

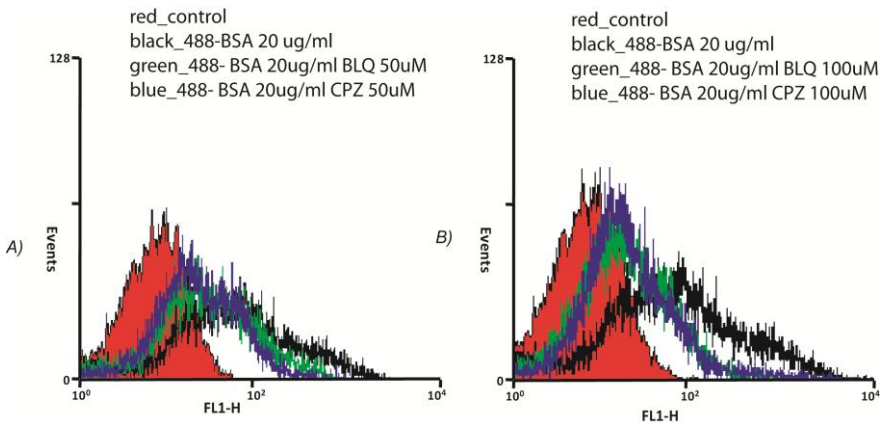

Fig 32. (A-B) FACS analysis of 488-BSA uptake in THP1 macrophages in presence and absence of different concentrations of BLQ and CPZ. Ctr: cells incubated in normal cell growth.

The same data, reported as percentage of 488-BSA internalization (**figure 33**), clearly showed that both BLQ and CPZ decrease the uptake of 488-BSA in a dose dependent fashion, with a potency of action of CPZ slightly higher than BLQ.

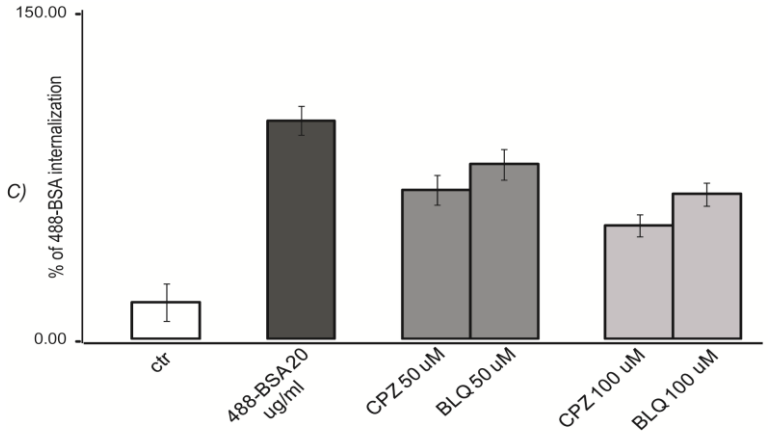

Fig. 33. Histograms representing the percentage of 488-BSA internalization calculated by the median fluorescence intensity values measured by CellQuest Software. The 488-BSA internalization at 20 μg/ml was set as 100%, the data are representing three different experiments ±sd.

Since 488-BSA is tagged with a fluorescence probe, we decided to evaluate BLQ and CPZ modulation of BSA internalization also by miscroscopy analysis. As expected, CPZ and BLQ reduced the uptake of 488-BSA (**figure 34**).

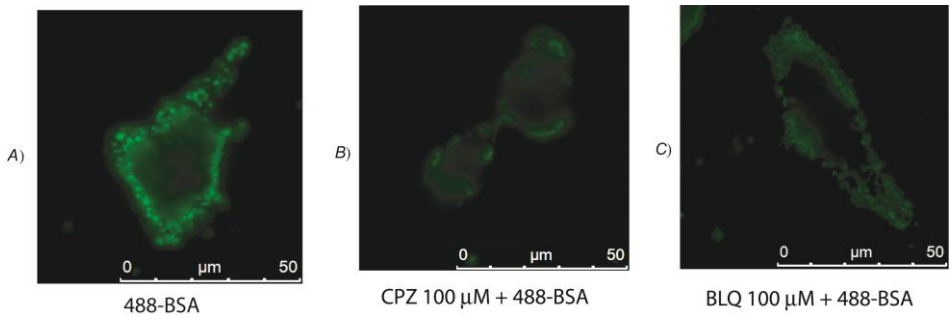

Fig. 34. Cells microscopy analysis: (A) after incubation with 488-BSA, (A) after preincubation with CPZ 100µM and incubation with 20 µg/ml 488-BSA, (C) after preincubation with BLQ 100µM and incubation with 20 µg/ml 488- BSA.

All these data clearly demonstrated the ability of BLQ to inhibit the clathrin-dependent internalization process in a dose-dependent manner (**figure 33-34**). Since only few organic compounds are known to modulate clathrin-dependent endocytosis (for instance CPZ and amantadine[107]), BLQ could be considered as a biotechnological tool with a novel chemical scaffold for the investigation of cellular internalization and trafficking pathways.

-CHAPTER 4-

Towards the Identification of Perthamide C Biological Partners

Based on: *Manuscript in preparation*

4.1 Chemical Proteomics applied to the discovery of Perthamide C interactome

Perthamide C (PRT, **Figure 35**) is a cyclic peptide isolated from an Australian collection of a *Theonella swinhoei* sponge, by Festa and co-workers in 2009[110].

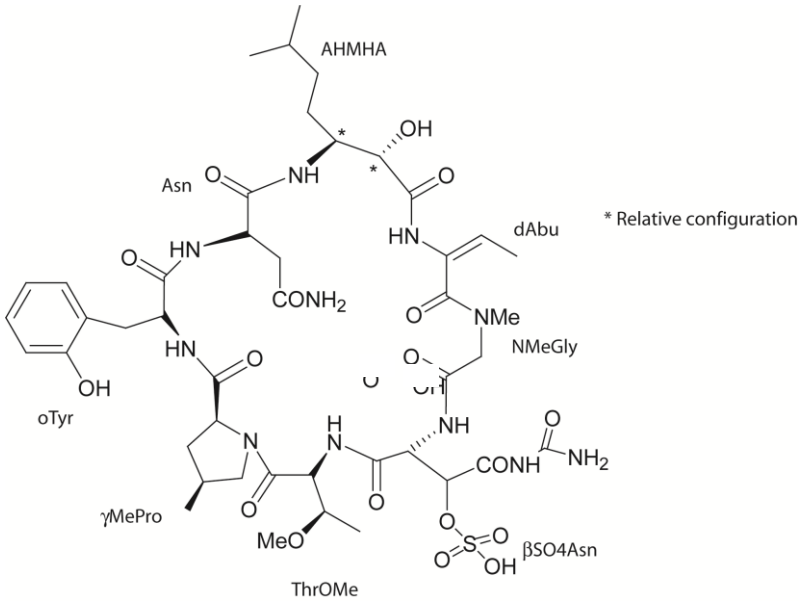

Fig. 35. Chemical structure of Perthamide C (PRT).

Chemically, PRT is a cyclic peptide containing both natural and un-natural aminoacids such as O-methylthreonine (ThrOMe), 2-amino-2-butenoic acid (dAbu), N-methylglycine (NMeGly), γ-methylproline (γMePro) and β-hydroxyasparagine (bOHAsn) leading an additional sulfate and amidic group.
Since marine sponges of the genus *Theonella* are an excellent source of bioactive peptides with interesting biological activities, PRT has been subjected to an *in vivo* investigation to test its anti-proliferative and anti-inflammatory activities. PRT C did not show anti-proliferative activity on KB cell lines up to a dose of 10 mg/mL. However, it is able to significantly reduce

carrageenan-induced paw oedema both in the early (0–6 h) and in the late phases (24–96 h). Moreover, PRT showed a dose dependent anti-inflammatory profile, which lead to a 60% reduction of the oedema, in mice, when administered at 300 μg/Kg. Its anti-inflammatory profile resulted 100 times more potent than naproxen (ED50 40 mg/kg), one of the most known non steroidal anti-inflammatory drug[110].

Since cyclic peptides are rarely found in the marine ecosystem, with the exception of cyclomarins[111], salinamides[112] and halipeptins[113], PRT anti-inflammatory profile has opened the way to further investigations on its origin. Aiming to a comprehensive characterization of PRT interactome in a cellular system, a chemical proteomics based approach has been employed.

The experimental approach could be divided into the following steps: (i) generation of functional PRT-modified beads, (ii) affinity purification and MS identification of PRT specific interacting partner(s), and (iii) surface plasmon resonance (SPR) experiments to measure the affinity between PRT and its target proteins.

4.2 Generation of PRT functional matrix

4.2.1 PRT reaction profile with 4,7,10-trioxa-1,13-tridecanediamine

As mentioned into previous chapters, the immobilization of a small molecule on the matrix beads needs a spacer arm to minimize steric hindrance between the ligand and its macromolecular *partners* during the affinity purification step. Moreover, in BLQ based experiment (see chapter 3), we have demonstrated that the modification of the drug with the spacer before the immobilization on the beads strongly reduces the amount of non-specific adsorption. On this basis, we decided to modify PRT with 4,7,10-trioxa-1,13-

tridecanediamine (NH_2-$(PEG)_2$-NH_2) before its immobilization on the matrix. The reaction was monitored by HPLC-MS allowing the identification of a covalent adduct (Mw: 1226.54 Da) generated through a nucleofilic attack of the spacer amino group onto the β-sulfated Asn residue, followed by urea loss (**Figure 36**).

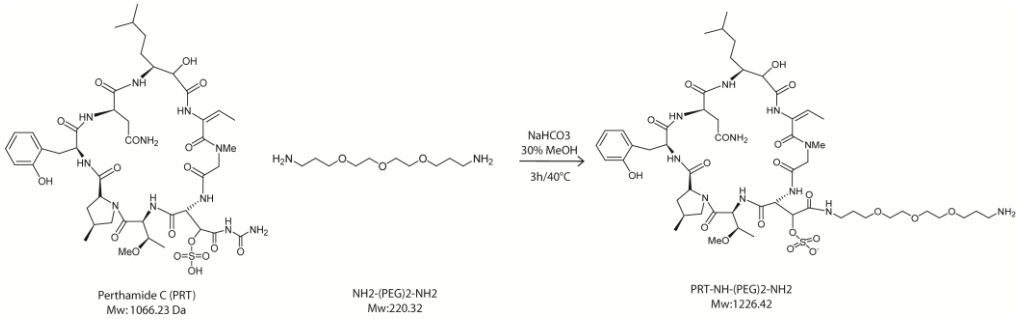

Fig. 36. Reaction scheme of PRT chemical modification with 7,10-Trioxa-1,13-tridecanediamine.

Several HPLC attempts were carried out to isolate the PRT modified species, even if unfortunately the adduct was unstable, since its degradation occurred during the first 36 h. On this basis, a change in the immobilization procedure was needed, and consequently PRT was put in reaction directly with the beads already modified with the spacer.

4.2.2 PRT on beads immobilization

PRT on beads immobilization was carried out using the agarose Reacti-Gel (6X) beads previously reacted with 4,7,10-Trioxa-1,13-tridecanediamine (NH_2-$(PEG)_2$-NH_2). A nucleophilic attack of the spacer terminal amino group onto the activated carbonyl function of the resin gave rise to the beads

chemical modification (**figure 37**). A following Kaiser test was useful to demonstrate the presence of free NH_2 function on the beads. The experimental conditions such as pH, temperature and amount of linker (see Material and Methods section) were optimized to avoid a complete covering of the particle surface.

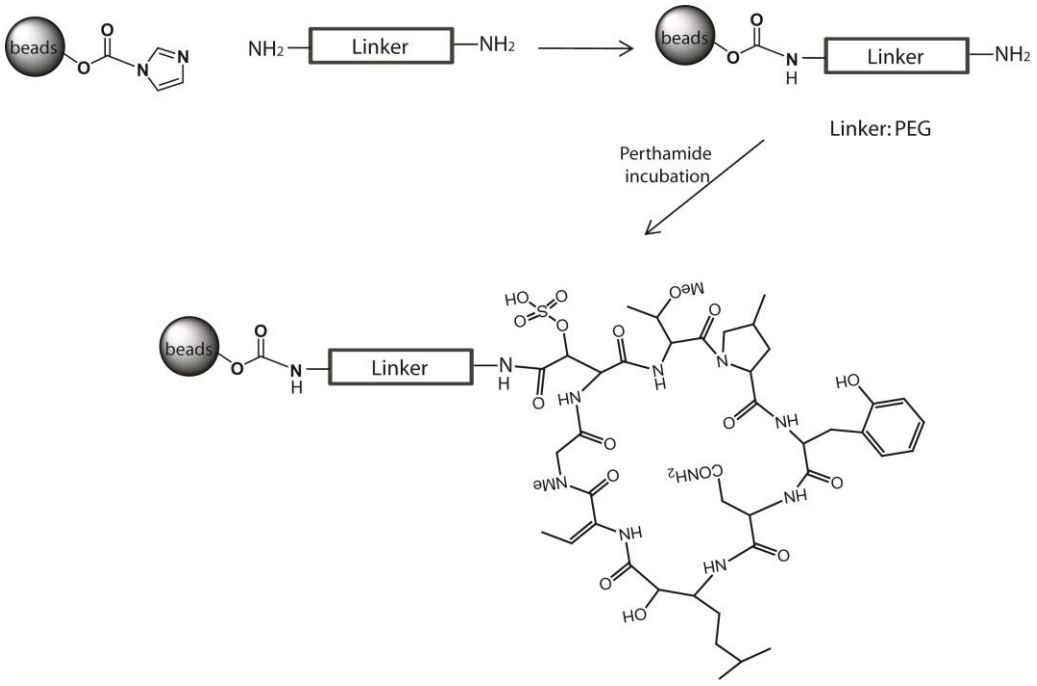

Fig. 37. Reaction Scheme of Perthamide immobilization on beads.

In the second step PRT was treated with the spacer-bearing matrix beads, and, as reported in **figure 37**, PRT immobilization most likely occurred through a nucleophilyc attack of the matrix free NH_2 groups onto the β-sulfated (Asn) residue followed by urea loss, as previously reported.

The immobilization yield was calculated by integration of RP-HPLC peaks of the free PRT before and after the reaction. The measure of peak area reduction after 16 h gave a 50% immobilization yield (**figure 38**).

The experimental procedures, reported in the experimental section, were optimized to reach a final concentration of 0.9 μmol drug/mL resin. A sample of control matrix was prepared by reaction of the activated Reacti-Gel (6X) support with a trytilated spacer species.

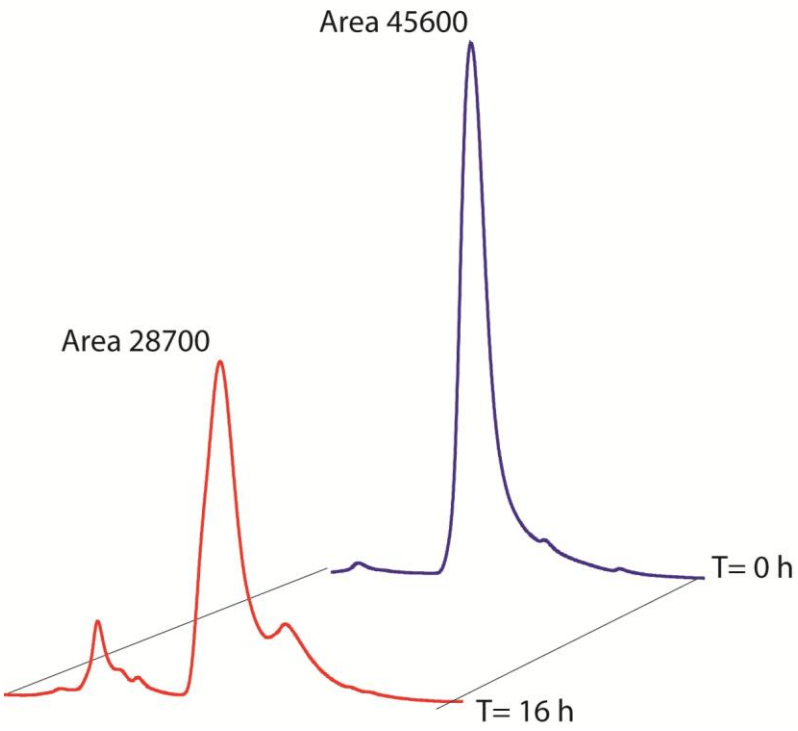

Fig. 38. Chromatographic profile of free PRT after 0 and 16 h incubation with Reacti-Gel agarose matrix modified with 4,7,10-Trioxa-1,13-tridecanediamine.

4.3 Affinity purification of Perthamide C partners

Crude cell extracts of J774.1 cells were loaded on the PRT-bearing matrix, to promote the interaction between PRT and its *partners* in the cell lysate. To distinguish between specifically and non-specifically bound components, the same amount of cell lysate was also incubated with a control matrix sample.

After several washing steps needed to reduce the amount of non-specific adsorption, proteins tightly bound were eluted by treating the beads with SDS-gel loading buffer. Finally, proteins eluted by PRT matrix and control beads were resolved using 12% SDS PAGE gel electrophoresis.

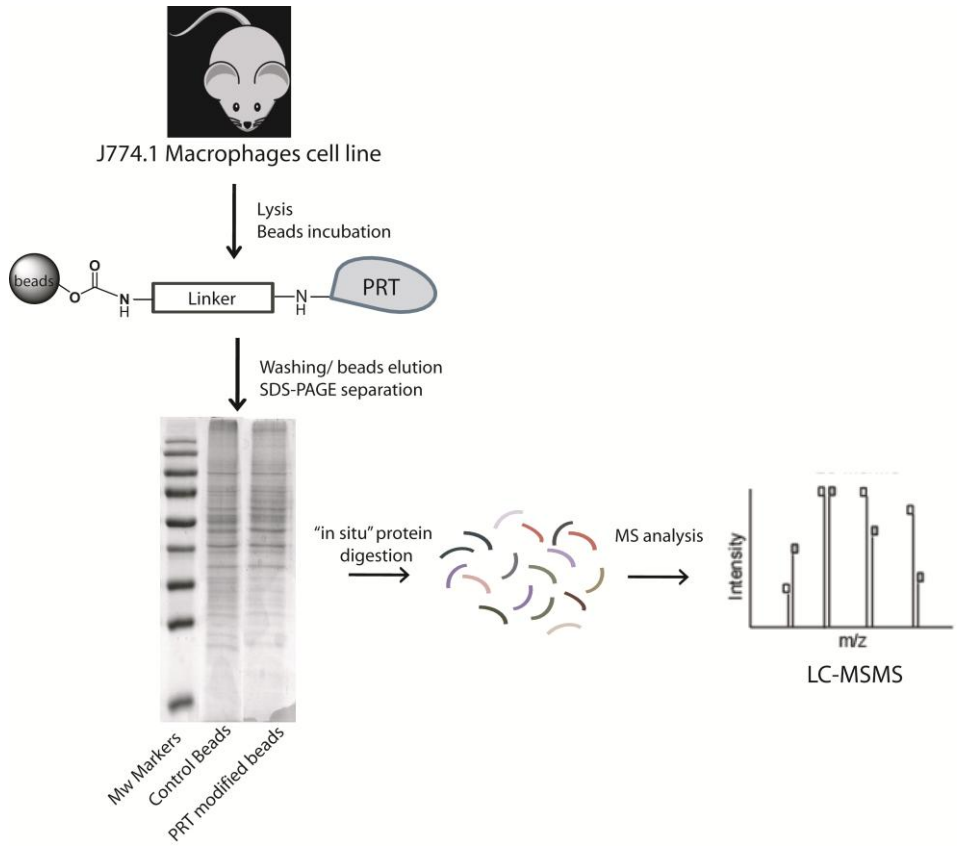

Fig. 39. Experimental workflow used to profile PRT C interactome.

Since no differences were evident simply looking at the comassie stained bands, both gel lanes (from PRT-bearing beads and control) were cut in ten pieces and subjected to *in situ* trypsin digestion. The resulting peptides mixture were analyzed by mass spectrometry through nanoflow reversed-phase HPLC MS/MS (**figure 39**). Doubly and triply charged peptide species were fragmented, and all the MS/MS spectra converted into a peak list using

the ProteinLynx software. Finally, protein identification were achieved by submitting all peak lists to a protein database search on SwissProt engine.

4.4 PRT interactome identification

Database search produced two list of identified proteins for both gel lanes (PRT-bearing and control matrix), that were compared to establish the PRT specific *partners*. As reported in the Venn diagram (**figure 40**), all proteins identified in three independent experiments were clustered to generate three lists of putative PRT interactors, following overlapped to give a significative set of PRT protein interactors.

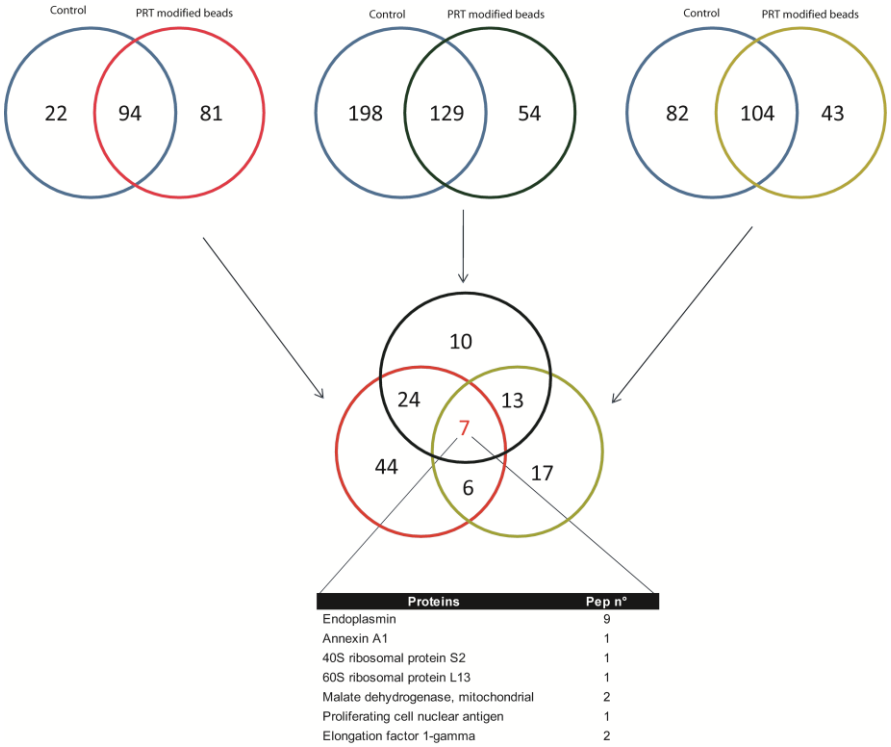

Fig. 40. Venn diagram showing the number of proteins identified in control and PRT based experiments. The overlapping of proteins identified only in PRT based experiments allow us to identify a smaller file of PRT interactors.

Based on this results, Endoplasmin, also known as glucose regulated protein 94 (GRP94) has been identified as PRT main partner.

GRP94 is a constitutively expressed endoplasmic reticulum (ER) lumenal protein, that is up-regulated in response to cellular stress such as heat shock, oxidative stress or glucose depletion.

GRP94 is thought to play a key role in the translocation of protein to the ER, in their subsequent folding and assembly, and in regulating protein secretion. GRP94 plays a role also in antigen presentation, by accessing the endogenous pathway and eliciting specific cytotoxic lymphocyte T (CTL) responses to chaperone bound peptides, via the major histocompatibility complex (MHC) class I pathway. GRP94 is a member of the Hsp90 family of stress proteins and shares 50% sequence homology over its N-domains and complete conservation in its ligand binding domains with Hsp90, its cytosolic isoform. Both Hsp90 and GRP94 are calcium binding proteins, but, despite their homology, they differ in binding affinity with the regulatory ligand ATP and hydrolysis activity. GRP94 exists as a homodimer, and the two subunits interact at two distinct intermolecular sites, the C-terminal dimerization domains and the N-terminal, cross-interacting with the middle domain of the opposing subunits. Furthermore, GRP94 contains a carboxy terminal KDEL (Lys-Asp-Glu-Leu) sequence, which is believed to cooperate in its ER localization.

4.5 Grp94-Perthamide interaction: SPR

Since GRP94 is involved in inflammation, cancer progression and immune system regulation, we decided to measure the interaction between PRT and GRP94, and to this end we evaluated the affinity and the binding specificity by surface plasmon resonance (SPR).

All the SPR experiments were performed using a commercially available canine isoform of GRP94, sharing a high degree of homology with the murine and human enzyme. As reported in **figure 41**, the sequence alignment reveals that these proteins have almost the same aminoacid sequence, and thus, canine protein can be considered a confident model.

Fig. 41. Sequence alignment of murine and canine GRP 94.

SPR is an optical technique suitable for characterizing macromolecular interactions, based on the evanescent wave phenomenon, useful to measure changes in refractive index very close to a sensor surface. The binding between a compound in solution eluting on its partner immobilized on a sensor surface results in a change in the refractive index.

The interaction is monitored in real time, and the amount of bound ligand and the rates of association and dissociation can be measured. Thus, GRP94 was immobilized on a CM5 sensor chip and PRT was injected over at concentrations ranging from 0.5 to 5 μM. In **figure 42**, the sensograms (association and dissociation SPR curves) obtained from the binding of PRT to GRP94 at two different concentrations are shown.

As expected, the increase of response units (RU) in the association phase and the slope of the dissociation phase of the complex are clearly dependent on the analyte concentration. The analysis of the ascendant region of the sensograms gave the k_a values, whereas k_d of the complex was evaluated on the basis of the time required to completely dissociate the complex and the slope of the curve in the descending region.

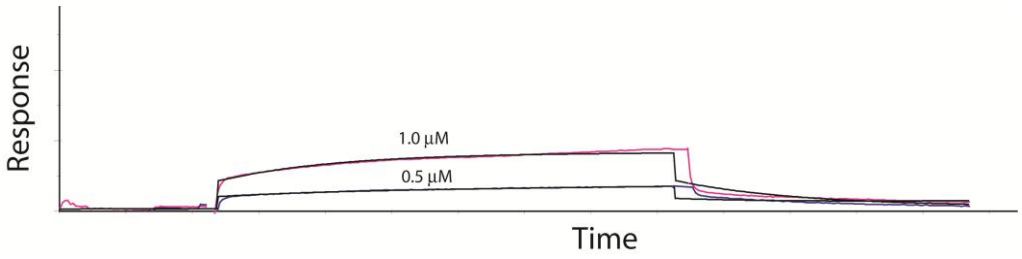

Fig. 42. Sensograms obtained from the binding of PRT to GRP94 at two different concentrations (0.5 μM blue curve and 1.0 μM violet curve).

The dissociation constant K_D of the PRT-GRP94 complex, calculated using a 1:1 Langmuir algorithm, was found to be 2.6 (±2.0) μM. Moreover, the binding selectivity of PRT for GRP94 was assessed comparing the PRT

response vs. bovine serum albumine (BSA). PRT was injected on a BSA-modified sensor chip in the concentration range between 0.5-5 μM, and produced a typical curve shape (red curve) corresponding to an absence of binding (**figure 43**).

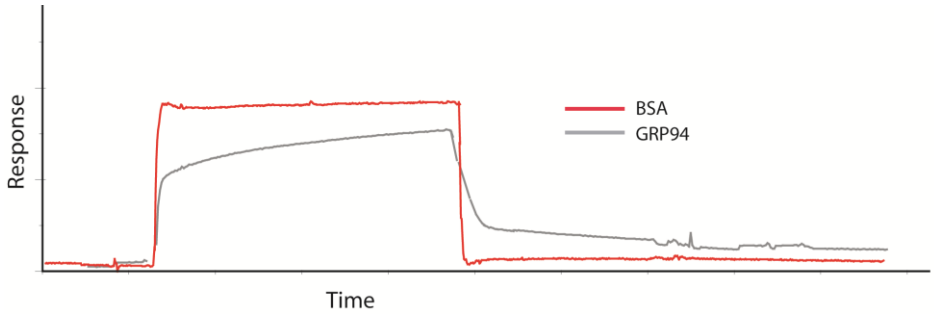

Fig. 43. Sensograms obtained from the binding of PRT to GRP94 (gray curve) and to BSA (red curve) at the same concentration (5 μM).

4.6 Hsp82-Perthamide interaction by SPR

Heat shock proteins (Hsp_s) are a class of functionally related proteins whose expression is increased when cells are exposed to elevated temperatures or other stress[114]. Moreover, intracellular heat shock proteins are highly expressed in cancerous cells and are essential to their survival. Considering the high homology occurring between GRP94 and Hsp90, we decided to test the binding affinity between PRT and Hsp82, the yeast Hsp90 homologue, by SPR. As reported for GRP94, we immobilized Hsp82 on a CM5 sensor chip. Then, PRT was injected over the enzyme-modified sensor chip in the concentrations range 0.5-5 μM. The sensograms (**figure 44**) were analyzed, using a 1:1 Langmuir algorithm through the BiaEvaluation software. The curves reported in figure 44 don't dissociate back to the baseline within a

reasonable time frame, possibly as a result of a strong binding. As a matter of fact, the K_D for the PRT-HSP82 adduct was estimated as 43.3 (±5.0) nM, demonstrating a fifty time stronger binding affinity than the PRT-GRP94 complex.

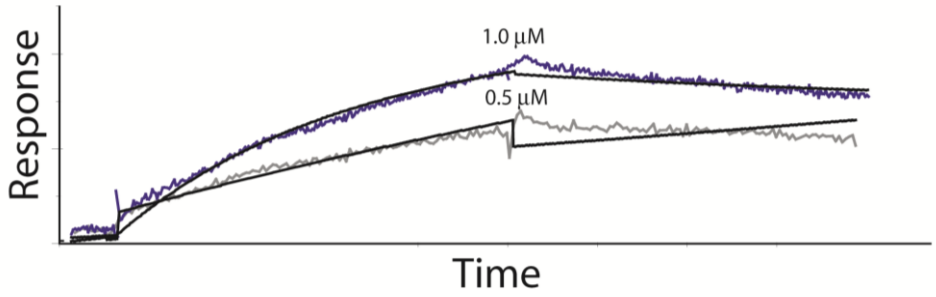

Fig. 44. Sensograms obtained from the binding of PRT to Hsp82 at two different concentrations (0.5 μM gray curve and 1.0 μM blue curve).

The ability of PRT to specifically bind the heat shock protein HSP90 opens the way to further investigation on the role of PRT in the modulation of the enzyme function *in vitro* and *in vivo*. It is noteworthy that Hsp90 was not included in the final list of PRT *partners* in the chemical proteomics approach. However, as reported by Rix and Superti-Furga in 2009[1], HSP90 is a 'frequent hitter protein' which is usually identified both in the drug-bound and control beads proteins lists, due to its high abundance in biological samples and sufficient affinity for the matrix. On this basis, it is usually excluded from the list of the specifically bound partners, as in our case. However, SPR validation assays gave us the chance to measure the PRT affinity for Hsp 90 homologue and to disclose this protein as a strong partner of our natural product.

-CHAPTER 5-

Collagen stimulation of platelets induces rapid spatial reorganizations in cAMP and cGMP signaling scaffolds

Based on: *Mol. BioSyst.* **2011**, Submitted

5.1 Background

Platelets are nuclear cells that play a key role in the control of haemostasis[115-117]. In the non-activated and resting state platelets circulate freely in the blood. The primary function of platelets is to occlude arteries, thereby preventing excessive bleeding after injury. Under pathological conditions, the same mechanisms are responsible for occlusion of vital arteries at the site of ruptured atherosclerotic plaques. Ischemic occlusions can lead to myocardial infarction and stroke[118, 119]. *In vivo*, platelet activation can be triggered by a number of stimuli, such as collagen, ADP, thrombin and serotonin. Direct contact of collagen with the platelets leads to their activation[120]. Platelet surface receptors, such as the glycoprotein VI receptor complex (GPVI) and integrin $\alpha 2\beta 1$,[121] accommodate binding to collagen with consequent adhesion, aggregation, cytoskeletal reorganization and granule secretion of the platelets[122]. All the above-mentioned stimuli act through binding to specific membrane G-coupled receptors, which activate their down-stream intracellular signaling pathways. These tyrosine kinase mediated pathways are responsible for the observed initial physiological responses[122, 123]. In order to maintain intact healthy vessel physiology, a tight regulation of platelet functions and of all these intracellular pathways is required. In general, the actual view of how signaling pathways are regulated is shifted from a more linear controlled system to a dynamic and localized set of events, taking place in a complex network of proteins each having a specific function in time and space[124]. Spatio-temporal control of signaling proteins is an emerging concept that combines the omnipotency and high specificity of many signaling molecules and proteins, even within a single cell. A well-documented example of such a controlled system is the cAMP (3'-5'-cyclic-adenosine monophosphate) regulated signaling that is translated into very specific events at very specific loci within the cell[125].

The main target of cAMP is the cAMP-dependent protein kinase (PKA), which can interact with different members of the A-kinase associated proteins (AKAP) family to achieve spatial specificity. AKAPs physically localize PKA's activity close to its substrates to avoid cross-reactivity of different PKA pathways[126]. Further specificity is achieved by generation of localized pools of cAMP that are generated close to the site of action and not throughout the whole cell[127]. These pools are spatially, but also time-wise controlled by phosphodiesterases (PDEs),[127] that have been shown to co-localize with PKA at specific AKAPs. PDEs degrades cAMP[128] to terminate signaling, and they are themselves dependent on phosphorylation by PKA[129]. Another layer of control is implemented by localization of specific phosphatases to AKAPs to also counteract PKA activity at the level of the substrate[125].

Dynamics in signaling complex constitution, through specific phosphorylation of AKAPs, seems a likely additional level of control. Such modifications could trigger binding/release of specific components in a similar manner as SH2/SH3 domains in tyrosine signaling. However, very few examples have emerged until now[130]. In a more specific context to this work, it has been shown that phosphorylation of the type IIa regulatory subunit of PKA (PKA-RIIa) at Ser99 increases its affinity for AKAPs[131], hinting at potential regulatory dynamics at the level of complex constitution.

It is well known that high intracellular concentrations of cAMP, but also of 3'-5'-cyclic-guanosine monophosphate (cGMP), interfere with the platelet activation pathways[132], mainly through their kinases PKA and cGMP-dependent protein kinase (PKG)[132]. cAMP and cGMP operate downstream[128] of resting signals such as adenosine, ß-adrenergic signals, PGE1, PG-I2 and nitric oxide, respectively. Although characterized to a lesser extent, PKG is also found to localize to specific cellular compartments through interaction with G kinase associated proteins (GKAPs)[133]. How platelets engage in activation and how they respond at the level of cyclic nucleotide

regulated proteins is currently not well understood, but very important to recognize the transition from the resting into the active state.

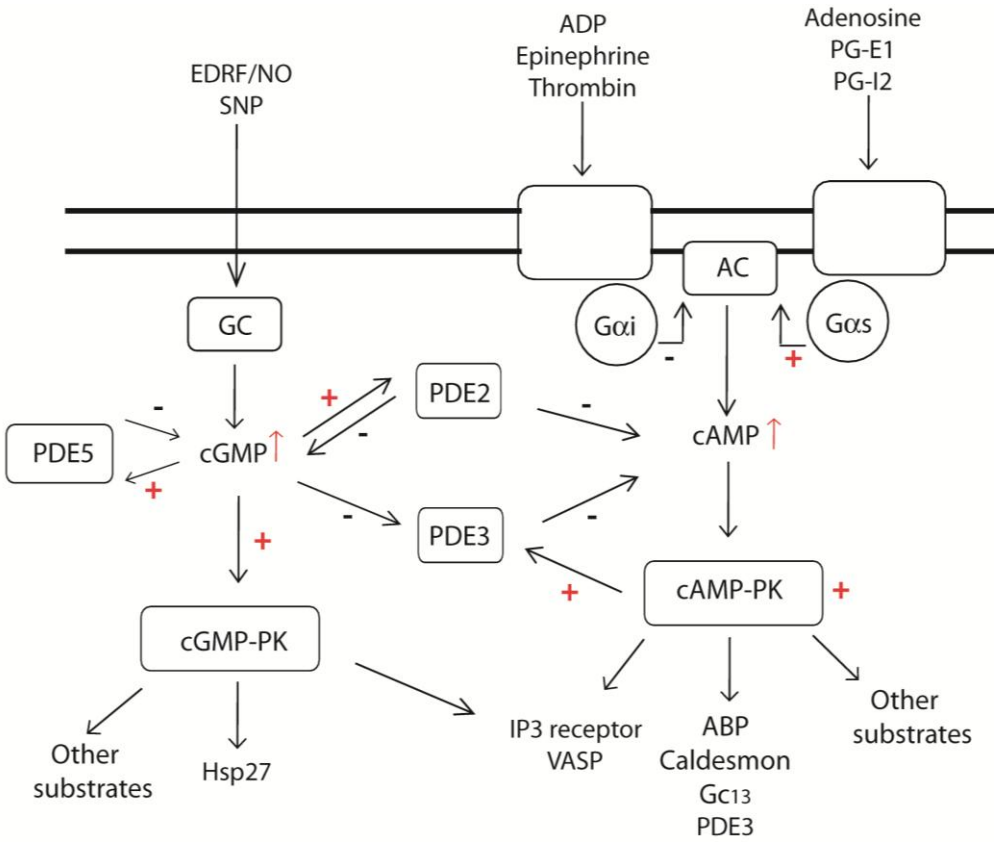

Fig. 45. Regulation and known effector sites of cyclic nucleotides in platelets[132].

Large scale proteomics in combination with stable isotope based quantitation has emerged as an excellent tool to study temporal changes of signaling cascades, especially when focused on phosphorylation[134, 135]. However, the potential to look at protein-protein interaction dynamics has only marginally been exploited.

To study cyclic nucleotide signaling, large-scale phosphoproteomics is not the method of choice as PKA and PKG, but especially their corresponding

AKAPs are generally quite low abundant and therefore often missed in large-scale studies[136]. In this field, we decided to zoom into the specific spatio-temporal alterations of cyclic nucleotide regulated proteins in platelet activation. Thus, we applied a targeted quantitative chemical proteomics approach, using immobilized cAMP and cGMP beads, to specifically enrich this class of signaling proteins[136, 137], and to evaluate the differential cAMP/cGMP-interactome of resting and (for 5 minutes) collagen stimulated platelets. Finally, we focus our attention on several (differential) protein phosphorylation events identified on our pulled down proteins, which can drive the spatial reorganization.

5.2 Isolating Specific Proteins of Interest

A quantitative chemical proteomics approach using dimethyl stable isotope labeling[136, 137] was adapted to monitor downstream changes in cyclic nucleotide dependent proteins upon activation of platelets by collagen (**figure 45**). CRP (collagen related peptide), a specific GPVI agonist, was used to stimulate the platelets, while parallel pathways were blocked (see experimental section).

Differential quantitative pull downs were performed using platelets of five individual human donors, whereby each time CRP-activated (for 5 minutes) and resting platelets of the same donor were compared. After combining all acquired data, we compared this set of enriched proteins with a global unbiased inventory of the whole platelet proteome, allowing us to differentiate background from specific interacting proteins (see experimantal section). This resulted in a small but stringent core cAMP/cGMP interactome of proteins, whose the enrichment in the pull-down was at least 4-fold compared to the global platelet proteome.

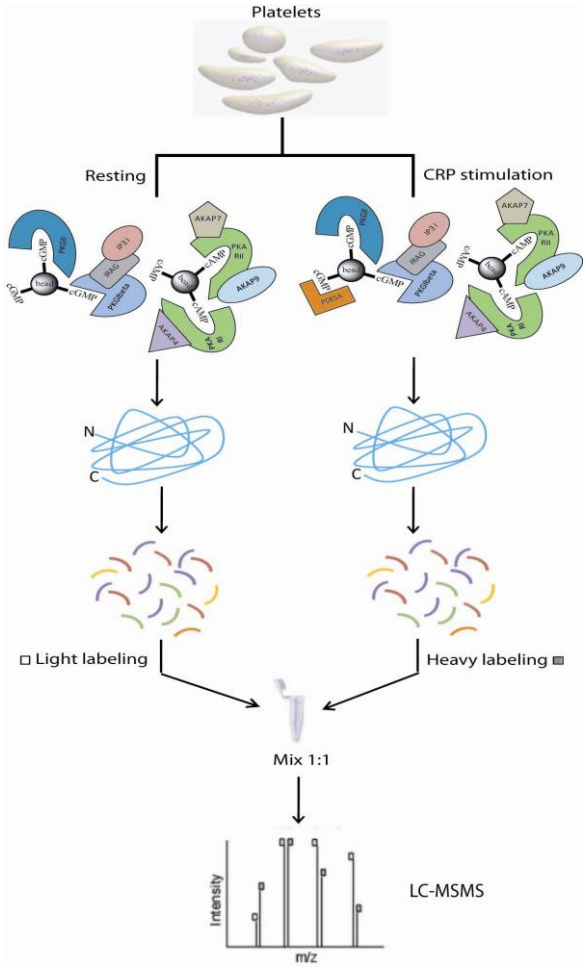

Fig. 46. Chemical proteomics strategy to enrich and differentially quantify pulled-down cyclic nucleotide signaling proteins and their interacting *partners* in resting and CRP stimulated platelets. Isolated platelets were divided in two 80 equal fractions and treated with CRP (active) or saline (resting). In parallel, lysis was performed and proteins were extracted prior to incubation with the immobilized cyclic nucleotide beads. cAMP/cGMP interacting core proteomes were subjected to an in solution digestion prior to stable isotope labeling with regular (light) and deutered (heavy) formaldehyde. Labeled peptides were mixed in a 1:1 total protein amount ratio followed by LC-MS/MS analysis for protein identification and quantitation.

Fifteen proteins within this group have a well-documented connection to cAMP/cGMP signaling, such as several PKA's, PKG's, AKAPs, GKAPs and

PDEs. The other twenty are putative interactome candidates. The differential abundances of these 35 proteins in the pull-downs from activated *versus* resting platelets are summarized in **table 2**.

PKA/PKG/AKAps/GKAP protein	Avg Ratio	Stdev
cAMP-dependent protein kinase type I-alpha	0.98	0.20
cAMP-dependent protein kinase type I-beta	1.03	0.25
cAMP-dependent protein kinase type II-alpha	1.14	0.05
cAMP-dependent protein kinase type II-beta	1.18	0.11
cGMP-dependent protein kinase 1, beta	0.86	0.13
cGMP-dependent protein kinase 2	0.66	0.12
cGMP-specific 3',5'-cyclic phosphodiesterase	2.53	1.24
cGMP-dependent 3',5'-cyclic phosphodiesterase	1.02	0.04
A-kinase anchor protein 7 isoform gamma	1.17	0.06
A-kinase anchor protein 9 OS=Homo sapiens	1.82	0.55
A-kinase anchor protein 2 OS=Homo sapiens	2.04	0.32
cAMP-dependent protein kinase catalytic subunit alpha	2.22	0.99
cAMP-dependent protein kinase catalytic subunit beta	1.75	0.94
Protein MRVI1	2.09	0.54
Inositol 1,4,5-trisphosphate receptor type 2	2.78	1.34
Inositol 1,4,5-trisphosphate receptor type 1	2.58	1.04
Putative cAMP/cGMP interactome	**Avg Ratio**	**Stdev**
Trans-Golgi network integral membrane protein 2	1.92	0.90
Cation-dependent mannose-6-phosphate receptor	1.63	0.82
Lysophospholipase-like protein 1	1.59	1.05
Heterogeneous nuclear ribonucleoprotein H3	1.49	1.08
Calcium-transporting ATPase type 2C member 1	1.44	0.85
Metalloproteinase inhibitor 3 O	1.43	0.44
Galectin-3-binding protein	1.41	0.60
Zinc-binding alcohol dehydrogenase domain-containing protein	1.36	0.27
Short/branched chain specific acyl-CoA dehydrogenase	1.35	1.32
Isobutyryl-CoA dehydrogenase, mitochondrial	1.16	0.58
ATP-dependent RNA helicase DDX3X	1.13	0.28
Ubiquitin	1.09	0.25
Tight junction protein ZO-2	1.06	0.11
Glycogen debranching enzyme	1.04	0.52
Glutaryl-CoA dehydrogenase, mitochondrial	0.95	0.24
Serglycin	0.93	0.25
Transforming growth factor beta-1-induced transcript 1	0.92	0.31
Protein-lysine 6-oxidase	0.88	0.24
Desmoplakin	0.69	0.05
Filaggrin-2	0.65	0.31

Tab. 2. Differential abundances of proteins from cAMP/cGMP signaling and putative cAMP/cGMP interactome identified in the pull-downs from activated *versus* resting platelets. The values, reported ±st. dev, are the average of 5 individual experiments.

5.3 Spatial reorganization occurring in signaling nodes upon collagen activation of platelets

The primary interactors PKA-R and PKG Iß, exhibited a stimulated/resting abundance ratio of around 1.0 (0 on 2log10 scale, **figure 47 A**) in all donors, revealing that both their abundance and affinity to the beads is not altered upon stimulation. In contrast, the amount of PDE5A bound to the beads increased significantly (3.0-fold) upon CRP-activation, whereas the amount of PKG type II (PKG2) decreased slightly (ratio 0.7).

This increased/decreased enrichment reflects more likely a change in affinity towards the beads or availability in the soluble proteome, as we assume that the amount of protein turn-over is negligible in the 5 minute time frame of activation. It is well documented that PDE5 affinity for cGMP increases upon phosphorylation at Ser102[138], therefore we investigated the peptides identified for PDE5A for presence of this modification, but we were unable to observe this specific site. However, in PDE5A, Ser92 was increasingly phosphorylated (data not shown) in activated platelets, and may thus also plays a role in the observed increased affinity of PDE5 for cGMP in stimulated platelets. PDE2, another member of the PDE-family captured in our experiments, displayed no differential affinity in activated platelets (**figure 47 A**).

Next to primary interactors (PKA-R, PKG, PDEs) our approach allowed us to simultaneously monitor the differential association of several known secondary interactors (PKA-C, AKAPs, GKAPs) to the pool of primary interactors. It is well documented that overall cAMP levels and hence overall PKA activity diminish upon platelet activation[139]. This is in agreement with our findings that upon CRP-stimulation the association of the PKA catalytic subunits PKA-Cα and PKACß to PKA-R is increased (2.2-fold and 1.8-fold, **figure 47 B**).

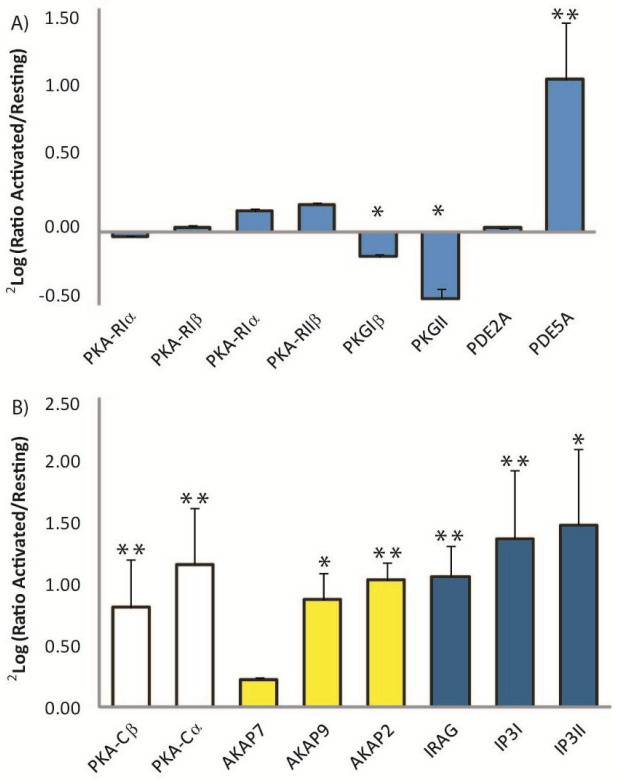

Fig. 47. Differential affinity analysis upon CRP induced platelet activation. (**A**) Differential enrichment ratios (Logscale) of cAMP and cGMP primary interactors. (**B**) Differential enrichment ratios of secondary interactors. The used colors represent different categories; PKA catalytic subunits (white), AKAPs (yellow), PKG interactors (blue). Ratios are normalized *versus* the ratio of their corresponding primary binders (Tab. 2). Significant changes are marked with a * for $p<0.05$ and ** for $p<0.01$.

Increased formation of holo-enzyme leads to reduced kinase activity[140]. A different set of secondary interactors are the AKAPs and GKAPs. Enrichment changes observed for these proteins reflect altered composition of the various signaling scaffolds in activated platelets. As illustrated in **figure 47 B**, binding of AKAP9 and AKAP2 increased significantly upon activation, whereas association to AKAP7 remained unaltered. Some other AKAPs also showed

increased binding, however, these could not be significantly quantified in all five donors (**Table 3**).

Other AKAPs	Avg Ratio	Stdev
A kinase anchor protein 10	**2.2**	1.2
Microtubule-associated protein 2	**4.8**	n.a.
A-kinase anchor protein 11	**1.8**	n.a.
A kinase anchor protein 1	**1.3**	n.a.

Tab. 3. The AKAPs reported in the table showed increased binding upon CRP treatment. These proteins, due to their low abundance, were not quantified in all five donors.

In platelets, the inositol-1,4,5-trisphosphate receptor–associated PKG substrate (IRAG, MRVI1) is assembled in a macromolecular complex together with PKG Iß and the inositol-1,4,5-trisphosphate receptor type I (IP3RI)[141]. Although known to be quite low abundant, we were able to detect all known components of this macro-molecular scaffold complex, following capture of the PKG Iß primary interactor. Interestingly, the association of this PKG/IRAG/IP3R signaling scaffold increased by over 2-fold upon CRP stimulation (IRAG 2.1-fold, IP3R1 2.8-fold, **figure 47 B**), although the primary interactor PKG Iß displayed no changes. Interestingly, also IP3R type 2 (IP3R2) showed the same differential enrichment as IP3R1.

Other proteins in the core proteome of 35 pulled-down proteins have, at present, little known biological connection to the cAMP/cGMP primary interactors (**table 2**, putative cAMP/cGMP interactome). These are potential novel, and /or less specific, interactors of the cAMP/cGMP signaling nodes in platelets.

Using classification programs[142, 143], their involvement in different biological pathways and molecular functions could be divided into several subsets. (**figure 48**). Among them, there is a receptor (Cationdependent mannose-6-

phosphate receptor (M6PR), also referred to as the IGF-II receptor), a Ca^{2+} ion channel (ATP2C1) and several cell-junction/cell adhesion proteins such as TGFB1I1 (Hic5)[144], which is the platelet alternative for paxilin, and Galectin binding protein 3 (LG3BP).

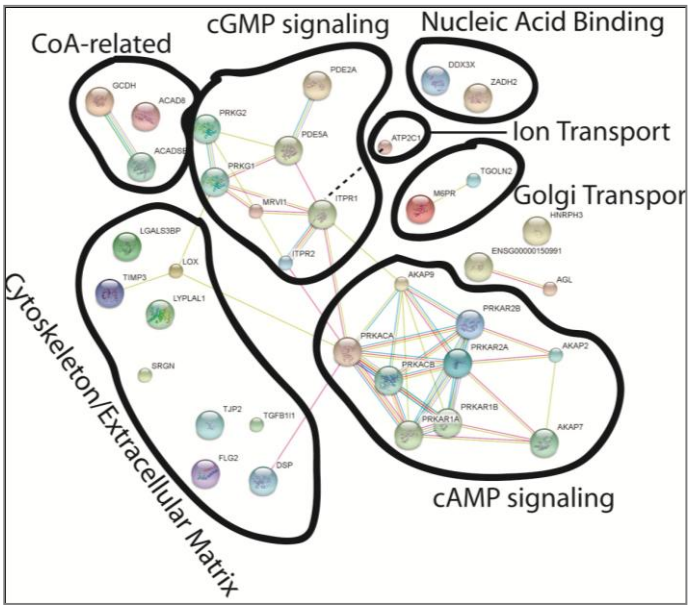

Fig 48. Proteins interaction network obtained using STRING (http://string-db.org/). Proteins with or without an evident biological connection to the cAMP/cGMP system were submitted to STRING to better understand their biological interactions. In the network, links between proteins signify the various interaction data supporting the network, colored by evidence type as outlined in STRING.

5.4 Differential phosphorylation occurring in signaling nodes upon collagen activation of platelets

Crucial steps of platelet resting are regulated by phosphorylation events, many of them mediated by PKA and PKG, which can also be subjected to phosphorylation themselves.

Protein	Peptide	Site	Avg ratio Active/Resting	Avg site ratio	Stdev	n	p-value	Max PTM score
PKGIß	SVIRPATQQAQKQ**S**ASTLQGEPR	S63	0.50	**0.50**	n.a.	1	0.04	26.9
	Q**S**ASTLQGEPR	S63	0.50		0.03	2		46.8
	K**T**WTFCGTPEYVAPEIILNK	T530	0.74	**0.74**	n.a.	1	n.a.	87.2
PKA-RIα	AGTRTDSREDEI**S**PPPPNPVVK	S83	0.97			3		40.3
	TDSREDEI**S**PPPPNPVVK	S83	1.51	**1.19**	0.35	2	>0.05	78
PKA-RIIα	RV**S**VCAETYNPDEEEEDTDPR	S99	1.58			4		103.83
	RV**S**VCAETYNPDEEEEDTDPRVIHPK	S99	1.44	**1.54**	0.40	2	0.01	37.1
	VADAKGD**S**E**S**EEDEDLEVPVPSR	S86+ S88	0.90	**0.90**	n.a.	1	n.a.	no
PKA-RIIß	RA**S**VCAEAYNPDEEEDDAESR	S114	1.10			2		103.84
	RA**S**VCAEAYNPDEEEDDAESRIIHPK	S114	0.91	**1.04**	0.15	1	>0.05	42
MRVI1 (IRAG)	SRSSPGDSPSAVSPNL**S**PSASPTSSR	S189	0.80			1		174.19
	SSPGDSPSAVSPNL**S**PSASPTSSR	S189	0.86	**0.83**	0.04	1	>0.05	92.4
	GL**S**WDSGPEEPGPR	S367	0.72	**0.72**	0.17	2	>0.05	87.6
	RRV**S**VAVVPK	S670	0.4	**0.38**	n.a	1	n.a	51.7

Tab. 4. Differential abundance of phosphorylation sites on cyclic nucleotide based signaling proteins before and after CRP stimulation. The active *versus* resting ratio for each observed phosphorylation is given including their standard deviations and amount of peptides observed. These ratios were normalized against the observed protein ratios (based on detected non-modified peptides, supplemental table 3). T-tests for significance of change were performed by comparing the phosphorylation site ratios with the protein ratios. The maximum PTM score for each phosphopeptide was obtained from MSQuant to provide confidence in the site localization[145].

Although we did not specifically enrich for phosphoproteins or phosphopeptides, we were able in our experiments to identify and differentially quantify 14 different phosphopeptides (**table 4**), representing 9 different phosphorylation sites (**table 4**). Although this number is relatively low compared to high-throughput phosphoproteomics datasets, it should be noted that several proteins we detected are novel, likely due to the strong enrichment of very low abundant signaling proteins. The differential extent of phosphorylation was calculated following normalization to their protein ratio (based on all non-phosphorylated peptides). We observed that PKA-RIIα was up-phosphorylated at Ser99, while PKG Iβ showed a decreased phosphorylation at Ser63 upon CRP stimulation as illustrated by the mass spectra displayed in **figure 49**.

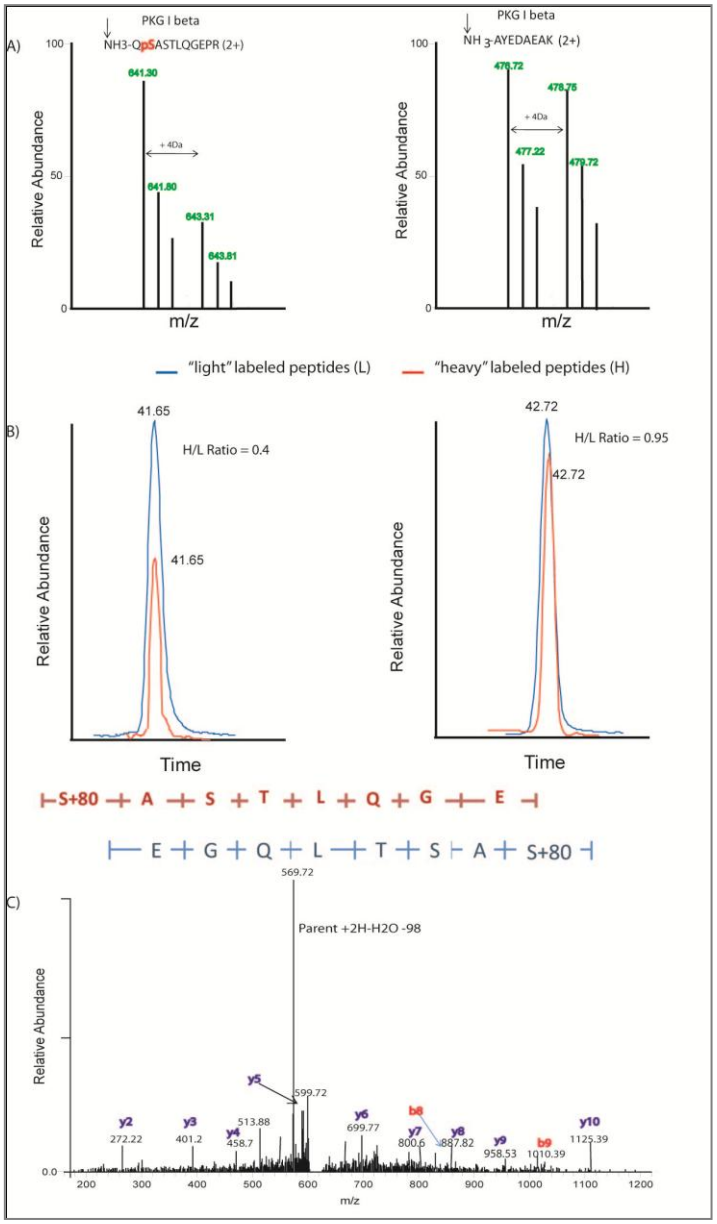

Fig. 49. PKG Iß phosphorylation at Ser63 is reduced upon platelet activation with CRP (**A**) Dimethylated peak pair of the phosphorylated PKGI_ peptide Q**pS**ASTLQGEPR (left) and of the non-phosphorylated PKG Iß peptide AYEDAEAK 5 (right). Extracted ion chromatograms of the phosphopeptide Q**pS**ASTLQGEPR compared with a non-phosphorylated peptide of PKGIß (AYEDAEAK). (**B**) The corresponding extracted ion chromatograms of this peptide show a ~50% decrease in phosphorylation of the Q**pS**ASTLQGEPR (**C**) The tandem mass spectrum of the phosphopeptide unambiguously identifies Ser63 to be the site of modification.

Also several, either reported or novel, phosphorylation sites on IRAG were detected, and did not change upon CRP stimulus, except S670 wherefore the phosphorylation decreased by about 60% upon activation.

5.5 Spatial alterations in specific signaling nodes

cAMP and cGMP and their respective kinases are heavily involved in platelet homeostasis, however their localized nature in platelets has not been investigated. Our quantitative chemical proteomic approach was used here to characterize the dynamic nature of the cAMP/cGMP core interaction proteome in resting *versus* activated platelets to reveal how the cyclic nucleotide system adapts to this transformation.

Up to now, this was only addressed at the level of cAMP and cGMP concentrations and PKA/PKG activity[132] (that was observed to decrease upon stimulus); however the downstream effects of this have not been addressed previously. Our data show that the constitution of several signaling complexes changes already significantly and rapidly within the 5 minute stimulation time window. In other words, upon platelet stimulus, PKA and PKG rearrange in different signaling complexes of which details are shown in **figure 50** that will be further discussed below.

5.6 Alterations in cGMP/PKG signaling nodes

We identified two isoforms of PKG in human platelets; PKGIα and PKG2. The former is a well documented isoform in platelets, whereas the latter has no prior functional annotation in platelets.

The IP3RI receptor regulates IP3 mediated release of Ca^{2+} from intracellular stores, an important process in platelet activation[146]. PKG Iα inhibits this process through phosphorylation of IRAG at S657 and S670 (Uniprot sites on MRVI1_HUMAN), thereby locking IP3RI in an inactive state[141].

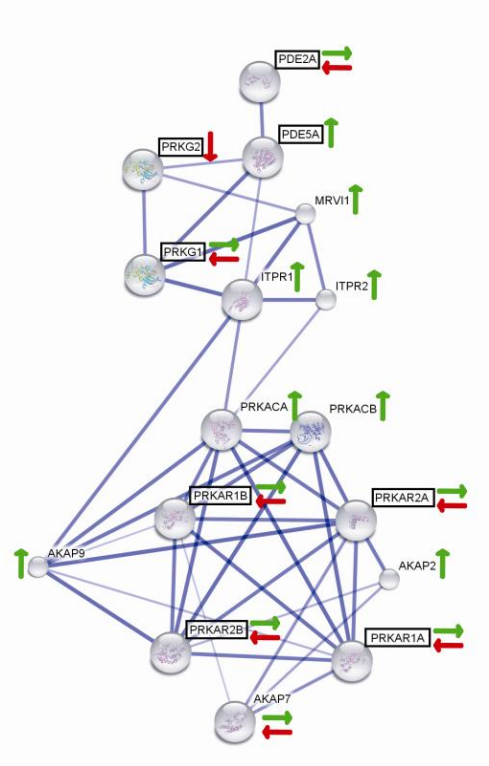

Fig. 50. Summary of the observed alterations in the PKA and PKG signaling scaffolds upon CRP induced platelet activation. Depicted is the STRING network (http://string.embl.org), evidence view. The thicker blue lines represent more robustly documented interactions of the core cAMP/cGMP platelet interactome. Boxed proteins are primary cAMP/cGMP-bead interactors, non-boxed proteins are secondary interactors. Red arrows indicate overall decrease in protein capture, green arrows indicate increase, horizontal red and green indicates unaltered enrichment after 5 minutes stimulation of platelets. Increased capture of secondary interactors indicates dynamic rearrangements of PKA/PKG signaling scaffolds.

We now show that upon platelet activation by collagen, the activity of this protein complex is affected at several levels of organization simultaneously.

First of all, the activity of PKGIα itself is reduced due to the observed reduced autophosphorylation at Ser63. Phosphorylation at this site is a measure of PKG's basal activity which renders it less dependent on cGMP[147].

As expected, we observed that Thr530 in the catalytic cleft of PKG Iα is constitutively phosphorylated[148]. Second, phosphorylation of IRAG at S670 was found to be reduced by 60%. This fits well with the observation by Antl *et al.* who showed that exogenous stimulus of platelets with cGMP or nitric oxide (induces resting) increased PKG-mediated phosphorylation at this site[141]. Both these decreased phosphorylation events will reduce activity of the PKG/IRAG couple and hence likely increase IP3-mediated Ca^{2+} release through the IP3RI to drive platelet activation. Antl *et al.* also showed that a small fraction of the total platelet PDE5 population is present in this complex and that only this portion of PDE5 is increasingly phosphorylated at Ser102[141, 149] upon platelet stimulus, likely to reduce local cGMP concentrations more actively, thereby increasing IP3RI activity. Although we were unable to detect phosphorylated Ser102, we did observe Ser92 to be increasingly phosphorylated in a highly substoichiometric amount upon activation. This suggests that also Ser92 may be involved in this process.

An intriguing observation is the general enlarge in enrichment of this intact scaffold complex following platelet activation, indicating increased tightness of the complex, possibly regulated by differential phosphorylation or other post-translational modifications. It seems there is a feedback mechanism in place here: Platelet activation leads to a decrease of PKG and IRAG activity, but to an increase in PKG/PDE5 localization to IRAG, probably to accommodate a rapid and efficient blockade of Ca^{2+} release from IP3R in case cGMP levels rise again. The cAMP/cGMP second messenger levels are regulated in space and time by a balance in production and degradation, catalyzed by localized PDEs. The major PDEs in platelets are thought to be PDE2 (hydrolyzes cAMP and cGMP, directly activated by cGMP), PDE3

(hydrolyzes cAMP and cGMP and is activated by PKA) and PDE5 (hydrolyzes cGMP and is activated directly by cGMP and by PKG)[132].
In this study, PDE5 is clearly the most dominant PDE, although PDE2 was also detected. PDE3 was not detected which may be due to the specific utilized capturing compounds, and/or its membrane localization properties. Upon CRP stimulation, we observed that the amount of captured PDE5 increased significantly whereas the level of PDE2 remained constant.
The increased affinity could be mediated by Ser92/Ser102 phosphorylation, however these phosphorylations can only occur to the small fraction of PDE5 that is localized to the IRAG/IP3RI complex (~1-2% at best)[141] and would not explain the overall increase of 3-fold in the total PDE5 pool. An alternative explanation may rise from the possibility that more PDE5 becomes available into the soluble proteome through release from a localized membrane-bound source.

5.7 Alterations in cAMP/PKA signaling nodes

In general, activation of platelets leads to reduced cAMP levels through an inhibitory G-protein coupled receptor mediated inhibition of cAMP production by adenylate cyclase[132]. A reduction in cAMP concentration then leads to dissociation of it from PKA-R and increased PKA-R/PKA-C holoenzyme formation. There are four distinct genetic isoforms of PKA-R. Our data reveal that based on spectral counts[137], PKA-RIα, RIIα and RIIβ constitute the major isoforms in platelets, whereas PKA-RIβ seems under-represented. We identified 7 AKAPs in platelets, whereby AKAP9, AKAP7 and AKAP2 were most abundant, although AKAP1, AKAP10, AKAP11 and MAP2 were also detected. Interestingly, similarly to PKG/IRAG, stimulation of platelets seems to lead to tighter association of PKA with certain AKAPs.

Our data reveal that collagen activation diminishes overall PKA activity as measured by the increase in pulled down holo-enzyme. Several phosphorylation sites were observed on PKA-R proteins (**table 4**), of which Ser99 of PKA-RIIα was the only one detected that changed upon collagen stimulation.

Recently, in the rat neonatal cardiomyocyte context[131], a higher level of this phosphorylation site was linked to a decreased affinity for PKA-C and thus higher activity of PKA, which contradicts the view of PKA being less active in activated platelets. Also, increased phosphorylation of Ser99 increases the affinity of PKA-RIIα for AKAPs both *in vitro* and *in vivo*[131], in line with what we observe here since AKAP9 is a known PKA-RII interacting AKAP[136]. In the same model, this increased AKAP interaction of PKA-RIIα leads to increased phosphorylation levels of the nearby substrates phospholamban and the ryanodine receptor through interaction with AKAP15/18 to ultimately increase the contractile Ca^{2+} response in these cells[131]. In platelets, increased phosphorylation could accommodate the observed increased calcium release upon activation, albeit not through AKAP7 and the ryanodine receptor, but perhaps through AKAP9 and IP3R, which have recently been reported to interact in cerebellar granule cells[150]. This would mean that one, or more, specifically localized pools of PKA-RIIα have a stimulatory effect on platelet activation, rather than on resting. This enforces the idea that different spatio-temporally controlled pools of cyclic nucleotide based signaling proteins have different functions.

Altogether, our quantitative chemical proteomics approach to monitor collagen stimulation of platelets presents a detailed characterization of the cyclic nucleotide signaling proteins that play a role in the platelet activation response. The role of the PKG/IRAG/IP3RI complex, but also that of PKA-C in platelet activation, is recapitulated here and validates our approach. We show that the constitution of several signaling scaffolds is highly dynamic

upon activation in platelets. This suggests that PKA and PKG relocation is important to accommodate the required intracellular changes induced by external signals. This interesting novel concept deserves extensive in-depth analysis at individual scaffold levels in the future, including the analysis of phosphorylation dynamics on AKAPs.

-CONCLUSIONS-

6.1 Conclusions

The target discovery of bioactive molecules endowed with intriguing pharmacological profiles is one of the main issues in the field of pharmaceutical sciences, since this is needed for a rational development of potential drugs. Indeed, a comprehensive characterization of a small molecule interaction profile inside a complex mixture, such as a cell environment, is necessary for a better comprehension of its poly-pharmacological activities and toxicities[2]. Moreover, the identification of the interactome of a potential drug needs a validation through biological evaluations, in which the role of the bioactive compound towards the identified target proteins has to be revealed and measured. Recent technological developments in the field of analytical methods, mainly mass spectrometry and liquid chromatography, gave and are still giving a significant improvement in the target discovery studies. In particular, mass spectrometry-based chemical proteomics is emerging as a powerful tool for a comprehensive characterization of a drug interactome, under physiological relevant conditions. Besides, even when the target of a drug is already known, information about the off-target activities are needed for a comprehensive evaluation of potential side effects and toxicities. Indeed, a drug hitting multiple targets can be applied in the therapy of several unrelated diseases or to increase its efficacy for a complex therapeutic application. On the other side, the modulation of multiple targets can also cause harmful drug side effects, which could be compensated, once known, by extra therapies or dose tuning.

In this appealing scenario, I have optimized a strategy focused on chemical proteomics-based target discovery of three marine metabolites, namely Petrosaspongiolide M (PM), Bolinaquinone (BLQ) and Perthamide C (PRT C), all showing relevant anti-inflammatory properties. Since their pharmacological profile has been shown to be related to multiple enzyme

inhibition, a full investigation of their interactome is of a broad interest to better understand the mechanism of action and the comprehensive effect on a living cell. The application of this method allowed us to successfully discover the interactome of the above mentioned marine bioactive metabolites.

The γ-hydroxy-butenolide terpenoid PM have been subjected, in the past, to a detailed *in vitro*[55] and *in vivo*[56] pharmacological investigation. It was found to inhibit human synovial PLA_2 with IC_{50} of 0.8 μM[54], and to reduce the levels of prostaglandin E2, tumor necrosis factor α , and leucotriene B4 in a dose-dependent fashion[55,56]. In addition, an in-depth pharmacological investigation revealed its interference with the NF-kB pathway, with a consequent decrease of NF-kB–DNA binding[56]. Since the NF-kB pathway plays a crucial role in the development of the inflammation response, it was desirable to identify the specific target modulated by PM, representing a potential therapeutic target. The proteasome complex has been established as the primary cytoplasmatic target of PM. This evidence has been also validated by SPR and both *in vitro* and *in cell* assays. SPR data gave equilibrium binding constants (K_D) (PM–proteasome) of 8 (±3.1), and 0.7 (±1.1) nM for the 20S proteasome and its PA28 complex, respectively, confirming a strong affinity between the ligand and its partner. Then, *in vitro* and *in cell* fluorescence experiments showed a relevant blocking of the proteasome activity by PM.

More in details, PM was able to inhibit caspase- and chimotrypsin-like activity with an IC_{50} of 0.85 (±0.15) μM and 0.64 (±0.11) μM, respectively, while the trypsin-like activity of the proteasome resulted to be increased. This is not surprising, since this effect has been already reported for several inhibitors of caspase-like sites which allosterically stimulates the trypsin-like activity[87]. These results gave evidence of the reported effect of Petrosaspongiolide M on the NF-KB pathway[151].

The same approach has been used to determine the interacting partners of BLQ, a marine hydroquinone isolated from the marine sponge *Dysidea sp.* BLQ was extensively studied as anti-inflammatory compound, indeed its PLA_2-inhibition properties[96, 97] and anti-inflammatory pharmacological profile were thoroughly examined, both *in vitro* and *in vivo*[57]. In particular, BLQ is able to reduce the production of mediators in acute and chronic inflammation, and is a modulator of the oxidative stress parameters in 2,4,6-trinitrobenzenesulphonicacid (TNBS)-induced colitis in mice [55]. Moreover, as reported by Busserolles and co-workers, BLQ dramatically reduces nitrotyrosine immuno-detection and colonic superoxide anion production, and decreases apoptosis, suggesting a potential protective action in intestinal inflammatory diseases[55]. Due to this wide anti-inflammatory profile, BLQ represented a good candidate for a target discovery-oriented chemical proteomics study. In this case, a so-called 'off-target' partner has been found, since clathrin was detected as major specific BLQ target[152]. The high affinity showed by BLQ versus clathrin was also proved through serial affinity chromatography approaches, opening the way to further investigation on the role of BLQ in the cellular uptake processes. Clathrin is a main component of the coated vesicles responsible for receptor-mediated endocytosis at the plasma membrane and for the receptor-mediated sorting of lysosomal enzyme. Clathrin-mediated endocytosis plays an important role in the selective uptake of proteins, viruses and other biologically important macromolecules at the plasma membrane of eukaryotic cells.Therefore, its modulating agents are considered significant targets for bio-pharmacological studies. To verify the biological relevance of BLQ towards the clathrin-mediated endocytosis, we studied the clathrin-dependent internalization of albumin by means of fluorimetric assays. The cytofluorimetric and microscopy analysis performed using a fluorescence-tagged BSA let us to measure the ability of BLQ to strongly inhibit clathrin-dependent internalization processes. On this basis,

BLQ can be considered a good candidate as new biotechnological tool with a novel chemical scaffold for the investigation of cell endocytosis processes.

Pertamide C is a cyclic peptide isolated from the sponge *Theonella swinhoei*[110], containing both natural and un-natural aminoacids, and it has been subjected to an *in vivo* investigation to test its anti-proliferative and anti-inflammatory activities. PRT C did not show cytotoxic activity on KB cell line up to a dose of 10 mg/mL, whereas it is able to significantly reduce carrageenan-induced paw oedema both in the early phase (0–6 h) and in the late phase (24–96 h). Moreover, PRT C showed a dose dependent anti-inflammatory profile which lead to a 60% reduction of the oedema, in mice, when administered at 300 μg/Kg[110]. When compared with naproxen anti-inflammatory profile (ED50 40 mg/kg), PRT resulted about 100 times more potent.

Since an anti-inflammatory activity in the field of marine cyclic peptides is not common, with the exception of cyclomarins, salinamides and halipeptins, PRT C has been worthy of further investigations about the origin of its activity. A comprehensive characterization of PRT C interactome has been performed by chemical proteomics, revealing endoplasmin, the glucose regulated protein 94 (GRP94), as the major partners of PRT C (*unpublished data*). The affinity between PRT C and its partner has also been tested by SPR experiments, measuring a K_D of 2.5 μM (±2.1).

GRP 94 is an endoplasmic reticulum (ER) lumenal protein up-regulated in response to cellular stress such as heat shock, oxidative stress or glucose depletion, which plays a key role in the translocation of proteins to the ER, in their folding, assembly and in regulation of protein secretion. In addition, we tested the ability of PRT to bind another protein chaperone, called Hsp82, the yeast homolog of Hsp90. It has to be noted that Hsp90 was not included in the final list of PRT C *partners* obtained upon chemical proteomics approach,

since, due to its high abundance, was identified as a matrix interactor. However, the SPR validation assays gave us the chance of measure PRT real affinity for Hsp 90 homolog and disclose this protein as an additional partner of our natural product. Indeed, PRT strongly binds Hsp82 with a K_D of 80.3 (±5) nM, opening the way to further investigation on role of PRT in the modulation of heat shock protein function.

A complementary point of view about the effect of a small bioactive molecule on cellular systems can be given by a quantitative chemical proteomics based approaches. On this basis, I employed this technique to discover the effect of collagen on platelet activation. Since cAMP and cGMP play a key role in platelet activation[132], a combination of quantitative chemical proteomics approach with the specific enrichment of cAMP/cGMP signaling nodes has been performed[135, 136], to investigate how cAMP-dependent protein kinases (PKA), and cGMP-dependent protein kinases (PKG) spatially reorganize in activated human platelets.

Evaluating the differential cAMP/cGMP-interactome of resting and collagen stimulated platelets of healthy human donors, I have revealed that both PKA and PKG significantly alter their intracellular localization, in particular, through attachement to different AKAPs and GKAPs. This evidence suggests that dynamic re-arrangement of these kinase scaffolds is a mean to adapt the system in response to the stimulus. Using protein phosphorylation data, several (differential) protein phosphorylation events were identified on our pulled-down proteins, which putatively are correlated to the observed spatial reorganization.

EXPERIMENTAL SECTION

-CHAPTER 7-

Chemical proteomics applied to Petrosaspongiolide M, Bolinaquinone, Perthamide C target discovery: Experimental procedures

7.1 Petrospongiolide M target discovery

7.1.1 Material

Reacti-Gel (6X) CDI support was obtained from Pierce. The diamine linker (PEG, 4,7,10-trioxa-1,13-diamine) such asthe protease inhibitor cocktail were purchased from Sigma Aldrich. 20S Proteasome (human recombinant) and PA28 activator (human recombinant) were obtained from Boston Biochemical. All fluorogenic substrates (Suc-LLVY-amc, Boc-LRR-amc and Ac-GPLD-amc) were purchased from Biomol International.

7.1.2 Generation of a Functional Petrosaspongiolide M Affinity Matrix

0.5 ml (dry volume) of the CDI activated Reacti-Gel (6X) beads was treated with 4,7,10-Trioxa-1,13-tridecanediamine (PEG) at 100 μM for 16 h at 25°C in NaHCO3 (10 mM) at pH 10. Then, the modified Reacti-Gel was washed three times with PBS and the presence of free amine groups on the modified Reacti-Gel surface was detected by Kaiser Test[153].

To obtain PM-fixed beads, the amine-beads were treated with 15 μmol of PM in 30% ACN/ 70% PBS at pH 10, and the mixture was kept for 16 h at 37 °C under continuous shaking.

The amount of immobilized PM was calculated integrating the peaks relative to free PM after HPLC injections of supernatants at t = 0 h and t= 16 h using an Agilent 1100 Series chromatographer, on a Phenomenex C18 column (250 x 2.0 mm) at a flow rate of 200 μl/min. The gradient (Solution A: 0.1% TFA, solution B: 0.07% TFA, 5% H2O 95% ACN) started at 10% and ended at 95% B after 15 min.

Time	%A	%B
0	90	10
5	90	10
15	5	95
20	5	95

Tab. 5. HPLC gradient used to quantify PM immobilization yield

The imine bond occurred between PM aldehyde and free amine groups was reduced to amine with NaBH4 100 mM in sodium borate buffer (10 mM) at pH 8.5 for 30 min. The residual amino groups were blocked with 300 mM acetic anhydride dissolved in DMF at 10% TEA.
To obtain the control matrix, the activated Reacti-Gel (6X) Support was mixed with PEG (100 μM) in PBS at pH 10 followed by the coupling with acetic anhydride. The matrices were stored at 4 °C.

7.1.3 Purification of Cellular Petrosaspongiolide M Targets by Affinity Chromatography

THP-1 monocytic cell line was cultured in RPMI medium (Sigma) supplemented with 10% (v/v) foetal bovine serum (Sigma), 100 U/ml penicillin and 100 μg/ml streptomycin (Sigma) at 37 °C in a 5% CO2 atmosphere. THP-1 cell line was differentiated into a macrophage-like

phenotype by incubation with phorbol-12-myristate-13-acetate (PMA). To induce an inflammatory response, bacterial lipopolysaccharides (LPS) were added to the culture medium at a final concentration of 100 μg/ml for 24 h. Induced cells were scraped off and harvested by centrifugation at 4000g, 4°C for 10 min and immediately frozen. Cell pellets were lysed in PBS 1X (50 mM Natrium Phosphate, 150 mM Natrium chloride), 0.1% Igepal, supplemented with protease inhibitor cocktail and clarified by centrifugation 12000g, 4°C for 20 min. Protein concentration was determined by Bradford assay [154, 155] and adjusted to 1 mg/ml.

PM-fixed beads (50 μl dry volume) and the control beads (50 μl dry volume) were separately mixed with 500 μl of crude cell extract (1mg/ml) and incubated at 4°C for 16 h on a rotating wheel. After six washing with PBS, the bound proteins were eluted with SDS-PAGE sample buffer (60 mM Tris/HCl pH 6.8, 2% SDS, 0.001% Bromophenol blue, 10% Glicerol, 2% 2-Mercaptoethanol), separated by electrophoresis and stained with Comassie brilliant blue G-250 Bio-Rad Laboratories[156-158].

Each lane of the SDS-PAGE separation was cut in 13 pieces. Gel pieces were subsequently washed with MilliQ Water and Acetonitrile and the proteins were digested *in situ* as described in Shevchenko protocol[159]. Briefly, gel slices were reduced in 1,4-dithiothreitol (10 mM) and alkylated with iodoacetamide (50 mM), then washed and rehydrated in trypsin solution (12 ng/μL) on ice for 1h. After the addition of 30 μL ammonium bicarbonate (10 mM, pH 7.5), samples were digested overnight at 25 °C. 5 μL of the obtained peptide mixture were injected onto a nano Acquity LC system (Waters Corp. Manchester, United Kingdom).

The peptides were separated on a 1.7 μm BEH C-18 column (Waters Corp. Manchester, United Kingdom) at a flow rate of 200 nl/min. The gradient (Solution A: 0.1% formic acid, solution B: 0.1% formic acid, 100% ACN) started at 5% and ended at 50% B after 55 min. MS and MS/MS data were

acquired using a Q-TOF Premier mass spectrometer (Waters Corp., Micromass, Manchester, United Kingdom, **figure 51**).

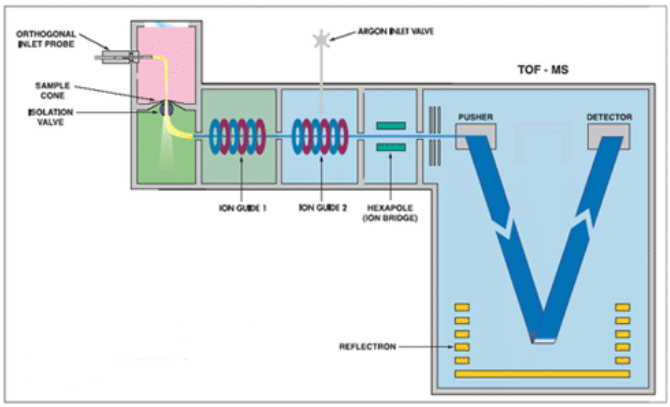

Fig. 51. Schematic rapresentation of Q-tof Premier mass spectrometer (Waters Corp., Micromass, Manchester, United Kingdom).

Doubly and triply charged peptide-ions were automatically chosen by the MassLynx software and fragmented. MS data were automatically processed and peaklists for protein identifications by database searches were generated by the ProteinLynx software. Database searches were carried out with MASCOT server using the SwissProt protein database. The SwissProt human database (514212 sequences; 180900945 residues) was searched allowing 2 missed cleavages, carbamidomethyl (*C*) as fixed modification, oxidation (M) and phosphorylation (ST) as variable modifications. The peptide tolerance was set to 80 ppm and the MS/MS tolerance to 0.8 Da.

7.1.4 Cell Viability Assay

Cell viability was assessed by 3-(4,5-dimethylthiazol-2-yl)-2,5-diphenyltetrazolium bromide (MTT) assay[161]. After PM treatment in a

concentration range from 1 nM to 1000 nM, the mitochondrial-dependent reduction of 3-(4,5- dimethylthiazol-2-yl)-2,5-diphenyltetrazolium bromide (MTT) to formazan was used to assess the cytotoxic effect of PM.

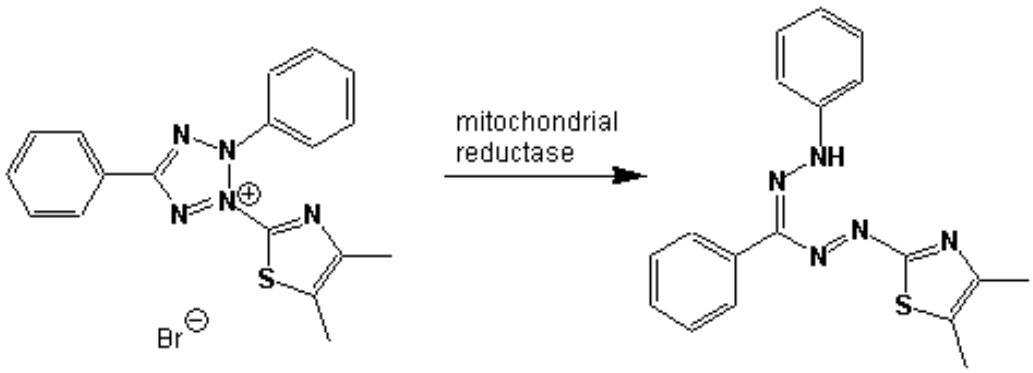

Fig. 52. Mitochondrial-dependent reduction of 3-(4,5- dimethylthiazol-2-yl)-2,5-diphenyltetrazolium bromide (MTT) to formazan.

7.1.5 In vitro Inhibition of 20S Proteasome Activity by Petrosaspongiolide M

The fluorogenic peptides Suc-LLVY-amc (10 μM), Boc-LRR-amc (10 μM) and Ac-GPLD-amc (10 μM) were used to measure the chymotrypsin-like, trypsin-like and peptidylglutamyl hydrolyzing activities of the 20S proteasome, respectively.

To increase the 20S proteasome activity, 0.1 μg of purified 20S proteasome was pre-incubated with PA28 activator (0.2 μg) for 15 min at 37 °C in 100 μl assay buffer (25 mM HEPES, 0.5 mM EDTA, pH 8.5). This step was followed by an additional incubation with either solvent (control) or PM at different concentrations ranging between 0.5-5 μM at 37°C for 30 min. The reaction was started by the addition of one of the substrates (10 μM). The released 7-

amino-4- methylcoumarin (amc) was monitored continuously (excitation, 380 nm; emission, 460 nm) using a multi-well plate Perkin Elmer LS55 Fluorescence Spectrometer.

7.1.6 Cellular Inhibition of 26S Proteasome Activity by Petrosaspongiolide M

The human monocytic cell line THP-1 was differentiated as described above and then incubated with 0.1, 0.5 and 1 μM PM or 1 μM MG132 for 24 h. As the small molecules were withdrawn from 100X stock solutions in Me_2SO equal amounts of Me_2SO were added to control samples.
Cells were then scraped off and harvested by centrifugation. The cell pellets were incubated with lysis buffer (PBS 1X, 10% glycerol, 0.1% Igepal supplemented with a protease inhibitors cocktail) for 5 min on ice and sonicated for two pulses of 10 s, at 30% output power, using a *Vibracell* sonicator. Lysates were then centrifuged for 10 min at 10000g and 4 °C to remove cellular debris, and the protein concentration was determined according to Bradford using BSA as standard[154].

7.2 Bolinaquinone target discovery

7.2.1 Chemicals

Reacti-Gel (6X) CDI support was obtained from Pierce. The linker 4,7,10-trioxa-1,13-tridecanediamine (NH_2-$(PEG)_2$-NH_2) and the protease inhibitor cocktail were purchased from Sigma Aldrich. The Trt-NH-$(PEG)_2$-NH_2 was from Merck. Chlorpromazine was from Sigma. Alexa Fluor 488 - Bovine

serum albumin (BSA) conjugate was from Molecular Probes (Invitrogen detection technologies). THP1 cell line was from ATCC Cell Bank.

7.2.2 BLQ chemical modification with 4,7,10-trioxa-1,13-tridecanediamine

10 mg of BLQ (25 mmol) were incubated with NH_2-$(PEG)_2$-NH_2 (50 mM) in 1 ml of $NaHCO_3$ (10 mM) containing 40% of ACN. The reaction mixture was maintained under shaking for 2h at 50°C. After the RP-HPLC fractionation, the mass spectrometry analysis was carried out on the major product of the reaction using a Q-TOF Premier Instrument (Waters, Manchester UK). The BLQ-NH-$(PEG)_2$-NH_2 adduct was purified using an Agilent 1100 Series chromatographer equipped with a Phenomenex C18 column (250 x 4.6 mm). The gradient (Solution A: 0.1% TFA, solution B: 0.07% TFA, 5% H_2O 95% ACN) started at 10% and ended at 95% B after 15 min at flow rate of 1 ml/min.

7.2.3 Generation of a Functional Boliquinone Affinity Matrix

0.5 ml (dry volume) of the CDI activated Reacti-Gel (6X) beads were treated with 7.5 mg of BLQ-NH-$(PEG)_2$-NH_2 (13 mM) at 37 °C in $NaHCO_3$ (10 mM) at pH 10. The mixture was maintained under continuous shaking for 16 h. The amount of immobilized BLQ-NH-$(PEG)_2$-NH_2 was calculated integrating the peaks of the free BLQ-NH-$(PEG)_2$-NH_2 species after HPLC injections of supernatants at t = 0 h, t= 2h and t=16h, using an Agilent 1100 Series chromatographer. The HPLC runs were carried out onto a Phenomenex C18 column (250 x 2.0 mm) at a flow rate of 200 µl/min. The gradient (Solution A:

0.1% TFA, solution B: 0.07% TFA, 5% H_2O 95% ACN) started at 10% and ended at 95% B after 15 min. The residual CDI groups were inactivated with 100 mM ethanolamine dissolved in H_2O. To obtain the control matrix, activated Reacti-Gel (6X) support was mixed with Trt-NH-$(PEG)_2$-NH_2 (100 µM) in a buffer containing 10 mM $NaHCO_3$ (pH 10) at 37 °C. The mixture was manteined under shaking for 4 h. The amount of immobilized Trt-NH-$(PEG)_2$-NH_2 has been calculated as reported for BLQ (see before). The matrices were stored at 4 °C.

7.2.4 BLQ interactome identification by affinity chromatography and mass spectrometry

THP-1 monocytic cell line were grown in RPMI medium (Sigma) supplemented with 10% (v/v) fetal bovine serum (Sigma), 100 U/ml penicillin and 100 µg/ml streptomycin (Sigma) at 37 °C in a 5% CO_2 atmosphere. THP-1 cell line was differentiated into a macrophage-like phenotype by incubation with phorbol-12-myristate-13-acetate (PMA). To induce an inflammatory response, bacterial lipopolysaccharides (LPS) were added to the culture medium at a final concentration of 100 µg/ml for 24 h. The cells were washed once with phosphate-saline buffer (PBS), collected by centrifugation at 96 x g for 3 min. The obtained pellets were lysed in ice-cooled PBS 1X, 0.1% Igepal, supplemented with protease inhibitor cocktail. To remove cellular debris the cell suspension was centrifuged at 9617 x g for 10 min at 4°C. The supernatant was collected and the protein concentration was tested using Bradford assay and adjusted to 1 mg/ml. 50 µl of beads suspension of BLQ modified beads and the same amount of the control matrix were separately incubated with 500 µg of THP1 total proteins under continuous shaking for 16 h at 4°C. The beads were precipitated by centrifugation (865 x g, 3 min, 4°C) and subjected to six

washing with PBS. The bound proteins were eluted by boiling the beads in 30 µl of SDS-PAGE sample buffer (60 mM Tris/HCl pH 6.8, 2% SDS, 0.001% Bromophenol blue, 10% glycerol, 2% 2-Mercaptoethanol) and subjected to SDS-PAGE separation at 12% of polyacrylamide. After gel electrophoresis, gels were subjected to colloidal Coomassie (Biorad G-250) staining[156-158]. The gel band at an apparent MW of 190 kDa was cut out in both lanes. Briefly, gel pieces were washed with MilliQ water and AcN, reduced with DTT (10 mM) and alkylated with iodoacetamide reagent (54 mM). After few washing, pieces were incubated with 50 µl of trypsin (10 ng/µl) on ice for 1h. After the addition of 30 µL ammonium bicarbonate (10 mM, pH 7.5) samples were digested overnight at 37 °C[159]. The supernatant was collected and the peptides were extracted from the gel pieces by incubation with 100 µl of pure AcN. Finally, the supernatant was collected and both were combined. Each peptide mixture was dried out and dissolved in 10 µl of 10% formic acid. 5 µl, of the above mentioned peptides mixture, were injected onto a nano Acquity LC system (Waters Corp. Manchester, United Kingdom). The peptides were separated using a 1.7 µm BEH C-18 column (Waters Corp. Manchester, United Kingdom) at a flow rate of 400 nl/min. Peptide elution was achieved with a linear gradient from 15 to 60% B (Solution A: 0.1% formic acid, solution B: 0.1% formic acid, 100% ACN) in 55 min. MS and MS/MS data were acquired using a Q-TOF Premier mass spectrometer (Waters Corp., Micromass, Manchester, United Kingdom). Doubly and triply charged peptide-ions were automatically chosen by the MassLynx software and fragmented. After mass spectrometric measurements, data were automatically processed by ProteinLynx software to generate peak lists for protein identifications. Database searches were carried out with MASCOT server. The SwissProt database (release 57.13 of 19-Jan-2010, taxonomy Homo Sapiens, 514212 sequences; 180900945 residues) was searched, allowing 2 missed cleavages, carbamidomethyl (C) as fixed modification o and oxidation (M)

and phosphorylation (ST) as variable modifications. The peptide tolerance was set to 80 ppm and the MS/MS tolerance to 0.8 Da.

7.2.5 Serial affinity chromatography as a tool for identifying specific BLQ binding protein

THP1 cells lysate (1.0 mg) was incubated with 50 ul of BLQ affinity beads for 1h at 4 °C under continuously shaking. The supernatant obtained after beads precipitation (9617 x g, 2 min) was again incubated with freshly BLQ affinity beads at 4 °C, again for 1h. Then the new beads were precipitated (9617 x g, 2 min) and the supernatant used for a third affinity purification step with BLQ affinity resin. The three batch of precipitated beads, obtained from serial affinity chromatography, were washed six times with PBS buffer and boiled in 30 µl of SDS-PAGE sample buffer (60 mM Tris/HCl pH 6.8, 2% SDS, 0.001% Bromophenol blue, 10% Glicerol, 2% 2-Mercaptoethanol). The proteins eluted were separated by SDS-PAGE at 8% of poly-acrylamide and stained with colloidal Comassie brilliant blu[162].

7.2.6 Cell Viability Assay

Cell viability was assessed by 3-(4,5-dimethylthiazol-2-yl)-2,5-diphenyltetrazolium bromide (MTT) assay[161]. Cells were seeded in 96-well microtiter plates in 100 µl of growth medium.

After 16 h incubation at 37 °C, cells were exposed to different concentration of BLQ, ranging from 0.01 µM to 100 µM, containing 1% DMSO. The same amount the of DMSO has been applied as control and the incubation was carried out for 48 h. The mitochondrial-dependent reduction of 3-(4,5-

dimethylthiazol-2-yl)-2,5-diphenyltetrazolium bromide (MTT) to formazan was used to assess the possible BLQ cytotoxic effect. The experiment was carried out in triplicate and all the values were normalized to control.

7.2.7 Uptake of FITC-labeled BSA by THP1

THP1 (human acute monocytic leukemia cell line) were grown in RPMI 1640 + 10% FBS + 2mM L-Glutamine. The cells differentiated into macrophage-like cell line after incubation with 161nM PMA (Phorbol 12-Myristate 13-Acetate) for 72 hours. 5.0 $x10^5$ THP1 differentiated cells were grown on 12 well plates in presence of glass dishes. After removal of the culture medium, each dish was washed and pre-incubated with PBS buffer in the absence or presence of BLQ (50 μM and 100 μM in PBS from stock solution in DMSO) at 37°C for 10 min. A control experiment using chlorpromazine (50 μM and 100 μM in PBS from stock solution in DMSO), was performed in the same experimental condition.

The cells were then incubated in presence of 20 μg/ml AlexaFluor488-albumin (488-BSA) at 37°C for 1 hour. At the end of incubation, the uptake buffer was aspirated, and the dishes were rinsed rapidly three times with ice-cold PBS buffer.

The cells were scraped with a rubber policeman in ice-cold buffer, washed by centrifugation at 4°C for 4 minutes at 1500 *g* and analyzed for internalized 488-BSA by flow cytometry[162]. FACS analysis was carried out with a Becton Dickinson FACS Vantage flow cytometer (Becton Dickinson, Cowley, Oxford, United Kingdom). The excitation wavelength was 488 nm, and data were collected in FL-1 channel. For each analysis, 10000 events were recorded; data were analyzed with CellQuest software (Becton Dickinson, Chino, California, USA). As far as the microscopy analyses, 48 x 10^3 THP1

differentiated cells plated on glass dishes were incubated with 488-BSA in presence or absence of BLQ or chlorpromazine as described[34]. After incubation, cells were rinsed three times with PBS buffer and fixed with 3,7% formaldehyde in PBS. Uptake was analyzed with a Leica microscope AF-6000 with a HCX PL FLUOTAR 63.0×1.25 oil objective.

7.3 PRT C based target discovery

7.3.1 Chemicals

Reacti-Gel (6X) CDI support was obtained from Pierce. The linker 4,7,10-trioxa-1,13-tridecanediamine (NH_2-$(PEG)_2$-NH_2) and the protease inhibitor cocktail were purchased from Sigma Aldrich. The Trt-NH-$(PEG)_2$-NH_2 was from Merck. Biacore 3000, CM5 sensor chip, and coupling reagents (*N*-ethyl-*N'*-(3-dimethylaminopropyl) carbodiimide (EDC), N-hydroxy-succinimmide (NHS), and ethanolamine-HCl) were purchased from GE Healthcare (United Kingdom). Endoplasmin (GRP94) was from Assay Design.

7.3.2 PRT C reactivity profile

100 μmol of PRT were incubated with 500 μmol of NH_2-$(PEG)_2$-NH_2 in 200 μl of $NaHCO_3$ (50 mM) containing 40% of ACN. The reaction mixture was incubated at 50°C and maintained under shaking (1250 rpm), using Termomixer eppendorf, for 16 h.

5 μl of the above reaction mixture were subjected to RP-HPLC fractionation and each chromatographic peak were analyzed by mass spectrometry using a LCQ-Deca instrument (Thermo Quest).

The RP- HPLC analysis was carried out using an Agilent 1100 Series chromatographer equipped with a Phenomenex C18 column (250 x 2.0 mm). The gradient (Solution A: 0.1% TFA, solution B: 0.07% TFA, 5% H_2O 95% ACN) started at 10% and ended at 95% B after 15 min at flow rate of 0.2 ml/min.

7.3.3 Generation of a Perthamide Affinity Matrix

0.2 ml (dry volume) of the CDI activated Reacti-Gel (6X) beads was treated with 5 μmol of 4,7,10-Trioxa-1,13-tridecanediamine (TRT) dissolved in $NaHCO_3$ (50 mM) supplemented with 30% ACN at pH 8.5 and incubated for 16 h at 50°C under continuous shaking.

Then, to prove the presence of free amine groups on the modified Reacti-Gel surface, the beads were washed three times with ethanol and subjected to Kaiser test[153].

The obtained amine-beads were, then, treated with 3μmol of Perthamide (3 mg) dissolved in 200 μl of a phosphate buffer containing Na_2HPO_4 (10 mM), ACN 30% at pH 8.5. The reaction mixture was kept for 16 h at 50 °C under continuous shaking. The amount of immobilized PRT was estimated integrating the peaks of the free PRT species after HPLC injections of supernatants at t = 0 h, t= 2h and t=16h, using an Agilent 1100 Series chromatographer. HPLC runs were carried out using a Phenomenex C18 column (250 x 2.0 mm) at a flow rate of 200 μl/min. The gradient (Solution A: 0.1% TFA, solution B: 0.07% TFA, 5% H2O 95% ACN) started at 10% and ended at 95% B after 20 min.

The same experimental conditions were applied to the preparation of control matrix. Briefly, 200 μl of the activated Reacti-Gel (6X) Support were mixed with 5 μmol of TRT dissolved in $NaHCO_3$ (50 mM) containing 30% ACN at

pH 8.5. The HPLC runs, to estimate the yield of the immobilization reaction, were performed as described above. The matrices were stored at 4 °C in acetone.

7.3.4 Affinity purification of Perthamide C partners

J774.1 murine macrophages cell line were grown in DMEM medium (Sigma) supplemented with 10% (v/v) foetal bovine serum (Sigma), 100 U/ml penicillin and 100 µg/ml streptomycin (Sigma), 4 mM Glutamine (Sigma), 10 mM HEPES (Sigma), 10 mM Natrium Pyruvate (Sigma) at 37 °C in a 5% CO_2 atmosphere. The cells were collected by centrifugation at 96 x g for 3 min and washed once with phosphate-saline buffer (PBS, 50 mM Natrium Phosphate, 150 mM Natrium chloride). The obtained pellet was dissolved in ice-cooled PBS 1X containing 0.1% Igepal and 5% glycerol and supplemented with protease inhibitor cocktail.

The cells suspension were sonicated for 2 min with Vibracell (Sonics) setting an amplitude of 30% and clarified by centrifugation (9617 x g) for 10 min at 4°C. The supernatant was collected and the protein concentration was tested using Bradford assay[153] and adjusted to 1 mg/ml.

50 µl of PRT beads suspension and the same amount of the control matrix were separately incubated with 1 mg of J774.1 total proteins under continuous shaking for 16 h at 4°C. The beads were precipitated by centrifugation (865 x g, 3 min, 4°C) and washed six time with 5 mM Natrium Phosphate. The bound proteins were eluted by boiling the beads in 30 µl of SDS-PAGE sample buffer (60 mM Tris/HCl pH 6.8, 2% SDS, 0.001% Bromophenol blue, 10% glycerol, 2% 2-Mercaptoethanol). The eleuted proteins were subjected to SDS-PAGE separation at 12% of polyacrylamide. After gel electrophoresis, gels were subjected to colloidal Coomassie (Biorad G-250) staining[157, 158].

The SDS-PAGE gel lane from control and PRT based experiment were cut in 10 pieces. Each one was subsequently washed with MilliQ Water and Acetonitrile and subjected to *in situ* protein digestion as described in Shevchenko protocol[159]. Briefly, gel slices were reduced and alkylated using 1,4-dithiothreitol (10 mM) and iodoacetamide (50 mM) respectively, then washed and rehydrated in trypsin solution (12 ng/μL) on ice for 1h.

After the addition of 30 μL ammonium bicarbonate (10 mM, pH 7.5), samples were digested overnight at 37 °C. The supernatant were collected and peptides were extracted by the gel slices using 100% ACN. Finally, the supernatant was collected and both were combined. All peptides sample were dried out and ri-dissolved in 10% FA before mass spec analysis. 5 μL of the obtained peptide mixture were injected onto a nano Acquity LC system (Waters Corp. Manchester, United Kingdom).

The peptides were separated using a 1.7 μm BEH C-18 column (Waters Corp. Manchester, United Kingdom) at a flow rate of 400 nl/min. Peptide elution was achieved with a linear gradient from 15 to 50% (solution A: 95% H_2O, 5%ACN, 0.1% FA; solution B: 95% ACN, 5% H_2O, 0.1% FA) in 55 min.

MS and MS/MS data were acquired using a Q-TOF Premier mass spectrometer (Waters Corp., Micromass, Manchester, United Kingdom). Four most intense doubly and triply charged peptide-ions were automatically chosen by the MassLynx software and fragmented. After mass spectrometric measurements, data were automatically processed by ProteinLynx software to generate peak lists for protein identifications. Database searches were carried out with MASCOT server. The SwissProt database (release 2010_11 of 02 Nov 10, taxonomy Mus Musculus; 522019 sequences, 184241293 residues) was searched, allowing 2 missed cleavages, carbamidomethyl (C) as fixed modification o and oxidation (M) and phosphorylation (ST) as variable modifications. The peptide tolerance was set to 80 ppm and the MS/MS tolerance to 0.8 Da.

7.3.5 SPR analysis of PRT-GRP94/Hsp82 complex

GRP94 was immobilized onto CM5 sensor chip using standard amine coupling procedures. Phosphate–buffered saline, which consisted of 10 mM Na_2HPO_4 and 150 nM NaCl, pH 7.4, was used as running buffer. The carboxymethyl dextran surface was activated with a 5-min injection of a 1:1 ratio of 100 mM EDC and 100 mM M NHS at 5 μl/min. GRP94 was diluted to a final concentration of 30 ng/μl in 10 mM sodium acetate, pH 4.5 and 100 μl prior the injection onto the activated chip surface at flow rate of 5 μl/min. Protein concentration was selected to obtain an optimal response (around 13000 RU). Remaining active groups were blocked with a 7-min injection of 1.0 M ethanolamine-HCl, pH 8.5, at 5 μl/min.

PRT solution (0.5-5 μM), used into the biosensor experiments, were diluted in 10 mM phosphate saline buffer (pH 7.4) containing 2% DMSO. Each concentration was tested at least three times.

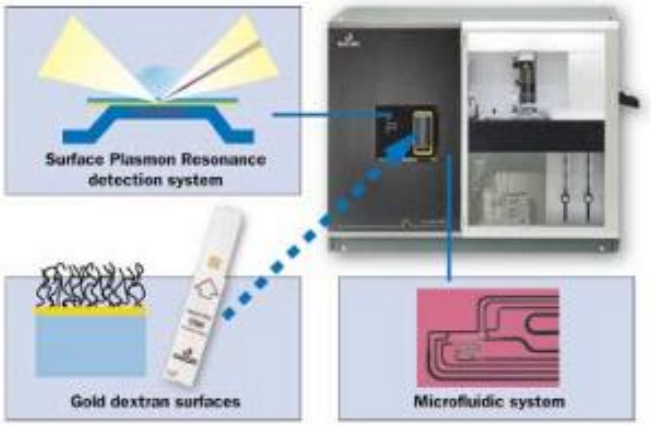

Fig. 53. Biacore 300 instrument, GE Healthcare (United Kingdom).

Since the dissociated back to baseline within a reasonable time frame, no regeneration has been required. The interaction experiments were carried out

at a flow rate of 10 µl/min, employing a 3 min injection time. The dissociation time was set at 600 seconds. Rate constants for association (k_a) dissociation (k_d) and the dissociation constant (K_D) were obtained by globally fitting data from all the injection of different concentration of each compound, using the BIAevaluation software, using the simple 1:1 Langmuir binding model.

The same procedure was used to calculate the K_D of PRT-Hsp82 complex.

-CHAPTER 8-

Collagen stimulation of platelets induces rapid spatial reorganizations in cAMP and cGMP signaling scaffolds : Experimental procedures

8.1 Materials

8-AHA-cAMP, 2-AHA-cGMP, Rp-8-AHA-cAMP, 8-AET-cGMP and 2-AHA-cAMP agarose beads were purchased from BIOLOG (Bremen, Germany). The amount of immobilized cyclic nucleotide on the beads was 6 µmol/ml.

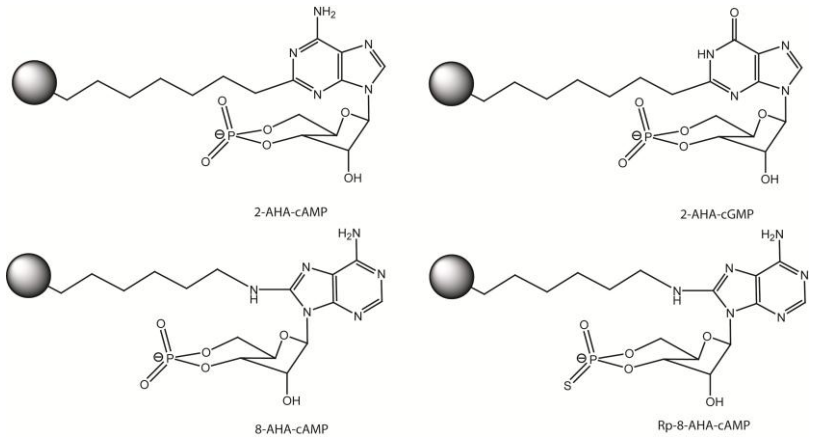

Fig. 54. Chemical structure of cAMP and cGMP beads

Protease inhibitor cocktail, complete mini, was from Roche Diagnostics, and phosphatase inhibitor cocktail was purchased from Sigma-Aldrich. Formaldehyde and isotope-labeled CD_2O formaldehyde (20% solution in D_2O) were also from Sigma-Aldrich. All the others chemicals (analysis grade) were purchased from commercial sources, unless stated otherwise. For all experiments high purity water, obtained from a Milli-Q system (Millipore, Bedford, MA), was used.

8.2 Donors, Platelet isolation and CRP activation

A total of 100 mL whole blood was drawn in citrate anticoagulated tubes to isolate platelets. Fresh whole blood was centrifuged at 156 G for 10 min, in

order to remove erythrocytes and leukocytes from the supernatant, resulting in platelets rich plasma. Blood platelets were separated from plasma by anther centrifugation step at 330 G for 10 min. The platelets were subsequently resuspended in Hepes Tyroid buffer, pH 6.5 + 10 ng/ml PGI2. After one wash step with Hepes Tyroid buffer, pH 9.0 + 10 ng/ml PGI2 followed by centrifugation at 330 G for 10 min, the pellet was resuspended in Hepes Tyroid buffer, pH 7.0 + 10 ng/ml PGI2 in a final concentration of $2^* 10^{11}$ platelets per liter. Platelets completely recover to the inactivated state by letting them rest for 30 minutes at room temperature. The "mean platelet volume" (MPV) was measured to exclude pre-activation of the platelets. Washed platelets were divided in two fractions. One of them was activated with the addition of 2.5 µg/mL Collagen Related Peptide (CRP), while HBS was added to the other fraction. After five minutes of incubation the solutions were centrifuged at 4000 g and the pellet was snap frozen in liquid nitrogen.

8.3 Platelet lysis

From each donor, the resting and CRP stimulated platelet samples were treated identically in parallel. The platelet fractions were taken up in 1.5 ml of ice-cold lysis buffer containing 50 mM KH_2PO_4/K_2HPO_4-buffer, pH 7.0, with 150 mM NaCl and 0.1% Tween 20 supplemented with protease (1 complete mini/15mL, Roche) and phosphatase inhibitor cocktail 2 (0.1%, Sigma-Aldrich).

Dounce homogenization was used for lysis. Cellular debris was removed by centrifugation in an eppendorf table top centrifuge at 10,000 rpm for 10 min at 4°C. The supernatant was carefully collected and the pellet resuspended in lysis buffer (500 µl) to increase the yield of the lysis. The second supernatant, obtained by centrifugation (10,000 rpm, 10min, 4°C), was added to the first one and the protein concentration was determined using a Bradford assay.

From each different donor, between 3 and 4 mg total protein lysate per 100 mL of whole blood was obtained.

8.4 Pulldown Assay

The pulldown experiment was carried out using a beads mixture composed of either four different immobilized cyclic nucleotides: 8-AHA-cAMP, Rp-8-AHA-cAMP, 2-AHA-cAMP and 2-AHA-cGMP (1:1:1:1), or a two-bead mixture of 2-AHA-cGMP and 8-AET-cGMP (1:1). Three different methods were used in which the applied beads, but also the sample analysis strategy was varied. Method 1 (Experiment 1) uses a mix of the 4 different cyclic nucleotide beads in combination with off-line TiO_2 based isolation of phosphopeptides. For method 2 (experiments 2 and 3) a 1:1 mixture of 2-AH-cGMP and 8-AET-cGMP beads was used to focus on PKG based signaling proteins. Method 3 (experiments 4 and 5) was performed with the same set of 4 beads as in method 1, but now strong cation exchange (SCX) of the eluted fraction was used to to analyze, and quantitate, more in depth the captured proteome. For both methods 2 and 3, 10mM ADP/GDP was added to compete for less specifically binding proteins as observed in experiment 1[163, 164]. Prior to pulldown the beads mixture was washed with 1mL of lysis buffer for each 100µL of beads. After lysis, equal amounts of resting and activated platelet lysate were used. Prior to addition of the beads, the lysate was diluted to a final concentration of 2 mg/mL using lysis buffer. Depending on the yield of total protein from the isolated platelets, in each pull-down, 10µL of beads mixture was used per mg of protein. The obtained lysate-beads suspension was incubated for 2 h at 4°C by rotary shaking. The unbound fraction was removed and the beads were washed 6 times with 1 mL of lysis buffer. To further increase bead specificity, where applicable the first three washing steps were performed with lysis buffer supplemented with ADP/GDP (10 mM)[163, 164].

After washing, the bound proteins were eluted with 50 µl of 8 M urea in 50mM of ammonium bicarbonate buffer (50mM, pH 8). The eluted proteins were digested with LysC (5 µg, Roche Diagnostics) for 4 h at 37 °C, reduced and alkylated (10 mM DTT and 54 mM iodoacetamide) in 2 M urea and finally subjected to trypsin digestion (5 µg, Roche Diagnostics) for 16 h at 37°C.

8.5 Stable Isotope Labeling Strategy

The trypsin digested peptides were subjected to C18 (Sep-PAK, Waters Corporation) for desalting and subsequent on-column stable isotope dimethyl labeling as described previously[165]. Peptides coming from the resting platelets were labeled using "*light*" reagent (each N-terminus and lysine side chain will obtain two $-CH_3$-groups) while, the peptides originating from the CRP induced platelets were labeled with "*intermediate*" reagent (two $-CHD_2$ added to each N-terminus and lysine side chain). After elution, the light and intermediate peptides were mixed in a 1:1 ratio, dried *in vacuo* and re-suspended in 10% formic acid for mass spectrometric analysis. For the phospho-peptide analysis in method 1, the peptide mixture was subjected to TiO_2 enrichment (Titansphere 5µM, GL science) using in-house packed micro columns. Briefly, the peptide mixture was loaded on the column pre-equilibrated with buffer A (50% ACN, 5% FA), subjected to several washing steps with the same buffer before the elution of the phospho-peptides with buffer B (1.25% NH3, pH 10.5). The eluted peptide mixture was neutralized with 5% formic acid before MS analysis[165, 166].

8.6 MS analysis and Quantitation

LC-MS analysis was performed using an Agilent 1100 series liquid chromatography system equipped with an 20-mm Aqua C18 (Phenomenex, Torrance, CA) trapping column (packed in-house, i.d. 100 µm; resin 5 µm) and a 400 mm ReproSil-Pur C18-AQ analytical column (packed in-house, i.d. 50 µm; resin 3 µm). Trapping was performed at 5 µl/min solution A (0.6% acetic acid) for 10 min. Peptide elution was achieved with a linear gradient from 13 to 32% of solution B (80% acetonitrile, 0.6%acetic acid) in 60 min at a flow rate of 100 nl/min obtained by passively splitting the flow from 0.6 ml/min.

Nanospray was achieved using a distally coated fused silica emitter (New Objective, Cambridge, MA; outer diameter 360 µm; i.d. 20 µm, tip i.d. 10 µm) biased to 1.8 kV. The LC system was coupled to a Finnigan Orbitrap Discovery mass spectrometer (Thermo Electron, Bremen, Germany). Briefly, the mass spectrometer was operated in the data-dependent mode to automatically switch between MS and MS/MS acquisition. Survey full scan MS spectra were acquired from *m*/*z* 350 to *m*/*z* 1500 in the OrbiTrap. The five most intense ions were fragmented in the linear ion trap using collisionally induced dissociation (CID) at a target value of 10,000.

The obtained data was processed by Bioworks 3.3 (Thermo, Bremen, Germany) software to generate a txt file used for database searching with Mascot (version 2.1.0, Matrix Science, London, UK).

The SwissProt human database database 56.2 (398181 protein sequences; 143572911 residues) was searched, allowing 2 missed cleavages, carbamidomethyl as fixed modification on cysteines, as well as “light” and “intermediate” di-methylation of peptide N termini and lysine residues and oxidation (M) and phosphorylation (ST) as variable modifications. The peptide tolerance was set to 15 ppm and the MS/MS tolerance to 0.9 Da. Proteins were organized using the Scaffold software package (Proteomesoftware). Quantification was performed using an in-house modified version of MSQuant[167], (version 1.4.2a). Peptide ratios between the

monoisotopic peaks of “light” and “intermediate” forms of the peptide were calculated and averaged over consecutive MS cycles for the duration of their respective LC-MS peaks in the total ion chromatogram using only MS scans; intermediate and light labeled peptides were found to co-elute. For comparison, all protein ratios were normalized. Initially normalization to the average ratio of PKA-Rs, PDE2, PKGIß and PKG2 was performed at individual experiment level. Subsequently, all secondary associating proteins (AKAPs, GKAPs etc) were normalized to their respective primary interactor(s) as reported by us previously[168]. Significance of difference was tested using a t-test between the obtained normalized ratios of different proteins. Molecular, biological and pathway analysis of enriched proteins was performed using String and Panther[169, 170].

8.7 Data analysis

Through the use of the three different methods in which the applied beads, but also the sample analysis strategy was varied, specific, less-specific and non-specific interactors of cAMP could be evaluated. Spectral counting across methods was used to isolate the core-cAMP interactome in human platelets. Method 1 (Experiment 1) showed good coverage on primary interactors, however secondary interactors (AKAPs, GKAPs) were obscured by other nucleotide binding proteins such NDKB and LDHA and LDHB. For both method 2 and 3, 10mM ADP/GDP was added to compete for less specifically binding proteins and increase coverage on secondary interactors. From all combined experiments, only proteins with a robust identification and specific enrichment rate were included based on the following criteria; (i) at least 10 spectra summed over all experiments, (ii) identified in at least 3 out of 5 experiments. In the remaining dataset, proteins specifically competed by ADP/GDP could be marked , as these had high spectral counts in Experiment

1, but low, or no counts at all in the others. Also a set of proteins that seemed to have affinity for cAMP, but not cGMP could be annotated based on spectral count features (data not shown), meaning their enrichment is bead specific and not PKA/PKG-dependent, since these kinases bind to all four beads with ~equal affinity. The remaining 35 proteins could be annotated as the core cAMP/cGMP interactome of human platelets and were further evaluated quantitatively for their differential enrichment upon CRP stimulation.

Bibliography

[1] U. Rix, G. Superti-Furga. *Nat. Chem. Biol.* **2009**, *5*(9), 616-624.

[2] M. Bantscheff, A. Scholten, A. J. Heck. *Drug Discov. Today* **2009**, *14*(21-22), 1021-1029.

[3] D. A. Jeffery, M. Bogyo. *Curr. Opin. Biotechnol.* **2003**, *14*(1), 87-95.

[4] U. Rix, O. Hantschel, G. Durnberger, L. L. Remsing Rix, M. Planyavsky, N. V. Fernbach, I. Kaupe, K. L. Bennett, P. Valent, J. Colinge, T. Kocher, G. Superti-Furga. *Blood* **2007**, *110*(12), 4055-4063.

[5] J. Wissing, K. Godl, D. Brehmer, S. Blencke, M. Weber, P. Habenberger, M. Stein-Gerlach, A. Missio, M. Cotten, S. Muller, H. Daub. *Mol. Cell Proteomics.* **2004**, *3*(12), 1181-1193.

[6] A. Kaiser, K. Nishi, F. A. Gorin, D. A. Walsh, E. M. Bradbury, J. B. Schnier. *Arch. Biochem. Biophys.* **2001**, *386*(2), 179-187.

[7] J. B. Schnier, G. Kaur, A. Kaiser, S. F. Stinson, E. A. Sausville, J. Gardner, K. Nishi, E. M. Bradbury, A. M. Senderowicz. *FEBS Lett.* **1999**, *454*(1-2), 100-104.

[8] M. Knockaert, P. Lenormand, N. Gray, P. Schultz, J. Pouyssegur, L. Meijer. *Oncogene* **2002**, *21*(42), 6413-6424.

[9] K. Godl, J. Wissing, A. Kurtenbach, P. Habenberger, S. Blencke, H. Gutbrod, K. Salassidis, M. Stein-Gerlach, A. Missio, M. Cotten, H. Daub. *Proc. Natl. Acad. Sci. U. S. A* **2003**, *100*(26), 15434-15439.

[10] N. Shimizu, K. Sugimoto, J. Tang, T. Nishi, I. Sato, M. Hiramoto, S. Aizawa, M. Hatakeyama, R. Ohba, H. Hatori, T. Yoshikawa, F. Suzuki, A. Oomori, H. Tanaka, H. Kawaguchi, H. Watanabe, H. Handa. *Nat. Biotechnol.* **2000**, *18*(8), 877-881.

[11] M. Furuya, Y. Tsushima, S. Tani, T. Kamimura. *Bioorg. Med. Chem.* **2006**, *14*(15), 5093-5098.

[12] D. Guiffant, D. Tribouillard, F. Gug, H. Galons, L. Meijer, M. Blondel, S. Bach. *Biotechnol. J.* **2007**, *2*(1), 68-75.

[13] L. Sleno, A. Emili. *Curr. Opin. Chem. Biol.* **2008**, *12*(1), 46-54.

[14] K. Yamamoto, A. Yamazaki, M. Takeuchi, A. Tanaka. *Anal. Biochem.* **2006**, *352*(1), 15-23.

[15] P. Dadvar, D. Kovanich, G. E. Folkers, K. Rumpel, R. Raijmakers, A. J. Heck. *Chembiochem* **2009**, *10*(16), 2654-2662.

[16] F. W. McLafferty, K. Breuker, M. Jin, X. Han, G. Infusini, H. Jiang, X. Kong, T. P. Begley. *FEBS J.* **2007**, *274*(24), 6256-6268.

[17] J. R. Yates, C. I. Ruse, A. Nakorchevsky. *Annu. Rev. Biomed. Eng* **2009**, *11*, 49-79.

[18] B. T. Chait. *Science* **2006**, *314*(5796), 65-66.

[19] W. J. Henzel, C. Watanabe, J. T. Stults. *J. Am. Soc. Mass Spectrom.* **2003**, *14*(9), 931-942.

[20] J. V. Olsen, M. Mann. *Proc. Natl. Acad. Sci. U. S. A* **2004**, *101*(37), 13417-13422.

[21] A. I. Nesvizhskii, O. Vitek, R. Aebersold. *Nat. Methods* **2007**, *4*(10), 787-797.

[22] R. G. Sadygov, D. Cociorva, J. R. Yates, III. *Nat. Methods* **2004**, *1*(3), 195-202.

[23] D. N. Perkins, D. J. Pappin, D. M. Creasy, J. S. Cottrell. *Electrophoresis* **1999**, *20*(18), 3551-3567.

[24] S. Bach, M. Knockaert, J. Reinhardt, O. Lozach, S. Schmitt, B. Baratte, M. Koken, S. P. Coburn, L. Tang, T. Jiang, D. C. Liang, H. Galons, J. F. Dierick, L. A. Pinna, F. Meggio, F. Totzke, C. Schachtele, A. S. Lerman, A. Carnero, Y. Wan, N. Gray, L. Meijer. *J. Biol. Chem.* **2005**, *280*(35), 31208-31219.

[25] A. Y. Lee, C. P. Paweletz, R. M. Pollock, R. E. Settlage, J. C. Cruz, J. P. Secrist, T. A. Miller, M. G. Stanton, A. M. Kral, N. D. Ozerova, F. Meng, N. A. Yates, V. Richon, R. C. Hendrickson. *J. Proteome. Res.* **2008**, *7*(12), 5177-5186.

[26] X. Liang, M. Hajivandi, D. Veach, D. Wisniewski, B. Clarkson, M. D. Resh, R. M. Pope. *Proteomics.* **2006**, *6*(16), 4554-4564.

[27] M. Bantscheff, M. Schirle, G. Sweetman, J. Rick, B. Kuster. *Anal. Bioanal. Chem.* **2007**, *389*(4), 1017-1031.

[28] S. E. Ong, M. Mann. *Nat. Chem. Biol.* **2005**, *1*(5), 252-262.

[29] M. J. MacCoss, D. E. Matthews. *Anal. Chem.* **2005**, *77*(15), 294A-302A.

[30] S. E. Ong, M. Mann. *Nat. Protoc.* **2006**, *1*(6), 2650-2660.

[31] Y. Shiio, R. Aebersold. *Nat. Protoc.* **2006**, *1*(1), 139-145.

[32] M. Munchbach, M. Quadroni, G. Miotto, P. James. *Anal. Chem.* **2000**, *72*(17), 4047-4057.

[33] J. L. Hsu, S. Y. Huang, N. H. Chow, S. H. Chen. *Anal. Chem.* **2003**, *75*(24), 6843-6852.

[34] P. J. Boersema, R. Raijmakers, S. Lemeer, S. Mohammed, A. J. Heck. *Nat. Protoc.* **2009**, *4*(4), 484-494.

[35] P. J. Boersema, T. T. Aye, T. A. van Veen, A. J. Heck, S. Mohammed. *Proteomics.* **2008**, *8*(22), 4624-4632.

[36] J. L. Hsu, S. Y. Huang, S. H. Chen. *Electrophoresis* **2006**, *27*(18), 3652-3660.

[37] R. Raijmakers, C. R. Berkers, J. A. de, H. Ovaa, A. J. Heck, S. Mohammed. *Mol. Cell Proteomics.* **2008**, *7*(9), 1755-1762.

[38] J. Colinge, A. Masselot, M. Giron, T. Dessingy, J. Magnin. *Proteomics.* **2003**, *3*(8), 1454-1463.

[39] P. Mortensen, J. W. Gouw, J. V. Olsen, S. E. Ong, K. T. Rigbolt, J. Bunkenborg, J. Cox, L. J. Foster, A. J. Heck, B. Blagoev, J. S. Andersen, M. Mann. *J. Proteome. Res.* **2010**, *9*(1), 393-403.

[40] M. P. Washburn, D. Wolters, J. R. Yates, III. *Nat. Biotechnol.* **2001**, *19*(3), 242-247.

[41] H. Liu, R. G. Sadygov, J. R. Yates, III. *Anal. Chem.* **2004**, *76*(14), 4193-4201.

[42] W. M. Old, K. Meyer-Arendt, L. veline-Wolf, K. G. Pierce, A. Mendoza, J. R. Sevinsky, K. A. Resing, N. G. Ahn. *Mol. Cell Proteomics.* **2005**, *4*(10), 1487-1502.

[43] H. Schmidinger, A. Hermetter, R. Birner-Gruenberger. *Amino. Acids* **2006**, *30*(4), 333-350.

[44] M. J. Evans, B. F. Cravatt. *Chem. Rev.* **2006**, *106*(8), 3279-3301.

[45] A. E. Speers, B. F. Cravatt. *Chembiochem* **2004**, *5*(1), 41-47.

[46] T. Bottcher, M. Pitscheider, S. A. Sieber. *Angew. Chem. Int. Ed Engl.* **2010**, *49*(15), 2680-2698.

[47] L. Bohlin, U. Goransson, C. Alsmark, C. Weden, A. Backlund. *Phytochem. Rev.* **2010**, *9*(2), 279-301.

[48] F. Folmer, M. Jaspars, M. Dicato, M. Diederich. *Biochem. Pharmacol.* **2008**, *75*(3), 603-617.

[49] J. W. Blunt, B. R. Copp, W. P. Hu, M. H. Munro, P. T. Northcote, M. R. Prinsep. *Nat. Prod. Rep.* **2009**, *26*(2), 170-244.

[50] P. Garcia-Pastor, A. Randazzo, L. Gomez-Paloma, M. J. Alcaraz, M. Paya. *J. Pharmacol. Exp. Ther.* **1999**, *289*(1), 166-172.

[51] C. Giannini, C. Debitus, R. Lucas, A. Ubeda, M. Paya, J. N. Hooper, M. V. D'Auria. *J. Nat. Prod.* **2001**, *64*(5), 612-615.

[52] C. Festa, S. De Marino, V. Sepe, M. C. Monti, P. Luciano, M. V. D'Auria, C. Dèbitus, M. Bucci, V. Vellecco, A. Zampella. *Tetrahedron* **2009**, *65*(50), 10424-10429.

[53] M. C. Monti, A. Casapullo, C. N. Cavasotto, A. Tosco, P. F. Dal, A. Ziemys, L. Margarucci, R. Riccio. *Chemistry* **2009**, *15*(5), 1155-1163.

[54] M. C. Monti, M. G. Chini, L. Margarucci, A. Tosco, R. Riccio, G. Bifulco, A. Casapullo. *J. Mol. Recognit.* **2009**, *22*(6), 530-537.

[55] J. Busserolles, M. Paya, M. V. D'Auria, L. Gomez-Paloma, M. J. Alcaraz. *Biochem. Pharmacol.* **2005**, *69*(10), 1433-1440.

[56] I. Posadas, M. C. Terencio, A. Randazzo, L. Gomez-Paloma, M. Paya, M. J. Alcaraz. *Biochem. Pharmacol.* **2003**, *65*(5), 887-895.

[57] R. Lucas, C. Giannini, M. V. D'Auria, M. Paya. *J. Pharmacol. Exp. Ther.* **2003**, *304*(3), 1172-1180.

[58] S. Terracciano, M. Aquino, M. Rodriquez, M. C. Monti, A. Casapullo, R. Riccio, L. Gomez-Paloma. *Curr. Med. Chem.* **2006**, *13*(16), 1947-1969.

[59] M. J. Alcaraz, M. Paya. *Curr. Opin. Investig. Drugs* **2006**, *7*(11), 974-979.

[60] F. Folmer, M. Jaspars, M. Dicato, M. Diederich. *Biochem. Pharmacol.* **2008**, *75*(3), 603-617.

[61] J. Busserolles, M. Paya, M. V. D'Auria, L. Gomez-Paloma, M. J. Alcaraz. *Biochem. Pharmacol.* **2005**, *69*(10), 1433-1440.

[62] I. Posadas, M. C. Terencio, A. Randazzo, L. Gomez-Paloma, M. Paya, M. J. Alcaraz. *Biochem. Pharmacol.* **2003**, *65*(5), 887-895.

[63] M. C. Monti, A. Casapullo, C. N. Cavasotto, A. Tosco, P. F. Dal, A. Ziemys, L. Margarucci, R. Riccio. *Chemistry* **2009**, *15*(5), 1155-1163.

[64] M. C. Monti, A. Casapullo, R. Riccio, L. Gomez-Paloma. *Bioorg. Med. Chem.* **2004**, *12*(6), 1467-1474.

[65] J. Busserolles, M. Paya, M. V. D'Auria, L. Gomez-Paloma, M. J. Alcaraz. *Biochem. Pharmacol.* **2005**, *69*(10), 1433-1440.

[66] K. Godl, O. J. Gruss, J. Eickhoff, J. Wissing, S. Blencke, M. Weber, H. Degen, D. Brehmer, L. Orfi, Z. Horvath, G. Keri, S. Muller, M. Cotten, A. Ullrich, H. Daub. *Cancer Res.* **2005**, *65*(15), 6919-6926.

[67] K. Godl, J. Wissing, A. Kurtenbach, P. Habenberger, S. Blencke, H. Gutbrod, K. Salassidis, M. Stein-Gerlach, A. Missio, M. Cotten, H. Daub. *Proc. Natl. Acad. Sci. U. S. A* **2003**, *100*(26), 15434-15439.

[68] J. Wissing, K. Godl, D. Brehmer, S. Blencke, M. Weber, P. Habenberger, M. Stein-Gerlach, A. Missio, M. Cotten, S. Muller, H. Daub. *Mol. Cell Proteomics.* **2004**, *3*(12), 1181-1193.

[69] D. Guiffant, D. Tribouillard, F. Gug, H. Galons, L. Meijer, M. Blondel, S. Bach. *Biotechnol. J.* **2007**, *2*(1), 68-75.

[70] A. Scholten, M. K. Poh, T. A. van Veen, B. B. van, M. A. Vos, A. J. Heck. *J. Proteome. Res.* **2006**, *5*(6), 1435-1447.

[71] A. Scholten, T. A. van Veen, M. A. Vos, A. J. Heck. *J. Proteome. Res.* **2007**, *6*(5), 1705-1717.

[72] A. Dupont, C. Tokarski, O. Dekeyzer, A. L. Guihot, P. Amouyel, C. Rolando, F. Pinet. *Proteomics.* **2004**, *4*(6), 1761-1778.

[73] K. Ferrell, C. R. Wilkinson, W. Dubiel, C. Gordon. *Trends Biochem. Sci.* **2000**, *25*(2), 83-88.

[74] N. Qureshi, S. N. Vogel, W. C. Van, III, C. J. Papasian, A. A. Qureshi, D. C. Morrison. *Immunol. Res.* **2005**, *31*(3), 243-260.

[75] D. Hoeller, C. M. Hecker, I. Dikic. *Nat. Rev. Cancer* **2006**, *6*(10), 776-788.

[76] R. L. Rich, Y. S. Day, T. A. Morton, D. G. Myszka. *Anal. Biochem.* **2001**, *296*(2), 197-207.

[77] D. Casper, M. Bukhtiyarova, E. B. Springman. *Anal. Biochem.* **2004**, *325*(1), 126-136.

[78] M. J. Cannon, G. A. Papalia, I. Navratilova, R. J. Fisher, L. R. Roberts, K. M. Worthy, A. G. Stephen, G. R. Marchesini, E. J. Collins, D. Casper, H. Qiu, D. Satpaev, S. F. Liparoto, D. A. Rice, I. I. Gorshkova, R. J. Darling, D. B. Bennett, M. Sekar, E. Hommema, A. M. Liang, E. S. Day, J. Inman, S. M. Karlicek, S. J. Ullrich, D. Hodges, T. Chu, E. Sullivan, J. Simpson, A. Rafique, B. Luginbuhl, S. N. Westin, M. Bynum, P. Cachia, Y. J. Li, D. Kao, A. Neurauter, M. Wong, M. Swanson, D. G. Myszka. *Anal. Biochem.* **2004**, *330*(1), 98-113.

[79] G. A. Papalia, S. Leavitt, M. A. Bynum, P. S. Katsamba, R. Wilton, H. Qiu, M. Steukers, S. Wang, L. Bindu, S. Phogat, A. M. Giannetti, T. E. Ryan, V. A. Pudlak, K. Matusiewicz, K. M. Michelson, A. Nowakowski, A. Pham-Baginski, J. Brooks, B. C. Tieman, B. D. Bruce, M. Vaughn, M. Baksh, Y. H. Cho, M. D. Wit, A. Smets, J. Vandersmissen, L. Michiels, D. G. Myszka. *Anal. Biochem.* **2006**, *359*(1), 94-105.

[80] P. F. Dal, A. Casapullo, A. Randazzo, R. Riccio, P. Pucci, G. Marino, L. Gomez-Paloma. *Chembiochem* **2002**, *3*(7), 664-671.

[81] J. R. Knowlton, S. C. Johnston, F. G. Whitby, C. Realini, Z. Zhang, M. Rechsteiner, C. P. Hill. *Nature* **1997**, *390*(6660), 639-643.

[82] J. M. Peters, W. W. Franke, J. A. Kleinschmidt. *J. Biol. Chem.* **1994**, *269*(10), 7709-7718.

[83] V. Su, A. F. Lau. *Cell Mol. Life Sci.* **2009**, *66*(17), 2819-2833.

[84] G. Nalepa, M. Rolfe, J. W. Harper. *Nat. Rev. Drug Discov.* **2006**, *5*(7), 596-613.

[85] M. Groll, L. Ditzel, J. Lowe, D. Stock, M. Bochtler, H. D. Bartunik, R. Huber. *Nature* **1997**, *386*(6624), 463-471.

[86] A. F. Kisselev, A. Callard, A. L. Goldberg. *J. Biol. Chem.* **2006**, *281*(13), 8582-8590.

[87] A. F. Kisselev, M. Garcia-Calvo, H. S. Overkleeft, E. Peterson, M. W. Pennington, H. L. Ploegh, N. A. Thornberry, A. L. Goldberg. *J. Biol. Chem.* **2003**, *278*(38), 35869-35877.

[88] C. P. Ma, P. J. Willy, C. A. Slaughter, G. N. DeMartino. *J. Biol. Chem.* **1993**, *268*(30), 22514-22519.

[89] L. J. Crawford, B. Walker, H. Ovaa, D. Chauhan, K. C. Anderson, T. C. Morris, A. E. Irvine. *Cancer Res.* **2006**, *66*(12), 6379-6386.

[90] H. A. Braun, S. Umbreen, M. Groll, U. Kuckelkorn, I. Mlynarczuk, M. E. Wigand, I. Drung, P. M. Kloetzel, B. Schmidt. *J. Biol. Chem.* **2005**, *280*(31), 28394-28401.

[91] I. M. Shah, N. M. Di. *Cardiovasc. Hematol. Disord. Drug Targets.* **2007**, *7*(4), 250-273.

[92] F. de Guzman, B. Coop, C. Mayne, G. Conception, G. Mangalindan, L. Barrows, C. Ireland. *J. Org. Chem.* **1998**, *63*(22), 8042-8044.

[93] P. Stahl, L. Kissau, R. Mazitschek, A. Huwe, P. Furet, A. Giannis, H. Waldmann. *J. Am. Chem. Soc.* **2001**, *123*(47), 11586-11593.

[94] P. Stahl, L. Kissau, R. Mazitschek, A. Giannis, H. Waldmann. *Angew. Chem. Int. Ed Engl.* **2002**, *41*(7), 1174-1178.

[95] Q. Wang, D. Dube, R. W. Friesen, T. G. LeRiche, K. P. Bateman, L. Trimble, J. Sanghara, R. Pollex, C. Ramachandran, M. J. Gresser, Z. Huang. *Biochemistry* **2004**, *43*(14), 4294-4303.

[96] M. C. Monti, A. Casapullo, C. Santomauro, M. V. D'Auria, R. Riccio, L. Gomez-Paloma. *Chembiochem* **2006**, *7*(6), 971-980.

[97] M. C. Monti, M. G. Chini, L. Margarucci, A. Tosco, R. Riccio, G. Bifulco, A. Casapullo. *J. Mol. Recognit.* **2009**, *22*(6), 530-537.

[98] R. Lucas, C. Giannini, M. V. D'Auria, M. Paya. *J. Pharmacol. Exp. Ther.* **2003**, *304*(3), 1172-1180.

[99] J. Busserolles, M. Paya, M. V. D'Auria, L. Gomez-Paloma, M. J. Alcaraz. *Biochem. Pharmacol.* **2005**, *69*(10), 1433-1440.

[100] D. Guiffant, D. Tribouillard, F. Gug, H. Galons, L. Meijer, M. Blondel, S. Bach. *Biotechnol. J.* **2007**, *2*(1), 68-75.

[101] A. Scholten, M. K. Poh, T. A. van Veen, B. B. van, M. A. Vos, A. J. Heck. *J. Proteome. Res.* **2006**, *5*(6), 1435-1447.

[102] A. Shevchenko, H. Tomas, J. Havlis, J. V. Olsen, M. Mann. *Nat. Protoc.* **2006**, *1*(6), 2856-2860.

[103] K. Yamamoto, A. Yamazaki, M. Takeuchi, A. Tanaka. *Anal. Biochem.* **2006**, *352*(1), 15-23.

[104] S. L. Schmid. *Annu. Rev. Biochem.* **1997**, *66*, 511-548.

[105] E. Smythe. *Biochem. Soc. Trans.* **2003**, *31*(Pt 3), 736-739.

[106] B. M. Pearse, C. J. Smith, D. J. Owen. *Curr. Opin. Struct. Biol.* **2000**, *10*(2), 220-228.

[107] R. Yumoto, H. Nishikawa, M. Okamoto, H. Katayama, J. Nagai, M. Takano. *Am. J. Physiol Lung Cell Mol. Physiol* **2006**, *290*(5), L946-L955.

[108] L. H. Wang, K. G. Rothberg, R. G. Anderson. *J. Cell Biol.* **1993**, *123*(5), 1107-1117.

[110] C. Festa, S. De Marino, V. Sepe, M. C. Monti, P. Luciano, M. V. D'Auria, C. Dèbitus, M. Bucci, V. Vellecco, A. Zampella. *Tetrahedron* **2009**, *65*(50), 10424-10429.

[111] M. K. Renner, Y. C. Shen, X. C. Cheng, P. R. Jensen, W. Frankmoelle, C. A. Kauffman, W. Fenical, E. Lobkovsky, J. J. Clardy. *J. Am. Chem. Soc.* **1999**, *121*(49), 11273-11276.

[112] J. A. Trischman, D. M. Tapiolas, R. Dwight, W. Fenical, T. C. McKee, C. M. Ireland, T. J. Stout, J. Clardy. *J. Am. Chem. Soc.* **2010**, *116*(2), 757-758.

[113] A. Randazzo, G. Bifulco, C. Giannini, M. Bucci, C. Debitus, G. Cirino, L. Gomez-Paloma. *J. Am. Chem. Soc.* **2001**, *123*(44), 10870-10876.

[114] C. Gachet. *Annu. Rev. Pharmacol. Toxicol.* **2006**, *46*, 277-300.

[115] J. Trepel, M. Mollapour, G. Giaccone, L. Neckers. *Nat. Rev. Cancer* **2010**, *10*(8), 537-549.

[116] R. I. Handin. *N. Engl. J. Med.* **1996**, *334*(17), 1126-1127.

[117] G. Davi, C. Patrono. *N. Engl. J. Med.* **2007**, *357*(24), 2482-2494.

[118] Z. M. Ruggeri. *Nat. Med.* **2002**, *8*(11), 1227-1234.

[119] A. D. Michelson. *Circulation* **2004**, *110*(19), e489-e493.

[120] R. W. Farndale, J. J. Sixma, M. J. Barnes, P. G. de Groot. *J. Thromb. Haemost.* **2004**, *2*(4), 561-573.

[121] J. M. Gibbins. *J. Cell Sci.* **2004**, *117*(Pt 16), 3415-3425.

[122] G. E. Jarvis, D. Best, S. P. Watson. *Platelets.* **2004**, *15*(5), 303-313.

[123] S. Murugappan, R. Chari, V. M. Palli, J. Jin, S. P. Kunapuli. *Biochem. J.* **2009**, *417*(1), 113-120.

[124] B. N. Kholodenko, J. F. Hancock, W. Kolch. *Nat. Rev. Mol. Cell Biol.* **2010**, *11*(6), 414-426.

[125] E. Jarnaess, K. Tasken. *Biochem. Soc. Trans.* **2007**, *35*(Pt 5), 931-937.

[126] W. Wong, J. D. Scott. *Nat. Rev. Mol. Cell Biol.* **2004**, *5*(12), 959-970.

[127] M. Mongillo, T. McSorley, S. Evellin, A. Sood, V. Lissandron, A. Terrin, E. Huston, A. Hannawacker, M. J. Lohse, T. Pozzan, M. D. Houslay, M. Zaccolo. *Circ. Res.* **2004**, *95*(1), 67-75.

[128] D. H. Maurice, D. Palmer, D. G. Tilley, H. A. Dunkerley, S. J. Netherton, D. R. Raymond, H. S. Elbatarny, S. L. Jimmo. *Mol. Pharmacol.* **2003**, *64*(3), 533-546.

[129] M. D. Houslay, G. S. Baillie, D. H. Maurice. *Circ. Res.* **2007**, *100*(7), 950-966.

[130] M. L. Dell'Acqua, M. C. Faux, J. Thorburn, A. Thorburn, J. D. Scott. *EMBO J.* **1998**, *17*(8), 2246-2260.

[131] S. Manni, J. H. Mauban, C. W. Ward, M. Bond. *J. Biol. Chem.* **2008**, *283*(35), 24145-24154.

[132] U. R. Schwarz, U. Walter, M. Eigenthaler. *Biochem. Pharmacol.* **2001**, *62*(9), 1153-1161.

[133] J. Schlossmann, A. Ammendola, K. Ashman, X. Zong, A. Huber, G. Neubauer, G. X. Wang, H. D. Allescher, M. Korth, M. Wilm, F. Hofmann, P. Ruth. *Nature* **2000**, *404*(6774), 197-201.

[134] J. V. Olsen, B. Blagoev, F. Gnad, B. Macek, C. Kumar, P. Mortensen, M. Mann. *Cell* **2006**, *127*(3), 635-648.

[135] S. Lemeer, A. J. Heck. *Curr. Opin. Chem. Biol.* **2009**, *13*(4), 414-420.

[136] T. T. Aye, S. Mohammed, H. W. van den Toorn, T. A. van Veen, M. A. van der Heyden, A. Scholten, A. J. Heck. *Mol. Cell Proteomics.* **2009**, *8*(5), 1016-1028.

[137] A. Scholten, M. K. Poh, T. A. van Veen, B. B. van, M. A. Vos, A. J. Heck. *J. Proteome. Res.* **2006**, *5*(6), 1435-1447.

[138] S. H. Francis, E. P. Bessay, J. Kotera, K. A. Grimes, L. Liu, W. J. Thompson, J. D. Corbin. *J. Biol. Chem.* **2002**, *277*(49), 47581-47587.

[139] B. O. Jensen, F. Selheim, S. O. Doskeland, A. R. Gear, H. Holmsen. *Blood* **2004**, *104*(9), 2775-2782.

[140] S. S. Taylor, C. Kim, D. Vigil, N. M. Haste, J. Yang, J. Wu, G. S. Anand. *Biochim. Biophys. Acta* **2005**, *1754*(1-2), 25-37.

[141] M. Antl, M. L. von Bruhl, C. Eiglsperger, M. Werner, I. Konrad, T. Kocher, M. Wilm, F. Hofmann, S. Massberg, J. Schlossmann. *Blood* **2007**, *109*(2), 552-559.

[142] H. Mi, N. Guo, A. Kejariwal, P. D. Thomas. *Nucleic Acids Res.* **2007**, *35*(Database issue), D247-D252.

[143] M. C. von, L. J. Jensen, M. Kuhn, S. Chaffron, T. Doerks, B. Kruger, B. Snel, P. Bork. *Nucleic Acids Res.* **2007**, *35*(Database issue), D358-D362.

[144] J. Hagmann, M. Grob, A. Welman, W. G. van, M. M. Burger. *J. Cell Sci.* **1998**, *111 (Pt 15)*, 2181-2188.

[145] P. Mortensen, J. W. Gouw, J. V. Olsen, S. E. Ong, K. T. Rigbolt, J. Bunkenborg, J. Cox, L. J. Foster, A. J. Heck, B. Blagoev, J. S. Andersen, M. Mann. *J. Proteome. Res.* **2010**, *9*(1), 393-403.

[146] H. A. Braun, S. Umbreen, M. Groll, U. Kuckelkorn, I. Mlynarczuk, M. E. Wigand, I. Drung, P. M. Kloetzel, B. Schmidt. *J. Biol. Chem.* **2005**, *280*(31), 28394-28401.

[147] J. A. Smith, S. H. Francis, K. A. Walsh, S. Kumar, J. D. Corbin. *J. Biol. Chem.* **1996**, *271*(34), 20756-20762.

[148] U. Rix, O. Hantschel, G. Durnberger, L. L. Remsing Rix, M. Planyavsky, N. V. Fernbach, I. Kaupe, K. L. Bennett, P. Valent, J. Colinge, T. Kocher, G. Superti-Furga. *Blood* **2007**, *110*(12), 4055-4063.

[149] S. D. Rybalkin, I. G. Rybalkina, R. Feil, F. Hofmann, J. A. Beavo. *J. Biol. Chem.* **2002**, *277*(5), 3310-3317.

[150] M. Collado-Hilly, J. F. Coquil. *Biol. Cell* **2009**, *101*(8), 469-480.

[151] L. Margarucci, M. C. Monti, A. Tosco, R. Riccio, A. Casapullo. *Angew. Chem. Int. Ed Engl.* **2010**, *49*(23), 3960-3963.

[152] L. Margarucci, M. C. Monti, B. Fontanella, R. Riccio, A. Casapullo. *Mol. Biosyst.* **2010**, *in press*.

[153] E. Kaiser, R. L. Colescott, C. D. Bossinger, P. I. Cook. *Anal. Biochem.* **1970**, *34*(2), 595-598.

[154] M. M. Bradford. *Anal. Biochem.* **1976**, *72*, 248-254.

[155] K. H. van, S. M. Hale. *Anal. Biochem.* **1977**, *81*(2), 485-487.

[156] N. Shimizu, K. Sugimoto, J. Tang, T. Nishi, I. Sato, M. Hiramoto, S. Aizawa, M. Hatakeyama, R. Ohba, H. Hatori, T. Yoshikawa, F. Suzuki, A. Oomori, H. Tanaka, H. Kawaguchi, H. Watanabe, H. Handa. *Nat. Biotechnol.* **2000**, *18*(8), 877-881.

[157] J. Wissing, K. Godl, D. Brehmer, S. Blencke, M. Weber, P. Habenberger, M. Stein-Gerlach, A. Missio, M. Cotten, S. Muller, H. Daub. *Mol. Cell Proteomics.* **2004**, *3*(12), 1181-1193.

[158] K. Godl, O. J. Gruss, J. Eickhoff, J. Wissing, S. Blencke, M. Weber, H. Degen, D. Brehmer, L. Orfi, Z. Horvath, G. Keri, S. Muller, M. Cotten, A. Ullrich, H. Daub. *Cancer Res.* **2005**, *65*(15), 6919-6926.

[159] A. Shevchenko, H. Tomas, J. Havlis, J. V. Olsen, M. Mann. *Nat. Protoc.* **2006**, *1*(6), 2856-2860.

[160] T. Mosmann. *J Immunol. Methods* **1983**, *65*(1-2), 55-63.

[161] K. Yamamoto, A. Yamazaki, M. Takeuchi, A. Tanaka. *Anal. Biochem.* **2006**, *352*(1), 15-23.

[162] R. Yumoto, H. Nishikawa, M. Okamoto, H. Katayama, J. Nagai, M. Takano. *Am. J. Physiol Lung Cell Mol. Physiol* **2006**, *290*(5), L946-L955.

[163] A. Scholten, T. A. van Veen, M. A. Vos, A. J. Heck. *J. Proteome. Res.* **2007**, *6*(5), 1705-1717.

[164] A. Scholten, M. K. Poh, T. A. van Veen, B. B. van, M. A. Vos, A. J. Heck. *J. Proteome. Res.* **2006**, *5*(6), 1435-1447.

[165] P. J. Boersema, R. Raijmakers, S. Lemeer, S. Mohammed, A. J. Heck. *Nat. Protoc.* **2009**, *4*(4), 484-494.

[166] M. R. Larsen, T. E. Thingholm, O. N. Jensen, P. Roepstorff, T. J. Jorgensen. *Mol. Cell Proteomics.* **2005**, *4*(7), 873-886.

[167] P. Mortensen, J. W. Gouw, J. V. Olsen, S. E. Ong, K. T. Rigbolt, J. Bunkenborg, J. Cox, L. J. Foster, A. J. Heck, B. Blagoev, J. S. Andersen, M. Mann. *J. Proteome. Res.* **2010**, *9*(1), 393-403.

[168] T. T. Aye, S. Mohammed, H. W. van den Toorn, T. A. van Veen, M. A. van der Heyden, A. Scholten, A. J. Heck. *Mol. Cell Proteomics.* **2009**, *8*(5), 1016-1028.

[169] H. Mi, N. Guo, A. Kejariwal, P. D. Thomas. *Nucleic Acids Res.* **2007**, *35*(Database issue), D247-D252.

[170] M. C. von, L. J. Jensen, M. Kuhn, S. Chaffron, T. Doerks, B. Kruger, B. Snel, P. Bork. *Nucleic Acids Res.* **2007**, *35*(Database issue), D358-D362.

List of Abbreviations

20S	Proteasome Subunit 20S
26S	Proteasome Subunit 26S
1D/2D SDS PAGE	Sodium Dodecyl Sulphate - PolyAcrylamide Gel Electrophoresis
488-BSA	488-Bovine Serum Albumin
ABPP	Activity Based Protein Profile
ADP	Adenosine Diphosphate
ATP	Adenosine Triphosphate
AMC	7-amino-4-methylcoumarine
ACN	Acetonitrile
AP2	Adaptor Protein 2
AKAP	A-Kinase Anchoring Protein
ATP2C1	ATPase type 2C member 1
Bcr-Abl	Oncogene Fusion Protein
BLQ	Bolinaquinone
CID	Collision Induced Dissociation
cAMP	Cyclic Adenosine Monophosphate
cGMP	Cyclic Guanosine Monophosphate
CRP	Collagen Related Peptide
CPZ	Chlorpromazine
CDK	Cyclin Dependent Kinase
DDR1	Receptor Tyrosine Kinase
DAP	1,5-diamino-pentane
DAD	1,12-diamino-dodecane
DMSO	Dimethyl Sulfoxide
ETD	Electron Transfer Dissociation

EDC	1-ethyl-3-(3-dimethylaminopropyl) carbodiimide
FKBP12	FK506 Binding Protein
GPVI	Glycoprotein VI
GKAP	G-Kinase Anchoring Protein
ICAT	Isotope Coated Affinity Tag
IRAG	Inositol-1,4,5-trisphosphate Receptor–Associated PKG Substrate
IP3	Inositol-1,4,5-trisphosphate Receptor
IC_{50}	Half Maximal Inhibitory Concentration
iTRAQ	Isobaric Tag for Relative and Absolute Quantitation
ITC	Isothermic Titration
Hic5	Cell-Junction/Cell Adhesion Proteins
Kd	Dissociation Constant
Ka	Association Constant
LC-MS	Liquid Chromatography Coupled Mass Spectrometry
LC-MSMS	Liquid Chromatography Coupled Tandem Mass Spectrometry
LDHA	Lactate Dehydrogenase A
LDHB	Lactate Dehydrogenase B
Lys-C	Endoproteinase *Lys-C*
LPS	Lipopolysaccharides
LG3BP	Galectin Binding Protein 3
MS	Mass Spectrometry
MALDI	Matrix Assisted Laser Desorption Ionization

MTT	3-(4,5-Dimethylthiazol-2-yl)-2,5-diphenyltetrazolium bromid
MRVI1	Inositol-1,4,5-trisphosphate Receptor–Associated PKG Substrate
M6PR	Mannose-6-Phosphate Receptor
$NaBH_4$	Sodium Borohydride
NDKB	Nucleoside Diphosphate Kinase B
NF-kB	Nuclear Factor-Kappa Beta
NQO2	Quinone Oxidoreductase 2
NOs	Nitric Oxide Synthase
NMR	Nuclear Magnetic Resonance
NHS	N-Hydroxysuccinimide
PEG	Poly-Ethylene Glycol
PDE	Phosphodiesterase
PMA	Phorbol Myristate Acetate
PMF	Peptide Mass Fingerprint
PTM	Post Translational Modification
PRT	Perthamide C
PM	Petrosaspongiolide M
PKA	Protein Kinase A
PKG	Protein Kinase G
PLA_2	Phospholipase A_2
PA28	Proteasome Activator 28
PHGH-like	Caspase Like
Poly-UP	Poly-Ubiquitin
PGE1	Prostaglandin E1
PGI2	Prostaglandin I2
Q-Tof	Quadrupole-Time of Flight
RU	Response Units

RP-HPLC	Reverse Phase- High Performance Liquid Chromatogrphy
SDS	Sodium Dodecyl Sulphate
SILAC	Stable Isotope Labeling with Aminoacids in Cell Culture
SET	Single Electron Transfer
$sPLA_2$	Secretory Phospholipase A_2
SPR	Surface Plasmon Resonance
TGFB1I1	Cell-Junction/Cell Adhesion Proteins
TNBS	2,4,6-trinitrobenzenesulphonicacid
TFA	Trifluoroacetic Acid
Trt	Trityl
UPS	Ubiquitin Proteasome System

Acknowledgements

This work was not possible without the enthusiasm and encouragements of the people that during the past three years worked with me in the organic chemistry lab. First of all, I'd like to thank my tutor Professor Raffaele Riccio for his guidance and support. Many thanks goes to Professor Agostino Casapullo for his effort in the field of marine natural product. Dear Prof, thanks for your encouragements and sounds advices which I really appreciated. My special thanks goes to Dr. Maria Chiara Monti; anything was possible without her help. Chiara, thanks for your enthusiasm, inspiration and endless support; our work made my PhD a success.

I'd like to thank Dr. Alessandra Tosco for introducing me in the biochemical world. Ale, your support was unique and endless also when I broken the centrifuge. I'd like to thank Dr. Fabrizio Dal Piaz for his training on Q-tof mass spectrometer for his experimental advises. Dear Fabri, today my BSA sometimes are better than yours.

I'd like to thank Dr. Bianca Fontanella for her cell images and Dr. Sandro Montefusco which make Agewandte Chemie cover possible.

Many thanks and appreciation goes to my students Germana, MariaAnna, Angela, Carmine, Rossana, Chiara, Maria and Dario that in various way helped me during this three years.

A special thanks goes to Dr. Rosa De Simone that from the degree day until now encourage me daily and contribute to make my research passion stronger.

I am also grateful to Dr. Annalisa Vilasi. Annalisa, thanks for introducing me to 2D-electrophoresis and for our friendly coffee break that now are becoming friendly tea break. Finally, I'd like to thank all the people of the Organic Chemistry lab especially Dr. Stefania Terracciano and Dr. Anna Falcone. Then, my thanks goes to Dr. Lucia Prota for our friendly chat during the daily

trip and for giving me the opportunity to have a sit on the bus (Agropoli-Fisciano) every day.

I like to thank Professor Albert J.R Heck for giving me the precious opportunity to join the "Biomolecular Mass Spectrometry and Proteomics Group". A special thanks to all Bimolecular Mass Spectrometry and Proteomics Group for welcoming me in the lab. Particularly, I have to thank Dr. Arjen Scholten for his help in developing my project. Arjen, I am grateful for your help throughout my stay at Utrecht University. Many thanks goes to Thijs for preparing me platelets on demand and Mark for his massive blood donation. Sara and Serena thank for everything; it was wonderfull to share my abroad experiences with two intalians. Sara, thanks for your daily encouragements which I really appreciate. Last but not least, I'd like to thank Michela which make all my life a success. Michela, we share a lot of experience and I am grateful to you for everything.

Finally, I'd like to thanks my parents that make my life wonderful. They encouraged me, loved me and supported me every day. For this reason I dedicated them this work.

Luigi Margarucci